Mathematical Problems in Engineering

Decision Making Problems Related to Modular Design Practices or Techniques

Lead Guest Editor: Vladimir Modrak
Guest Editors: R. Sudhakara Pandian, Ponnusamy Venkumar, and Chrysostomos Stylios

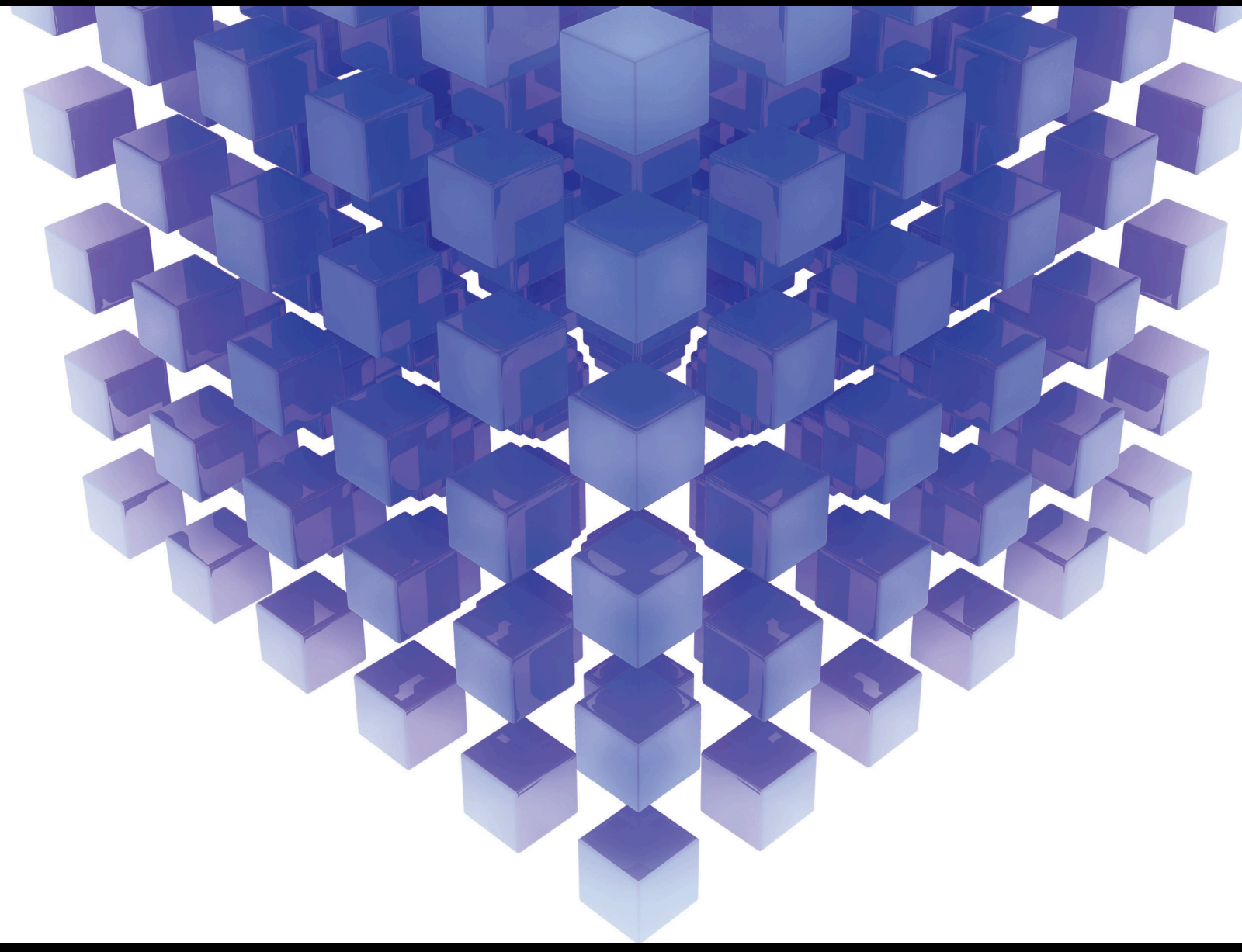

Decision Making Problems Related to Modular Design Practices or Techniques

Mathematical Problems in Engineering

Decision Making Problems Related to Modular Design Practices or Techniques

Lead Guest Editor: Vladimir Modrak
Guest Editors: R. Sudhakara Pandian, Ponnusamy Venkumar, and Chrysostomos Stylios

Contents

Hindawi
Mathematical Problems in Engineering
Volume 2022, Article ID 9870358, 2 pages
https://doi.org/10.1155/2022/9870358

Editorial

Decision Making Problems Related to Modular Design Practices or Techniques

Vladimir Modrak,[1] **R. Sudhakara Pandian**,[2] **Ponnusamy Venkumar**,[3] **and Chrysostomos Stylios**[4]

[1]*Dept. of Industrial Engineering & Informatics, Institute of Manufacturing Management, Technical University of Kosice, Kosice, Slovakia*
[2]*Dept. of Manufacturing Engineering, School of Mechanical Engineering, Vellore Institute of Technology, Vellore, India*
[3]*Dept. of Mechanical Engineering, VSB Engineering College in Karur, Affiliated to Anna University in Chennai, Chennai, India*
[4]*Dept. of Informatics & Telecommunications, University of Ioannina, Ioannina, Greece*

Correspondence should be addressed to Vladimir Modrak; vladimir.modrak@tuke.sk

Received 30 June 2022; Accepted 30 June 2022; Published 18 August 2022

Modularization, often treated as modular design, is a well-known approach subdividing a system or product or process into smaller parts called modules. These design elements are engineered to be grouped collectively so that a single module can be developed, modified, replaced, or swapped between other systems. Modular design is widely used in multiple disciplines, including the theory of interrelatedness and reconfigurability, axiomatic design theory, general modular systems theory, graph theory, complexity science, and system theory. System theory, as one of the major meta-synthetic disciplines, describes modular systems using mathematical concepts in the most generic way. In spite of its prevalence and importance for flexible systems or product or process development and improvement, there is still insufficient understanding of how to apply existing knowledge and techniques of modular design in specific application domains. In order to contribute to overcoming the situation, this Special Issue collects recent original contributions related to designing products, optimization models for decision making problems, process modularity, and manufacturing systems modularity.

Authors from five different countries submitted original research articles that made use of mathematical methodologies and tools, numerical solutions, computer programmes, and data handling procedures to cover, explicitly or implicitly, the defined and relevant subject fields. Contributions containing generalized formulations or results related to practical applications are also included.

This Special Issue has received more than ten manuscripts, from which eight of them complied with essential editorial requirements screened by members of the journal's Editorial Board, and five high-quality papers have been accepted and published. The published papers have addressed various real-time techniques and contributed to a wide range of application areas such as modelling of assembly process structures, designing of large-scale box structures, performance optimization in manufacturing systems, and causal reasoning in decision making. A brief description characterizing each contribution is provided in the following paragraphs.

G. Mazzuto et al. investigated and proposed a novel hybrid decision-support system based on the decision-making trial and evaluation laboratory and fuzzy cognitive maps. Their method increases decision makers' ability to make correct decisions, since it enables them to more effectively differentiate and understand system findings. The applicability and advantage of this approach are illustrated there through a case study focused on analysis of clinical risk in drug administration. Obtained results clearly show a promising potential of the proposed method for achieving better decision outcomes than by using traditional fuzzy cognitive mapping methodology.

The authors V. Modrak and Z. Soltysova stated about the assessment of the degree operational modularity issues. A novel approach of this research lies in measuring the relative modularity of various assembly process topologies. In order to validate its effectiveness, this novel technique is compared to other relative modularity metrics such as the single value modularity index, degree of process module, and process module independence. The expected result for the relative modularity indicator in the manufacturing assembly process structure is obtained using the new technique.

W.-Y. Wang and Y. Wang, in their article, discussed the development of a diagnostic index system for large-scale building projects. The indicators produced in this work are more structurally correlated than current index systems, with superior hierarchical development at all levels of the index system. It has been shown that the diagnosis index system generated by the recommended approach is capable of diagnosing macroscopic, mesostates, and microstates, as well as expressing systematic hierarchical linkages among all linked indices.

The paper written by Velmurugan et al. focuses on development and implementation of the new method to predict the most critical subsystems in the tyre manufacturing system of the rubber industry. Their research was motivated by the fact that any one maintenance parameter among reliability, availability, maintainability, and dependability parameters was not mathematically evaluated to identify the critical subsystems and their impact on the effectiveness of the tyre manufacturing system. In order to fill this research gap, this paper proposes an approach to identification of the critical subsystem of the tyre production system based on the Markov Birth Death approach. Besides, it also includes calculation of the performance of certain maintenance parameters concerning time such as mean time between failures, mean time to repair, and dependability ratio for each subsystem of the tyre production system.

Z. Wang et al. discussed various concerns of direct topology optimization as a result of large-scale box structure carrying moving loads by the primary load bearing structure of heavy machine tools, cranes, and other high-end types of equipment. As a result, for large-scale box structures, the authors presented multiworking condition topology optimization. For instance, using a crossbeam from a superheavy turning and milling machining centre, the optimization study shows that the crossbeam's stiffness and strength are enhanced while its weight is minimized.

We would like to conclude this editorial with the hope that the collection of the papers in this Special Issue will be beneficial to readers who are scientifically interested or practically involved in decision making problems related to modular design practices or techniques.

Conflicts of Interest

The editors declare that there are no conflicts of interest regarding the publication of this article.

Acknowledgments

The guest editors sincerely thank all the authors for their high-quality research articles in this Special Issue. The lead guest editor would also like to express the gratitude to other guest editors for their kind support and cooperation for the development of this Special Issue.

Vladimir Modrak
R. Sudhakara Pandian
Ponnusamy Venkumar
Chrysostomos Stylios

Hindawi
Mathematical Problems in Engineering
Volume 2022, Article ID 2749435, 14 pages
https://doi.org/10.1155/2022/2749435

Research Article

Improved Decision-Making through a DEMATEL and Fuzzy Cognitive Maps-Based Framework

Giovanni Mazzuto,[1] **Chrysostomos Stylios**,[2,3] **Filippo Emanuele Ciarapica**,[1] **Maurizio Bevilacqua**,[1] **and Georgopoulos Voula**[4]

[1]*Dipartimento Ingegneria Industriale e Scienze Matematiche, Università Politecnica Delle Marche, Ancona, Italy*
[2]*Dept of Informatics and Telecommunications, University of Ioannina, Arta, Greece*
[3]*Industrial Systems Institute, Athena RC, Patra, Greece*
[4]*School of Health Rehabilitation Sciences, University of Patras, Patra, Greece*

Correspondence should be addressed to Giovanni Mazzuto; g.mazzuto@univpm.it

Received 13 April 2021; Accepted 7 March 2022; Published 27 May 2022

Academic Editor: Adiel T. de Almeida-Filho

The decision-making process is highly demanding. There has been an increasing tendency to incorporate human thinking, individual experience about a problem, and pure mathematical approaches. Here, a novel integrated approach is investigated and proposed to develop an advanced hybrid decision-support system based on the decision-making trial and evaluation laboratory (DEMATEL) and fuzzy cognitive maps (FCMs). Indeed, knowledge acquisition and elicitation may present distortions and difficulties finding a consensus and an interpretation. Thus, the proposed combined approach aims to examine in depth the potential to improve FCMs' outcomes by integrating FCM with the DEMATEL approach. The combined methodology achieves at avoiding some of the drawbacks, such as the lack of a standardized FCM theoretical model. Thus, it provides advanced comparative analysis and results in better interpretation of the decision-making process. It is highlighted that the traditional FCM approach does not allow distinguishing the whole number of defined scenarios, in contrast to the hybrid one presented here, which increases the ability of users to make correct decisions. Combining the two approaches provides new capabilities to FCMs in grouping experts' knowledge, while the DEMATEL approach contributes to refining the strength of concepts' connections.

1. Introduction and Background

Decision-making is the process of making choices by identifying a decision, collecting information, and achieving alternatives. Since their first appearance in the 1970s, decision support systems developed rapidly; initially, they performed their task essentially on mainframes, using inflexible warehouses of corporate data. In the last decade, with the entrance in the information age (e.g., development of information technologies and Industry 4.0 paradigm), companies are accumulating a huge amount of data with little knowledge, transforming the way decisions are made [1]. One can generalise by saying that the decision-making process is essentially characterized by two types of elements: organisational and technical [2]. The formers are related to the day-to-day operation of companies, in line with corporate strategy; the latter includes a set of tools such as information systems, data repositories, formal modeling, and decision analysis. What evolves with Industry 4.0, however, is the source and nature of the information [3]. All the actors involved in the day-to-day running of the company produce data, structured and unstructured, which necessarily require standardisation mechanisms such as the adoption of PLM (product lifecycle management) systems, in the context of the integration brought about by Industry 4.0 [4]. Moreover, given the varied nature of the available information, according to [5], in order to improve the data management process and make full use of it, it is necessary to extract this knowledge from it by referring to big data analytics tools. Increasing data size also increases the

calculation and processing time: the whole process becomes quite demanding and creates the additional need to manage such data in an agile and flexible manner. In this regard, [6] suggests adopting cloud technology to manage huge sets of data and discover knowledge from them through data mining. With the support of cloud infrastructure, high levels of reliability and availability regarding data collection, management, and sharing can be obtained [7]. In addition, for a decision to be reliable, the information and knowledge on which it depends must be reliable. Thus, in their study, [8] introduced the emerging blockchain technology as a guarantee of reliability. In fact, according to [9], all the relevant information and past decisions cannot be corrupted or changed by any of the participants, unless all concerned agree to such a change. This provides reliable and unambiguous information for use in decision-making of both a structured and unstructured nature. However, the problem linked to the unstructured nature of the information still remains, since, in this case, the formulation of a quantitative model is difficult or almost impossible because of the scarcity of available data characterized by an unstructured nature. According to [10], understanding the events and factors affecting the whole problem domain is an indispensable condition for achieving decisions efficiently and adequately structuring the decision-making approach based on a wide range of related issues. For this reason, as asserted by [11], several types of problems can profit from an approach centered on people's knowledge and problem assessment and, mainly, those wherein the stakeholder's opinion is remarkable [12]. A large number of methods have been developed for the improvement of the decision-making process, focusing on the experts' opinion in many research and application fields: from economics [13, 14] to healthcare [15], from safety and security [16, 17] to manufacturing and supply chain [18–20], and so on. However, all of them highlight complexities in conflict mitigation due to the collaborative process [21].

Among the well-known decision-making techniques that can be mentioned are the analytic hierarchy process (AHP) [22], the technique for order of preference by similarity to ideal solution (TOPSIS) [23], or the most adopted Strengths, Weaknesses, Opportunities, and Threats (SWOT) matri [24]. However, because explaining human reasoning is a very hard task using only numbers, many decision-making techniques consider the fuzzy theory application [25]. For instance, [26] provided an integrated approach based on the multiobjective mathematical programming and fuzzy analytical hierarchy process for sustainable suppliers' selection and the definition of the best order allocation. Saidi Mehrabad [27] defined a method based on the preference ranking organization method for enrichment evaluations, taking advantage of the method, flexibility, and simplicity, jointly to the evaluation of fuzzy data for preferences, weights, and scores.

Interestingly, between 1972 and 1979, the Science and Human Affairs Program of the Battelle Memorial Institute of Geneva provided the DEMATEL method to study complex and intertwined issues. Thus, DEMATEL is a practical and helpful approach to envision the composition of complex causal relationships using diagrams or matrices [28]. Specifically, these matrices or diagrams can describe a contextual relationship among the system elements, and a numeric value characterizes the relevance strength [29]. DEMATEL allows decision-makers to identify the fundamental criteria to efficiently explain the problem and avoid evaluation overfitting [30]. For instance, [31] built a hybrid dynamic multiple criteria decision-making approach to solving problems related to the complex dynamics in the real world, combining DEMATEL with the analytic network process (ANP). Seleem et al. [32] developed an integrated model for the manufacturing organizations' support in selecting and managing appropriate initiatives using the theory of constraints, balanced scorecard, jointly to DEMATEL. Keskin [30], analogously, developed an integrated model through fuzzy DEMATEL and fuzzy C-means to increase quality in selecting and evaluating the supplier.

Moreover, [33] defined a hybrid framework referring to fuzzy AHP with fuzzy Delphi and fuzzy DEMATEL to overcome the weaknesses related to supplier selection. Unequivocally, the framework allows designing a methodology to achieve the performance scores of three PLC suppliers, taking into consideration 11 attributes. Tadić et al. [34] combined fuzzy ANP, fuzzy VIKOR, and fuzzy DEMATEL methods to select and analyze the concept related to Belgrade's city logistics to improve the city organization with more relevance. Some years later, still the hesitant fuzzy VIKOR was combined with the hesitant fuzzy DEMATEL by [35] to investigate the relationships among the customer requirements and determine their relevance weights to prioritize the engineering characteristics; this issue is also analyzed by [36].

Even [37] realized a DEMATEL-based approach for investigating barriers to the green supply chain in Canada. The barriers considered were investigated using causality and prominence relations to help decision-makers in providing successful practices. However, [38] pointed out that DEMATEL, in spite of the advantages listed above, is insufficient to provide a good decision-making tool when the information available is obtained from experts whose knowledge may be limited or incomplete. The same can be said when the information becomes innumerable as it would require complex mechanisms for its interpretation.

Some years after the introduction of DEMATEL, the fuzzy cognitive maps (FCMs) were proposed by [39] to model the causal relationship among concepts and evaluate inference patterns.

Indeed, causal reasoning in decision-making is important, since it is inherent to the human reasoning process [40], and thus, easily comprehensible, as well as based on cause-effect relations between components of the system being modeled. Pure mathematical modeling systems that are based on regression analysis rely on correlation, which does not confirm causation. Also, data-driven decision-making systems can be designed even without system-specific knowledge, since they use pattern recognition and statistical techniques [41]. Causal-based and model-driven systems such as FCMs and Bayesian belief networks (BBNs) are based on visual graphs consisting of nodes (variables) and

directional links between nodes that represent cause-and-effect relationships between the variables. The research findings show that in comparison to BBNs, FCMs are more suitable for use as a front-end modeling tool to elicit expert knowledge, since the causal model is simpler, more intuitive, and user-friendly, making easier their composition and decomposition [42, 43].

More, in particular, FCMs are a tool for knowledge and inference depiction, an essential step for any intelligent system. Remarkably, they offer a far more flexible and potent framework for human reasoning and knowledge representation [44]. In addition, always related to the application of FCMs for the decision-making process, many studies can be mentioned in many fields, from industrial plants to healthcare, mainly concerning risk assessment for complex systems [45, 46]. For example, [47] used FCM to explore and evaluate the importance of human factors affecting human reliability in the industrial sector. A hybrid model has been proposed by [48], based on competitive FCM for medical decision support systems introducing genetic algorithms. In addition, [49] developed an FCM tool for identifying the most critical injury causes in a refinery plant and addressing the economic efforts to reduce them, and then, [50] developed a decision-support system for the criticality ranking of the plant equipment. Poczęta et al. [51] presented how to optimize FCMs operation for better decision-making and prediction. Al-subhi et al. [52] proposed an extension of FCMs, the neutrosophic cognitive map, that was successfully applied to model multistage sequential decision-making problems.

Also focusing on the healthcare field, FCMs have been applied to assess the risks. Amirkhani et al. [53] have modeled with the help of the FCMs various aspects in the medical field. Smith [54] proposed a prototype for the IT risks evaluation in healthcare. Furthermore, [55] used FCMs to evaluate cancer thermography, finding in them a valuable tool to diminish medical errors. Bevilacqua et al. [56] referred to a similar approach to evaluating drug administration risk in an Italian hospital.

By analyzing the literature review, it is possible to assert that DEMATEL and FCM techniques are characterized by several similarities, as given in Table 1. At the same time, they also have differences demonstrating the complementarity of the two approaches.

Due to the many similarities and complementarity of DEMATEL with FCMs, as given in Table 1, the two modeling methods are chosen here for decision-making. For example, in 2014, fuzzy cognitive maps, DEMATEL, and ANP have been combined by [57] to realize an analytical hybrid multiple criteria-decision making (MCDM) model for a private primary school selection problem to help parents in the primary school selection problem.

In particular, the possibility of improving FCMs outcomes using the DEMATEL approach wants to be evaluated since

(i) Knowledge can present distortions once transferred among persons [58]

(ii) Extreme difficulty can be encountered in finding a consensus[59]

(iii) The traditional FCM approach does not allow to distinguish the entire number of defined scenarios for decision-making [60]

As [61] asserted, the lack of a standardized FCM theoretical model pinpoints the problem of comparative analysis in problem-solving. Axelrod [62] presented similar conclusions, stressing that the lack of formal methods for the construction of cognitive maps affects the results' reliability and the interpretability of problem situation analysis [63]. How the results' reliability and interpretability are also due to the oversized FCM models were also studied. Generally, human reasoning is characterized either by oversimplification or by overcomplicated mental processes. Indeed, as [64] asserted, the critical dependence on experts' knowledge is an important deficiency in managing FCMs in control processes, since the FCM output must describe the real system output as closely as possible. Therefore, researchers have developed several learning algorithms to reach this purpose [65]. Lee et al. [66] developed an FCM-based holistic method to solve the semantic ambiguity problems due to different FCMs, thus ensuring semantic enhancement and interoperability through effective collaboration. In addition, [67] highlighted the inability of the FCM to model the uncertainty introduced by people's hesitation in a complex system and how this can affect the reliability of the entire decision-making process. Therefore, they refer to the dual hesitant fuzzy sets (DHFSs) theory to consider the degree of membership and nonmembership to model uncertainty and epistemic uncertainty.

For all of these reasons, the proposed study investigates in a comparative approach and analyses the features of DEMATEL and FCM methodologies and how they could be used jointly, in a complementary way, as described in Section 2. Section 3 describes the case study used to underline pros and cons in their combined use, while in Section 4, the relative outcomes are discussed. Last, Section 5 focuses on the further analysis and improvement needed to model a hybrid decision-making support system.

2. Complementarity and Combination of DEMATEL and FCMs

2.1. The Need for Expanding FCM Methodology. As described in the introduction section, several methods have been developed for the decision-making process improvement, focusing on experts' opinion, but underlining how the transferred knowledge can be affected by biases [58], and concurrently, extreme difficulties can occur in obtaining a consensus [59] or in the results' interpretation [68]. Even though FCMs have been proposed as a unique methodology able to aggregate a significant amount of knowledge and beliefs [11, 69], the lack of a standardized FCM theoretical model pinpoints the problem of comparative analysis in problem-solving [61, 62]. Many applications solve this problem by developing learning algorithms or analogous but de facto, modifying, or even neglecting the experts' contribution. Indeed, referring to [70], experts can introduce realism for dynamic planning and modeling, improving the system's performance. This means that every developed

Table 1: Compared aspects of DEMATEL and FCM approaches.

	DEMATEL	FCM
Similarities	Cause-effect relationships Graph visualization Factor prioritization Based on matrices Structural modeling approach	
Differences	No threshold function for the algorithm convergence	A threshold function for the algorithm convergence is mandatory
	Only nonnegative judgments matrix	Negative and nonnegative judgments matrix
	No parameters to be set for the output readability	Few parameters to be set for the output readability

decision-making approach must seriously consider human expertise, but concurrently, it must avoid ambiguous results analysis for an effective decision-making procedure.

It is concluded that the proposed approach aims at showing how the combination of the traditional FCM approach with another experts-based decision-making tool allows to solve or reduce the questioned problem.

Moreover, given the analogy between DEMATEL and FCM, it is possible to adopt the same assumption for this research. Presume that m experts are involved in solving a complex problem described considering n main concepts. The grades assigned by all the experts (for example, adopting a 5-point Likert scale: 0, no influence; 1, very low influence; 2, low influence; 3, high influence; 4, very high influence) produce an $n \times$ n matrix X^k, with $1k \leq m$. Consequently, X^1, X^2,. . ., X^{m} are the resultant matrices for each expert, and each element of X^k (denoted with x_{ij}^k) assumes an integer value. The elements on the main diagonal of each X^{k} have a null value to neglect the effects of each concept with itself.

2.2. The DEMATEL Methodology. Zhu et al. [71] provided an in-depth description of the DEMATEL procedure. First, using the X^k matrices, a collective scores matrix A can be calculated using (1) as their average influence.

$$a_{ij} = \frac{1}{m} \sum_{k=1}^{m} x_{ij}^k. \tag{1}$$

Thus, by normalizing the average influence matrix A through (2) and (3), the direct influence matrix D can be determined.

$$D = sA, \tag{2}$$

$$s = \min\left[\frac{1}{\max\limits_{1\leq i\leq n} \sum_{j=1}^{n} a_{ij}}, \frac{1}{\max\limits_{1\leq i\leq n} \sum_{i=1}^{n} a_{ij}}\right]. \tag{3}$$

Once the direct influence matrix is defined, the total influence matrix T can be calculated according to the following equation [72].

$$\begin{aligned} T &= D + D^2 + D^3 + \cdots + D^{\infty} \\ &= \sum_{i=1}^{\infty} D^i = D(I - D)^{-1}. \end{aligned} \tag{4}$$

A threshold or benchmark value is chosen to ignore the concepts with negligible effects from the total influence matrix T. Therefore, a value lower than the threshold can be omitted from T to obtain the inner dependency matrix [37].

The influence-relations map can be provided by considering the values of $d + r$ and $d–r$, referring to the following equations It is possible to realize a visible structural model to figure out the complex causal connections in the set of all identified concepts.

$$r_i = \sum_{j=1}^{n} t_{ij}, \quad (i = 1, 2, \ldots, n), \tag{5}$$

$$d_i = \sum_{i=1}^{n} t_{ij}, \quad (j = 1, 2, \ldots, n). \tag{6}$$

In particular, the term $r_i + d_i$ represents the influences' strength by and on the i^{th} concept, measuring its relevance. Analogously, $r_i - d_i$, called relation, allows the concepts classification in a "cause" and "affected" unit: if $d_i - r_i$ has a nonnegative value, the i^{th} concept affects the other concepts more than those belonging to the cause group influencing it. Conversely, a negative value defines the i^{th} concept as belonging to the affected group [31].

2.3. FCM Approach. Kosko's elementary FCM approach [39], named in this study with "traditional approach," has been extensively expanded and applied by [73, 74] in the decision-making process to assign fuzzy weights to every FCM relationship. The expert or decision-maker is asked to express the degree of belief in terms of the strength of all the causal relationships for a particular organisational environment. Thus, the relationship weights can be personalized by each organization and industry sector. As shown in Figure 1, the first step of the map realization has been carried out by an experts' panel who were asked to give a numerical r_{ij} (the significance of the relation between concept i^{th} and j^{th}) to the R matrix where columns and rows identify the concepts. The expert panel session seeks to limit errors due to subjectivity. Once the experts agree on each interconnection, the proposed linguistic values are aggregated through the SUM method [75] for an overall linguistic weight evaluation. The defuzzification method of the centre of gravity allows changing to a numerical weight r_{ij} [76]. The so obtained r_{ij} describes the effect of concept C_i on C_j, varying in the range (1; 1). Specifically, if $r_{ij} = 0$, there is no causality; if $r_{ij} > 0$ can be identified as a relationship between the involved concepts

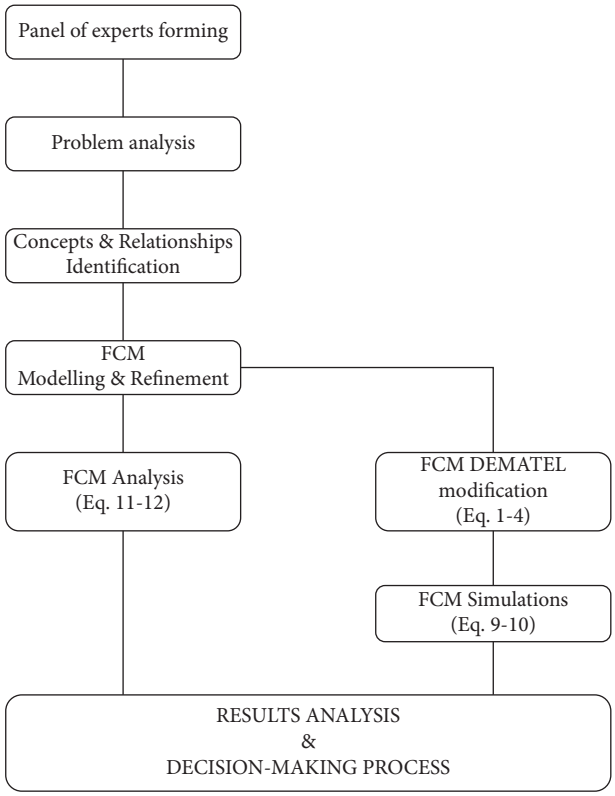

Figure 1: The proposed FCM modeling and analysis approach.

and if C_j increases, then C_i increases (or C_j decreases as C_i decreases); at the same time, if $r_{ij} < 0$, there is a causal decrease or negative causality. This means that if C_j j decreases, C_i increases (and or C_j increases as C_i decreases). The final adjacency matrix is

$$R = \begin{bmatrix} r_{11} & \cdots & r_{1n} \\ \vdots & r_{ij} & \vdots \\ r_{n1} & \cdots & r_{nn} \end{bmatrix}. \tag{7}$$

Moreover, a state vector $[C_1 \ldots C_n]$ describes the values of the current concepts (specifically, C_i represents the i^{th} concept). If $C_i = 0$, the concept is not active; if $C_i \neq 0$, it is active [77]. Bertolini[47] stated that equation (8) describes the time evolution of the map. A maximum iterations number can impose the stop condition or if between two successive iterations, there is a slight variation of the $[C_1 \ldots C_n]_{\text{NEW}}$ and $[C_1 \ldots C_n]_{\text{OLD}}$.

$$[C_1 \ \ldots \ C_n]_{\text{NEW}} = [C_1 \ \ldots \ C_n]_{\text{OLD}} \begin{bmatrix} r_{11} & \cdots & r_{1n} \\ \vdots & r_{ij} & \vdots \\ r_{n1} & \cdots & r_{nn} \end{bmatrix}. \tag{8}$$

Thus, simulate the cognitive map (CM) dynamics and analyze all CM paths. If A_i is the instantaneous value of concept C_i, its time evolution can be calculated by computing the impact of the related concepts C_j on the concept C_i, according to

$$A_i^{k+1} = f\left(A_i^k + \sum_{\substack{j=1 \\ j \neq i}}^{n} A_j^k r_{ij} \right), \tag{9}$$

where A_i^{k+1} is the value of concept C_i at the instant $k+1$, A_i^k is the value of concept C_j at simulation step k, and $f()$ is a threshold function for the algorithm convergence [78], since it is used to force the concept value to range into a normalized range [56, 79].

Generally, four activation functions can be used: hyperbolic tangent function, sigmoid function, step function, and threshold linear function.

Regardless of the lack of standard rules to choose activation functions, [78] thoroughly described the activation function's advantages and disadvantages, highlighting how they can modify FCM analysis. Decision-makers' predilections can decide the choice of a specific function. In the proposed study, the hyperbolic tangent function has been used, since it can tackle concepts varying in [−1, 1] interval, according to [80]. The normalization range is reached with λ close to 0.6 for the following equation.

$$f\left(A_i^k\right) = \frac{\left(e^{\lambda A_i^k} - e^{-\lambda A_i^k}\right)}{\left(e^{\lambda A_i^k} + e^{-\lambda A_i^k}\right)}. \tag{10}$$

The indirect and total causal effect evaluation is relevant in FCM analysis [81]. The indirect effect I_k of C_i concept on C_j concept is described by

$$I_k\left(C_i, C_j\right) = \min\left\{r\left(C_p, C_{p+1}\right)\right\}. \tag{11}$$

I_k is defined as the minimum value of the r_{ij} weight and a particular path starting from concepts i^{th} and ending in j^{th}. The total causal effect $T(C_i, C_j)$, expressed in (12), is subsequently evaluated as the maximum of all the indirect effects starting from C_i and ending in the concept C_j:

$$T\left(C_i, C_j\right) = \max\left\{I_k\left(C_p, C_{p+1}\right)\right\}. \tag{12}$$

$I_k(C_i, C_j)$ and $TE(C_i, C_j)$ must be interpreted according to the fuzzy mathematics theory and $e(C_p, C_{p+1})$ with the relationship weight expressed using fuzzy numbers. As explained by [39], $I_k(C_i, C_j)$ and $TE(C_i, C_j)$ are identified with t-norm (triangular-norm) operator t and t-conorm s. For instance, the connections between concepts $C1$ and $C5$ are

$$\begin{aligned} I_1(C_1, C_5) &= \min\{e_{13}, e_{35}\} \\ &= \min\{\text{much}, \text{lot}\} = \text{much}, \\ I_2(C_1, C_5) &= \text{some}, \\ I_3(C_1, C_5) &= \text{some}. \end{aligned} \tag{13}$$

The presence of three paths connecting the nodes $C1$ and $C5$ implies that the concept $C1$ can affect the final node ($C5$) in different ways. Thus, with the TE calculus, the maximum effect of $C1$ on $C5$ can be evaluated:

$$TE(C_1, C_5) = \max\{I_1(C_1, C_5), I_2(C_1, C_5), I_3(C_1, C_5)\} = \max\{\text{much}, \text{some}, \text{some}\} = \text{much}. \quad (14)$$

This means that concept C1 affects "much" concept C5.

In the same way, if a more complex evaluation scale is necessary, considering a symmetric scale with negative connections (i.e., ranging from very low to very high), it could be possible to identify situations in which some IEs manifest positive effects, while in other situations, they can manifest negative effects: "an indeterminate effect." If $I_1(C_1, C_5) = \text{very low}$ and $I_2(C_1, C_5) = \text{very high}$, both of the connections have a high impact on the concept $C5$. But they have different behaviors on the final concept: the first relationship negatively impacts them. In contrast, the second one has positive effects, so it is impossible to evaluate just one of them. Still, the analyzer must distinguish all the possible situations according to the analysis point of view.

2.4. DEMATEL and FCM Comparison. By comparing the mentioned methods, it is possible to underline that obtaining the finishing relationships matrix is quite comparable. Both derive the final matrix after experts have evaluated the more relevant concepts and their relationships.

Significantly, this connection has been investigated by [82], demonstrating that FCMs are a simplification of the DEMATEL approach if the threshold function $f()$ in (9) is the linear one to equal their convergence behaviors. Additionally, considering the previously mentioned condition, FCMs can manage the dynamic criteria status and overcome the limitation of the DEMATEL method adopting nonlinear dynamics. In contrast, many authors analyzed the chance to merge both approaches [83]. An efficient decision-making tool is provided to support leanness extent evaluation through DEMATEL to ascertain the impact of every leanness factor on others and FCM to identify several scenarios. These two methods are used differently in the decision-making process, and only in the final step, the relative results can be analyzed jointly. The literature review underscored the lack of the combined application of these two approaches. Possibly, this could be referred to as one of the main fundamentals of DEMATEL aspects. In fact, it is limited to a nonnegative assessments matrix, while FCMs also consider negative values. However, the matrix convergence is also ensured for a negative if its values range in $(-1, 1)$. The condition is verified for the FCM, since each evaluation mark varies in this range.

2.5. Combining DEMATEL and FCM. Under the discussed mathematical similarities and practical approaches, Figure 1 shows the proposed hybrid modeling application combining DEMATEL and FCM.

The proposed approach is the result of further development with respect to [84] which has been proposed to use a combined approach.

Beginning from the experts panel forming, each component has to be involved matching the criteria of competence and area. The panel of experts must describe all of the main aspects of the questioned problems.

The analysis aims at defining and classifying the internal and external aspects connected to the problem, as discussed in the problem analysis step. The analyzed system's requirements, regulations, and adequacy criteria must be clear, since they are considered "boundary conditions."

Using their experience and literature, experts are asked to express their opinions on the factors relating to the problem identified and the paired relations of concepts in the concepts and relationships identification step.

In the FCM modelling and refinement step, the different experts' experience produces different FCMs in terms of identified concepts and relationship and direction of the connection. They are analyzed to define a collective knowledge model helpful in analyzing the problem.

Therefore, the collective FCM can be analyzed to identify the most significant concept involved in the system, analyzing the hidden patterns and indirect/total effects. Then, to avoid the results understanding problem obtained during FCM simulation, the collective FCM has been revised, taking into account the DEMATEL procedure in the FCM DEMATEL modification step. In particular, the collective FCM becomes the collective scores matrix A (equation (1)), i.e., the starting point of the DEMATEL approach.

Finally, the results analysis can help managers adopt the proper corrective action or improve the proposed problem.

3. The Case Study

The examined case study analysis of clinical risk in drug administration was initially investigated by [56]. It is, in brief, used to show the efficacy of what has been proposed in [84]. Indeed, reducing the clinical risk reduces the likelihood of errors (prevention) or recovering and mitigating their effects (protection).

To continue the study with the simulation step for ranking and correcting critical situations, according to [61] and their assertion about the difficulty in defining concepts, so that the semantic and mathematical meaning is clear, the authors needed to modify the designed FCM for simulative purposes.

A new experts panel has been formed: two nurses, two physicians, and one pharmacist giving their own assessment on the involved relations referring to a fuzzy Likert scale with ten items, according to [85], to carry out and refine the collaborative relationships matrix for the considered problem.

The panel identified the main concepts connected to the clinical risk in drug administration and classified them into "Immediate Causes" and "Subordinate Causes." The first set causes immediate consequences on the system, while the second one remains dormant until a triggering event makes them manifest their potential and "Root Causes" or causes generating a reaction.

4. Results and Discussion

Concerning the previous analysis [56], a new panel of experts reduced by 40% the list of main concepts (from 30 to 17 concepts) due to the unfeasibility to give them a

Table 2: The FCM referred to the clinical risk due to the drug administration through the traditional approach.

		C1	C2	C3	C4	C5	C6	C7	C8	C9	C10	C11	C12	C13	C14	C15	C16	C17
Prescription errors	C1	0.00	0.53	0.66	0.69	0.51	0.00	0.00	0.00	0.00	0.96	0.00	0.00	0.00	0.00	0.00	0.00	0.49
Transcription errors	C2	0.23	0.00	0.71	0.55	0.60	0.00	0.00	0.00	0.00	0.28	0.00	0.24	0.00	0.00	0.00	0.00	0.87
Interpretation errors	C3	0.38	0.97	0.00	0.41	0.05	0.00	0.00	0.00	0.00	0.84	0.00	0.13	0.00	0.00	0.00	0.00	0.68
Preparation errors	C4	0.58	0.99	0.60	0.00	0.42	0.00	0.00	0.00	0.00	0.00	0.00	0.00	0.00	0.00	0.00	0.00	0.50
Drug management errors	C5	0.00	0.00	0.00	0.23	0.00	0.00	0.00	0.00	0.00	0.00	0.00	0.00	0.00	0.00	0.00	0.00	0.86
Experience	C6	−0.88	−0.52	−0.75	−0.12	−0.39	0.00	0.57	0.28	0.00	−0.46	−0.74	0.00	0.00	0.00	−0.75	0.00	0.00
Therapy knowledge	C7	−0.16	−0.65	−0.67	−0.20	0.00	0.00	0.00	0.00	0.00	−0.69	−0.17	0.00	0.00	0.00	0.00	0.00	0.00
Pathology knowledge	C8	−0.55	−0.15	−0.10	−0.14	0.00	0.00	0.51	0.00	0.00	0.00	0.00	0.00	0.00	0.00	0.00	0.00	0.00
Patient information	C9	−0.03	0.00	0.00	0.00	0.00	0.00	0.00	0.00	0.00	0.00	0.00	−0.57	0.00	−0.46	0.00	0.00	0.00
Mistaken procedures	C10	0.60	0.25	0.14	0.73	0.88	0.00	0.00	0.00	0.00	0.00	0.20	0.31	0.00	0.00	0.00	0.00	0.00
Lack of procedures	C11	0.89	0.14	0.65	0.12	0.35	0.00	0.00	0.00	0.00	0.56	0.00	0.04	0.45	0.80	0.00	0.00	0.00
Patient identification	C12	0.48	0.00	0.00	0.00	0.00	0.00	0.00	0.00	0.00	0.00	0.00	0.00	0.00	0.46	0.00	0.00	0.00
Work-related stress	C13	0.26	0.10	0.65	0.40	0.29	0.00	0.00	0.00	0.00	0.36	0.00	0.70	0.00	0.08	0.00	0.00	0.00
Binds occurrence	C14	0.00	0.00	0.00	0.00	0.00	0.00	0.00	0.00	0.00	0.17	0.00	0.00	0.63	0.00	0.00	0.00	0.00
External staff use	C15	0.00	0.00	0.00	0.00	0.00	0.00	0.00	0.00	0.00	0.65	0.00	0.00	0.48	0.82	0.00	0.00	0.00
Clinical documentation quality	C16	0.22	0.50	0.72	0.11	0.26	0.00	0.00	0.00	−0.10	0.52	0.00	0.05	0.00	0.11	0.00	0.00	0.00
Clinical risk	C17	0.00	0.00	0.00	0.00	0.00	0.00	0.00	0.00	0.00	0.00	0.00	0.00	0.00	0.00	0.00	0.00	0.00

mathematical meaning. The significance of the "Motivation" concept is unquestionable, but its mathematical formalization can be considered complex. Likewise, "Hurry," "Workload," and "Fatigue," representing the causes concerning work quality, cannot be easily quantified. Nevertheless, all of them can be clustered, considering their effects, in the unique "Stress" concept because, i.e., workload and fatigue are causes of work-related stress [86]. Then, studying the research approach in Figure 1, this section explores the improvement introduced by the DEMATEL equations into the FCM theory.

Table 2 provides the collective FCM realized considering the experts' FCMs on the discussed problem. Table 3 provides the collective FCM, once equations (2)–(4) have been used.

By comparing Tables 2 and 3, it is possible to identify five new relationships and the lack of 19 initial ones. The relationships among concepts increase their complexity, assuming more relevance than others, allowing algorithm convergence.

The comparison underlines one of the most relevant aspects, not judged directly by the experts. Four out of five added relationships refer to the concept C15 ("external staff use"). The experts negatively evaluate the presence of external staff because they do not know the internal system. Thus, seeking help from external personnel increases the probability of committing "mistaken procedures," producing "binds occurrence," and subsequently, increasing the level of "work-related stress." Subsequent to the application of equations from 1 to 4, what has been revealed is the influence of the "external staff use" concept on those concepts identified as "unsafe acts" with direct effects on the patient: "Prescription errors," "Interpretation errors," "Preparation errors," and "Drug management errors," despite their low relationship strength (about 0.11, weak strength). Considering those vanished, it is possible to mention, for example, the relationship of the concepts "Transcription errors" ($C2$) and "Interpretation errors" ($C3$) with "Patient identification" ($C12$). This means that the effects of "Transcription errors" and "Interpretation errors" on the "Patient identification" during the system evaluation are so scarce that they do not influence the system convergence.

By analyzing the relationships of the concepts, highlighting is possible as the concepts' centrality does not change considerably concerning the approach used, and

Table 3: The FCM referred to the clinical risk due to the drug administration through the revised approach.

		C1	C2	C3	C4	C5	C6	C7	C8	C9	C10	C11	C12	C13	C14	C15	C16	C17
Prescription errors	C1	0.00	0.24	0.23	0.27	0.23	0.00	0.00	0.00	0.00	0.28	0.00	0.00	0.00	0.00	0.00	0.00	0.26
Transcription errors	C2	0.12	0.00	0.21	0.19	0.20	0.00	0.00	0.00	0.00	0.13	0.00	0.00	0.00	0.00	0.00	0.00	0.30
Interpretation errors	C3	0.17	0.30	0.00	0.20	0.13	0.00	0.00	0.00	0.00	0.25	0.00	0.00	0.00	0.00	0.00	0.00	0.28
Preparation errors	C4	0.18	0.30	0.21	0.00	0.18	0.00	0.00	0.00	0.00	0.00	0.00	0.00	0.00	0.00	0.00	0.00	0.25
Drug management errors	C5	0.00	0.00	0.00	0.00	0.00	0.00	0.00	0.00	0.00	0.00	0.00	0.00	0.00	0.00	0.00	0.00	0.20
Experience	C6	−0.35	−0.31	−0.35	−0.22	−0.27	0.00	0.13	0.00	0.00	−0.32	−0.16	0.00	0.00	0.00	−0.16	0.00	−0.22
Therapy knowledge	C7	−0.12	−0.24	−0.23	−0.15	−0.11	0.00	0.00	0.00	0.00	−0.23	0.00	0.00	0.00	0.00	0.00	0.00	−0.13
Pathology knowledge	C8	−0.15	0.00	0.00	0.00	0.00	0.00	0.11	0.00	0.00	0.00	0.00	0.00	0.00	0.00	0.00	0.00	0.00
Patient information	C9	0.00	0.00	0.00	0.00	0.00	0.00	0.00	0.00	0.00	0.00	0.00	−0.12	0.00	−0.11	0.00	0.00	0.00
Mistaken procedures	C10	0.19	0.15	0.11	0.23	0.26	0.00	0.00	0.00	0.00	0.00	0.00	0.00	0.00	0.00	0.00	0.00	0.14
Lack of procedures	C11	0.28	0.16	0.25	0.16	0.20	0.00	0.00	0.00	0.00	0.24	0.00	0.00	0.12	0.18	0.00	0.00	0.15
Patient identification	C12	0.11	0.00	0.00	0.00	0.00	0.00	0.00	0.00	0.00	0.00	0.00	0.00	0.00	0.00	0.00	0.00	0.00
Work-related stress	C13	0.13	0.00	0.20	0.16	0.13	0.00	0.00	0.00	0.00	0.15	0.00	0.17	0.00	0.00	0.00	0.00	0.10
Binds occurrence	C14	0.00	0.00	0.00	0.00	0.00	0.00	0.00	0.00	0.00	0.00	0.00	0.00	0.13	0.00	0.00	0.00	0.00
External staff use	C15	0.11	0.00	0.11	0.10	0.12	0.00	0.00	0.00	0.00	0.22	0.00	0.00	0.14	0.22	0.00	0.00	0.00
Clinical documentation quality	C16	0.12	0.20	0.22	0.12	0.14	0.00	0.00	0.00	0.00	0.19	0.00	0.00	0.00	0.00	0.00	0.00	0.12
Clinical risk	C17	0.00	0.00	0.00	0.00	0.00	0.00	0.00	0.00	0.00	0.00	0.00	0.00	0.00	0.00	0.00	0.00	0.00

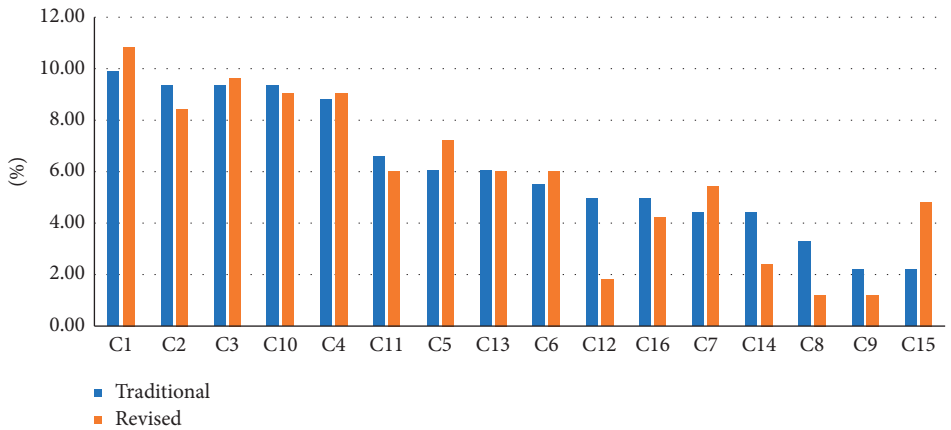

Figure 2: Comparison of the traditional and revised FCM approaches in terms of centrality.

Figure 2 shows this consideration. Indeed, it is shown that the percentage of influencing and influenced concepts (by each other) does not change. The unique variations are connected to the concepts that have shown a relationship change in the previous analysis. Thus, the experts' analysis of these changes could be an essential step in the FCM refinement phase.

Three critical scenarios have been defined mathematically in the simulation phase, imposing the value 1 for those concepts having negative effects on the system and 0 for

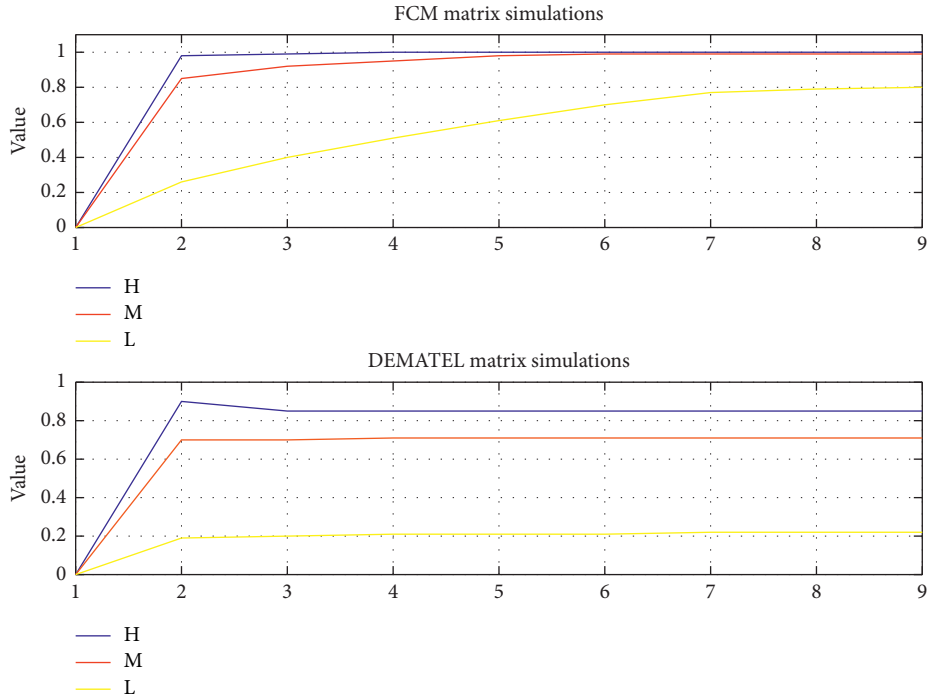

Figure 3: Comparison of different scenarios outcomes using the traditional and revised approach.

Table 4: The array to be considered as the input for calculating the criticality value.

C1	C2	C3	C4	C5	C6	C7	C8	C9	C10	C11	C12	C13	C14	C15	C16	C17
H	—	M	—	—	VL	VL	VL	VL	—	M	VL	VH	VH	—	VL	—

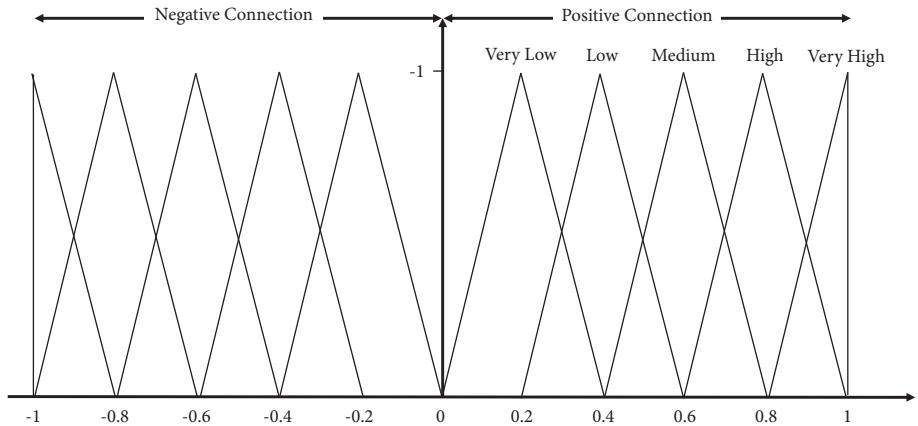

Figure 4: The adopted membership function for the fuzzy weights' definition.

those with positive effects to realize an extremely critical scenario. Then, the opposite represents a low critical scenario. The value of 0.5 has been given to all concepts to realize a medium-critical scenario (Figure 3).

This scenario highlights that the system outcomes, considering the same inputs but using different approaches, are not easily distinguishable. This is the validation of the problem mentioned in the introduction section. Indeed, the traditional FCM does not distinguish all the defined scenarios because the convergence value is always the same. Besides, the algorithm convergence time is variable according to specific cases. Contrariwise, the hybrid FCM allows distinguishing the different scenarios to make correct decisions.

Moreover, to test other discrepancies between both maps and understand the efficacy of the revised approach, several

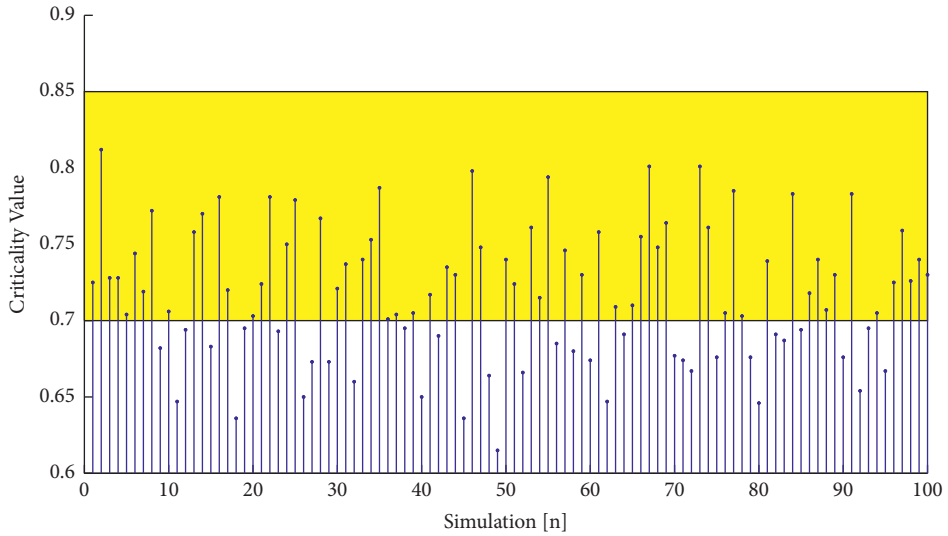

Figure 5: Criticality values for the considered scenario obtained by the revised FCM approach.

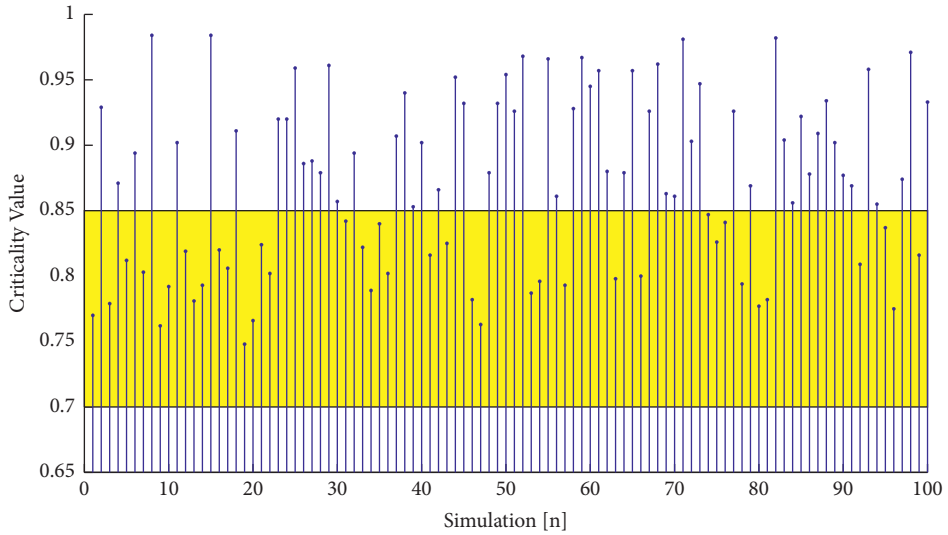

Figure 6: Criticality values for the considered scenario obtained by the traditional FCM approach.

critical situations have been provided with the experts' help, considering the concepts involved and giving a final value concerning the scenario's criticality.

For example, an identified scenario with a high criticality mark has referred to an actual event that happened to one of the experts.

"At about 3.00 am, an unknown patient with extreme difficulties in speaking arrived at the emergency department of the hospital at a very critical moment, since a terrible car crash had occurred on the highway, and many injured people had arrived at the same time. A young internist (who had started his activity only three weeks before) was delegated to help the patient. Due to misunderstanding what the patient was communicating, the internist misinterpreted the patient's symptoms and diagnosed a nonspecific upper airway respiratory infection. As a result, according to the guidelines, an oral antihistamine and nasal decongestant and a counter cough suppressant were prescribed. No antibiotics were prescribed to the patient. The patient improved slightly over the next couple of days but after 10 days returned with overall worsening of systems and with an additional symptom, specifically, a very high fever."

Table 4 provides the array identifying the scenario described, according to the Likert scale developed by the experts (Figure 4).

Because the mean value of each fuzzy label has been used to compute the numerical value of the simulation array, a set of one hundred arrays has been tested to evaluate the result. Figure 5 shows the criticality value of the revised FCM approach for the scenario explained, where the yellow area identifies the expected values for the specific example. Analyzing the available data, experts defined the criticality value as medium high according to the real situation. Consequently, the black points in the yellow area represent

the whole simulation responding to reality. Results are characterised by an accuracy equal to 65% by referring to the hybrid approach DEMATEL-FCM.

Conversely, Figure 6 shows the results of the traditional FCM, underlining an overestimation of the scenario. Good results are only 38% of the identified set.

By analyzing Figure 5, the experts agreed on the suitability of the outcome obtained with the DEMATEL matrix to simulate the system, since the standard FCM outputs do not highlight different situations.

5. Conclusion

This study presents an increasing interest in the human factor for the decision-making process, which raises attention to understanding human reasoning and the individual perception of a problem. However, knowledge transfer among persons can present distortions and difficulty in finding a consensus and interpretating the results. FCMs have been demonstrated as the best tool for grouping experts' knowledge, but the lack of a standardized FCM theoretical model pinpoints the problem of comparative analysis in problem-solving. Using FCMs learning algorithms, researchers have developed several methods. However, even if these approaches bring good results considering the system control, they show deficiencies if reference is made to the experts' opinion, which is sometimes neglected.

In terms of novelty, this study examines in depth the possibility of improving FCMs' outcomes by using the DEMATEL approach, and results highlight how the traditional FCM approach does not allow distinguishing the whole number of defined scenarios, in contrast to the hybrid one allowing users to make correct decisions. The combined use of these two approaches integrates the capability of FCMs in grouping experts' knowledge and DEMATEL's, aiming to refine the strength of concepts' connections. The experts' opinion is the core of the approach, and it is fundamental in each activity of the hybrid method. In light of the advantages of combining the two techniques, work is already underway to evaluate the methodology for an industrial case. Specifically, the approach defined and discussed in this study will be integrated with the decision-making environment in question, taking into account the technological innovations introduced by Industry 4.0, which are present in the field.

The considerations made by [84] have been consolidated by analyzing in depth the mathematical theory beyond both methods, and at the same time, their explanatory example has been structured and analyzed extensively considering a new panel of experts. Thus, the proposed approach, obtained by introducing specific DEMATEL considerations and equations, shows its great opportunities in reducing the results' interpretation problem, which is typical of the FCM theory. This allows decision-makers to distinguish and analyze the system outcomes more meaningfully, so that it is possible to discriminate, with no doubt, different situations without changing the FCM procedure radically.

Data Availability

The numerical matrix used to support the findings of this study are included within the article.

Conflicts of Interest

The authors declare that they have no conflicts of interest.

References

[1] F. Rosin, P. Forget, S. Lamouri, and R. Pellerin, "Enhancing the decision-making process through industry 4.0 technologies," *Sustainability*, vol. 14, p. 461, 2022.

[2] T. Poleto, V. D. H. de Carvalho, and A. P. C. S. Costa, "The roles of big data in the decision-support process: an empirical investigation," in *Decision Support Systems V – Big Data Analytics for Decision Making*, pp. 10–21, Springer, Berlin, Germany, 2015.

[3] J. Yan, Y. Meng, L. Lu, and L. Li, "Industrial Big data in an industry 4.0 environment: challenges, schemes, and applications for predictive maintenance," *IEEE Access*, vol. 5, pp. 23484–23491, 2017.

[4] J. S. Bedolla, G. D'Antonio, and P. Chiabert, "A novel approach for teaching IT tools within learning factories," *Procedia Manufacturing*, vol. 9, pp. 175–181, 2017.

[5] D. C. J. W. Wise, M. Logapriya, R. Padmavathy, D. C. J. Josephine, and P. B. Shamini, "Health decision support system based on machine learning via big data," in *Proceedings of the 2021 5th International Conference on Trends in Electronics and Informatics (ICOEI)*, pp. 1661–1666, Tirunelveli, India, June 2021.

[6] A. S. Varde, M. J. Pawlish, K. Hammond, J. Tancer, and S. Chandra, "Cloud technology for big data management and mining," Techical Report, Big Data Alliance (NJDBA) Symposium, Piscataway, NJ, USA, 2014.

[7] L. Jun, "Cloud computing based solution to decision making," *Procedia Engineering*, vol. 15, pp. 1822–1826, 2011.

[8] N. Tapus and M. A. Manolache, "Integrated decision making using the Blockchain," *Procedia Computer Science*, vol. 162, pp. 587–595, 2019.

[9] K. Zheng, Z. Zhang, Y. Chen, and J. Wu, "Blockchain adoption for information sharing: risk decision-making in spacecraft supply chain," *Enterprise Information Systems*, vol. 15, no. 8, pp. 1070–1091, 2021.

[10] R. Venkata Rao, "Decision making in the manufacturing environment using an improved PROMETHEE method," *International Journal of Production Research*, vol. 48, no. 16, pp. 4665–4682, 2010.

[11] U. Özesmi, "Ecological models based on people's knowledge: a multi-step fuzzy cognitive mapping approach," *Ecological Modelling*, vol. 176, no. 1–2, pp. 43–64, 2004.

[12] S. Elkosantini and D. Gien, "Integration of human behavioural aspects in a dynamic model for a manufacturing system," *International Journal of Production Research*, vol. 47, no. 10, pp. 2601–2623, 2009.

[13] R. E. Lenski, "Experimental evolution of bacteria across 60,000 generations, and what it might mean for economics and human decision-making," *Journal of Bioeconomics*, vol. 20, no. 1, pp. 107–124, 2018.

[14] C. E. Phelps, D. N. Lakdawalla, A. Basu, M. F. Drummond, A. Towse, and P. M. Danzon, "Approaches to aggregation and decision making—a health economics approach: an ISPOR

special task force report [5]," *Value in Health*, vol. 21, no. 2, pp. 146–154, 2018.
[15] J. Avorn, "The psychology of clinical decision making — implications for medication use," *New England Journal of Medicine*, vol. 378, no. 8, pp. 689–691, 2018.
[16] W. Ling, "Consumers' food safety risk perception of and consumption decision-making behaviour," *NeuroQuantology*, vol. 16, no. 6, 2018.
[17] H. g. Peng, J. q. Wang, and P. f. Cheng, "A linguistic intuitionistic multi-criteria decision-making method based on the Frank Heronian mean operator and its application in evaluating coal mine safety," *International Journal of Machine Learning and Cybernetics*, vol. 9, no. 6, pp. 1053–1068, 2018.
[18] M. Hariga, S. Babekian, and Z. Bahroun, "Operational and environmental decisions for a two-stage supply chain under vendor managed consignment inventory partnership," *International Journal of Production Research*, vol. 57, no. 11, pp. 3642–3662, 2018.
[19] R. V. Rao, "Flexible manufacturing system selection using a combinatorial mathematics-based decision-making method," *International Journal of Production Research*, vol. 47, no. 24, pp. 6981–6998, 2009.
[20] K. F. Yuan, S. H. Ma, B. He, and Y. Gao, "Inventory decision-making models for a closed-loop supply chain system with different decision-making structures," *International Journal of Production Research*, vol. 53, no. 1, pp. 183–219, 2015.
[21] K. Slimani, C. F. Da Silva, L. Médini, and P. Ghodous, "Conflict mitigation in collaborative design," *International Journal of Production Research*, vol. 44, no. 9, pp. 1681–1702, 2006.
[22] T. L. Saaty, "Decision making with the analytic hierarchy process," *International Journal of Services Sciences*, vol. 1, no. 1, p. 83, 2008.
[23] C.-L. Yoon, "Methods for multiple attribute decision making," in *Multiple Attribute Decision Making: Methods and Applications A State-Of-The-Art Survey*Springer Berlin Heidelberg, Berlin, Heidelberg, 1981.
[24] M. Kajanus, P. Leskinen, M. Kurttila, and J. Kangas, "Making use of MCDS methods in SWOT analysis—lessons learnt in strategic natural resources management," *Forest Policy and Economics*, vol. 20, pp. 1–9, 2012.
[25] L. A. Chang and S. S. L. Zadeh, "On fuzzy mapping and control," *Fuzzy Sets, Fuzzy Logic, and Fuzzy Systems*, World Scientific, Singapore, 1996.
[26] A. H. Azadnia, M. Z. M. Saman, and K. Y. Wong, "Sustainable supplier selection and order lot-sizing: an integrated multi-objective decision-making process," *International Journal of Production Research*, vol. 53, no. 2, pp. 383–408, 2015.
[27] M. Saidi Mehrabad, "Provident decision making by considering dynamic and fuzzy environment for FMS evaluation," *International Journal of Production Research*, vol. 48, no. 15, pp. 4555–4584, 2010.
[28] Q. Liu, M. Dong, F. F. Chen, W. Lv, and C. Ye, "Single-machine-based joint optimization of predictive maintenance planning and production scheduling," *Robotics and Computer-Integrated Manufacturing*, vol. 55, pp. 173–182, 2019.
[29] Y.-T. Chen, "Applying the DEMATEL approach to identify the focus of library service quality: a case study of a Taiwanese academic library," *The Electronic Library*, vol. 34, no. 2, pp. 315–331, 2016.
[30] G. A. Keskin, "Using integrated fuzzy dematel and fuzzy c: means algorithm for supplier evaluation and selection," *International Journal of Production Research*, vol. 53, no. 12, pp. 3586–3602, 2015.
[31] F.-H. Chen, "Application of a hybrid dynamic MCDM to explore the key factors for the internal control of procurement circulation," *International Journal of Production Research*, vol. 53, no. 10, pp. 2951–2969, 2015.
[32] S. N. Seleem, E.-A. Attia, and A. El-Assal, "Managing performance improvement initiatives using DEMA^{TEL} method with application case study," *Production Planning & Control*, vol. 27, no. 7–8, pp. 637–649, 2016.
[33] C.-H. W. Wu and H. S. Wu, "A novel framework to evaluate programmable logic controllers: a fuzzy MCDM perspective," *Journal of Intelligent Manufacturing*, vol. 27, no. 2, pp. 315–324, 2016.
[34] S. Tadić, S. Zečević, and M. Krstić, "A novel hybrid MCDM model based on fuzzy DEMATEL, fuzzy ANP and fuzzy VIKOR for city logistics concept selection," *Expert Systems with Applications*, vol. 41, no. 18, pp. 8112–8128, 2014.
[35] S.-M. Wu, H.-C. Liu, and L. E. Wang, "Hesitant fuzzy integrated MCDM approach for quality function deployment: a case study in electric vehicle," *International Journal of Production Research*, vol. 55, no. 15, pp. 4436–4449, 2017.
[36] J. Huang, X.-Y. You, H.-C. Liu, and S. L. Si, "New approach for quality function deployment based on proportional hesitant fuzzy linguistic term sets and prospect theory," *International Journal of Production Research*, vol. 57, no. 5, pp. 1283–1299, 2018.
[37] J. Kaur, R. Sidhu, A. Awasthi, S. Chauhan, and S. Goyal, "A DEMATEL based approach for investigating barriers in green supply chain management in Canadian manufacturing firms," *International Journal of Production Research*, vol. 56, no. 1–2, pp. 312–332, 2018.
[38] L. Abdullah, Z. Ong, and N. Rahim, "An intuitionistic fuzzy decision-making for developing cause and effect criteria of subcontractors selection," *International Journal of Computational Intelligence Systems*, vol. 14, no. 1, pp. 991–1002, 2021.
[39] B. Kosko, "Fuzzy cognitive maps," *International Journal of Man-Machine Studies*, vol. 24, no. 1, pp. 65–75, 1986.
[40] B. Zheng, Y.-F. Li, J. Guo, and H. Z. Huang, "Aeroengine performance prediction based on double-extremum learning particle swarm optimization," *International Journal of Turbo and Jet Engines*, vol. 37, no. 1, pp. 17–29, 2020.
[41] M. W. L. Moreira, J. J. P. C. Rodrigues, V. Korotaev, J. Al-Muhtadi, and N. Kumar, "A comprehensive review on smart decision support systems for health care," *IEEE Systems Journal*, vol. 13, no. 3, pp. 3536–3545, 2019.
[42] W.-P. Cheah, K.-Y. Kim, H.-J. Yang, S.-H. Kim, and J. S. Kim, "Fuzzy cognitive map and bayesian belief network for causal knowledge engineering: a comparative study," *The KIPS Transactions:PartB*, vol. 15B, no. 2, pp. 147–158, 2008.
[43] Y. Y. Wee, W. P. Cheah, S. C. Tan, and K. Wee, "An evaluation of the role of fuzzy cognitive maps and Bayesian belief networks in the development of causal knowledge systems," *Journal of Intelligent and Fuzzy Systems*, vol. 37, no. 2, pp. 1905–1920, 2019.
[44] C. D. Styliose and P. P. Groumpos, "Fuzzy Cognitive Maps in modeling supervisory control systems," *Journal of Intelligent and Fuzzy Systems*, vol. 8, no. 1, pp. 83–98, 2000.
[45] A. Jamshidi, D. Ait-kadi, A. Ruiz, and M. L. Rebaiaia, "Dynamic risk assessment of complex systems using FCM," *International Journal of Production Research*, vol. 56, no. 3, pp. 1070–1088, 2018.
[46] C. D. Stylios, E. Bourgani, and V. C. Georgopoulos, O. Kosheleva, S. P. Shary, G. Xiang, e R. Zapatrin, and A. c. di, Impact and applications of fuzzy cognitive map methodologies," in *Beyond Traditional Probabilistic Data Processing*

*Techniques: Interval, Fuzzy Etc. Methods and Their Applications*Springer, Berlin, Germany, 2020.

[47] M. Bertolini, "Assessment of human reliability factors: a fuzzy cognitive maps approach," *International Journal of Industrial Ergonomics*, vol. 37, no. 5, pp. 405–413, 2007.

[48] C. D. Stylios and V. C. Georgopoulos, "Genetic algorithm enhanced fuzzy cognitive maps for medical diagnosis," in *Proceedings of the 2008 IEEE International Conference on Fuzzy Systems*, pp. 2123–2128, IEEE World Congress on Computational Intelligence), Hong Kong, China, June 2008.

[49] M. Bevilacqua, F. E. Ciarapica, and G. Mazzuto, "Analysis of injury events with fuzzy cognitive maps," *Journal of Loss Prevention in the Process Industries*, vol. 25, no. 4, pp. 677–685, 2012.

[50] M. Bevilacqua, F. E. Ciarapica, and G. Mazzuto, "A fuzzy cognitive maps tool for developing a RBI&M model," *Quality and Reliability Engineering International*, vol. 32, no. 2, pp. 373–390, 2016.

[51] K. Poczęta, Ł. Kubuś, A. Yastrebov, and E. I. Papageorgiou, "Learning fuzzy cognitive maps using evolutionary algorithm based on system performance indicators," in *Automation 2017*Springer, Berlin, Germany, 2017.

[52] S. H. Al-subhi, E. I. Papageorgiou, P. P. Pérez, G. S. S. Mahdi, and e L. A. Acuña, "Triangular neutrosophic cognitive map for multistage sequential decision-making problems," *International Journal of Fuzzy Systems*, vol. 23, no. 3, 2021.

[53] A. Amirkhani, E. I. Papageorgiou, A. Mohseni, and M. R. Mosavi, "A review of fuzzy cognitive maps in medicine: taxonomy, methods, and applications," *Computer Methods and Programs in Biomedicine*, vol. 142, pp. 129–145, 2017.

[54] E. Smith, "A prototype for assessing information technology risks in health care," *Computers & Security*, vol. 21, no. 3, pp. 266–284, 2002.

[55] T. Z. Tan, C. Quek, G. S. Ng, and E. Y. K. Ng, "A novel cognitive interpretation of breast cancer thermography with complementary learning fuzzy neural memory structure," *Expert Systems with Applications*, vol. 33, no. 3, pp. 652–666, 2007.

[56] M. Bevilacqua, F. E. Ciarapica, and G. Mazzuto, "Fuzzy cognitive maps for adverse drug event risk management," *Safety Science*, vol. 102, pp. 194–210, 2018.

[57] A. Baykasoglu and Z. D. U. Durmusoglu, "A hybrid MCDM for private primary school assessment using DEMATEL based on ANP and fuzzy cognitive map," *International Journal of Computational Intelligence Systems*, vol. 7, no. 4, p. 615, 2014.

[58] N. Abramova, Z. Avdeeva, S. Kovriga, and D. Makarenko, "Subject-formal methods based on cognitive maps and the problem of risk due to the human factor," *Cognitive Maps*, 2010.

[59] M. S. Khan, "Group decision support using fuzzy cognitive maps for causal reasoning," *Group Decision and Negotiation*, vol. 13, no. 5, pp. 463–480, 2004.

[60] C. L. Ishizaka, "A scenario-based modeling method for controlling ECM performance," *Expert Systems with Applications*, vol. 97, pp. 253–265, 2018.

[61] N. Abramova, Z. Avdeeva, and A. Fedotov, "An approach to systematization of types of formal cognitive maps," *IFAC Proceedings Volumes*, vol. 44, no. 1, pp. 14246–14252, 2011.

[62] R. Axelrod, *Structure of Decision: The Cognitive Maps of Political Elites*, Princeton University Press, Princeton, NJ, USA, 2015.

[63] M. F. Hatwágner, E. Yesil, M. F. Dodurka, E. Papageorgiou, L. Urbas, and L. T. Koczy, "Two-Stage learning based fuzzy cognitive maps reduction approach," *IEEE Transactions on Fuzzy Systems*, vol. 26, no. 5, pp. 2938–2952, 2018.

[64] E. I. Papageorgiou, C. D. Stylios, and P. Groumpos, "Active Hebbian learning algorithm to train fuzzy cognitive maps," *International Journal of Approximate Reasoning*, vol. 37, no. 3, pp. 219–249, 2004.

[65] B. Kosko, "Fuzzy systems as universal approximators," *IEEE Transactions on Computers*, vol. 43, no. 11, pp. 1329–1333, 1994.

[66] S. Lee, S.-U. Cheon, and J. Yang, "Development of a fuzzy rule-based decision-making system for evaluating the lifetime of a rubber fender: fuzzy rule-based decision-making system," *Quality and Reliability Engineering International*, vol. 31, no. 5, pp. 811–828, 2015.

[67] Z. Wang, J. Wu, X. Liu, and H. Garg, "New framework for FCMs using dual hesitant fuzzy sets with an analysis of risk factors in emergency event," *International Journal of Computational Intelligence Systems*, vol. 14, no. 1, p. 67, 2020.

[68] C. D. Stylios, "Medical decision support systems based on soft computing techniques," *IFAC Proceedings Volumes*, vol. 44, no. 1, pp. 14115–14120, 2011.

[69] V. Kreinovich and C. D. Stylios, "Why fuzzy cognitive maps are efficient," *International Journal of Computers, Communications & Control*, vol. 10, pp. 65–6, 2015.

[70] D. Ivanov, S. Sethi, A. Dolgui, and B. Sokolov, "A survey on control theory applications to operational systems, supply chain management, and Industry 4.0," *Annual Reviews in Control*, vol. 46, pp. 134–147, 2018.

[71] Q. Zhu, J. Sarkis, and Y. Geng, "Barriers to environmentally-friendly clothing production among Chinese apparel companies," *Asian Business & Management*, vol. 10, no. 3, pp. 425–452, 2011.

[72] C. W. Li and G.-H. Tzeng, "Identification of a threshold value for the DEMATEL method using the maximum mean de-entropy algorithm to find critical services provided by a semiconductor intellectual property mall," *Expert Systems with Applications*, vol. 36, no. 6, pp. 9891–9898, 2009.

[73] V. C. Georgopoulose and C. D. Stylios, "Fuzzy cognitive maps for decision making in triage of non-critical elderly patients," in *Proceedings of the 2017 International Conference on Intelligent Informatics and Biomedical Sciences (ICIIBMS)*, pp. 225–228, Okinawa, Japan, November 2017.

[74] L. Concepción, G. Nápoles, I. Grau, K. Vanhoof, and R. Bello, C. Berger-Vachon, A. M. Gil Lafuente, J. Kacprzyk et al., Retracted chapter: towards the convergence in fuzzy cognitive maps based decision-making models," in *Complex Systems: Solutions and Challenges in Economics, Management and Engineering: Dedicated to Professor Jaime Gil Aluja*Springer International Publishing, Berlin, Germany, 2018.

[75] J. Fang, "Sums of L-fuzzy topological spaces," *Fuzzy Sets and Systems*, vol. 157, no. 6, pp. 739–754, 2006.

[76] A. Abraham, "Neuro fuzzy systems: state-of-the-art modeling techniques," in *Connectionist Models of Neurons, Learning Processes, and Artificial Intelligence*Springer, Berlin, Germany, 2001.

[77] W. B. Vasantha Kandasamye and F. Smarandache, *Fuzzy Cognitive Maps and Neutrosophic Cognitive Maps*, Infinite Study, West Conshohocken, PA, USA, 2003.

[78] S. Bueno, "Benchmarking main activation functions in fuzzy cognitive maps," *Expert Systems with Applications*, vol. 36, no. 3, pp. 5221–5229, 2009.

[79] D. G. Osei-Bryson, "Using fuzzy cognitive maps to assess MIS organizational change impact," in *Proceedings of the 38th*

Annual Hawaii International Conference on System Sciences, p. 263c, Big Island, HI, USA, January 2005.

[80] C. Stylios, "Modeling complex systems using fuzzy cognitive maps," *IEEE Transactions on Systems, Man, and Cybernetics - Part A: Systems and Humans*, vol. 34, no. 1, pp. 155–162, 2004.

[81] A. J. Miller, "Review of structure of decision: the cognitive maps of political elites, ; perception and misperception in international politics," *Can. J. Polit. Sci. Rev. Can. Sci. Polit.*vol. 12, no. 1, pp. 177–179, 1979.

[82] G.-H. Tzeng, W.-H. Chen, R. Yu, and M. L. Shih, "Fuzzy decision maps: a generalization of the dematel methods," *Soft Computing*, vol. 14, no. 11, pp. 1141–1150, 2010.

[83] A. Azadeh, M. Zarrin, M. Abdollahi, S. Noury, and S. Farahmand, "Leanness assessment and optimization by fuzzy cognitive map and multivariate analysis," *Expert Systems with Applications*, vol. 42, no. 15-16, pp. 6050–6064, 2015.

[84] G. Mazzuto, C. Stylios, and M. Bevilacqua, "Hybrid decision support system based on dematel and fuzzy cognitive maps," *IFAC-PapersOnLine*, vol. 51, no. 11, pp. 1636–1642, 2018.

[85] C. Stylios and V. C. Georgopoulos, "Develop fuzzy cognitive maps based on recorded data and information," in *Proceedings of the 2015 IEEE International Conference on Fuzzy Systems (FUZZ-IEEE)*, pp. 1–6, Istanbul, Turkey, August 2015.

[86] W. Rohmert and W. Laurig, "Work measurement psychological and physiological techniques for assessing operator and work load," *International Journal of Production Research*, vol. 9, no. 1, pp. 157–168, 1971.

Hindawi
Mathematical Problems in Engineering
Volume 2021, Article ID 4900748, 9 pages
https://doi.org/10.1155/2021/4900748

Research Article

Development of the Modularity Measure for Assembly Process Structures

Vladimir Modrak and Zuzana Soltysova

Department of Industrial Engineering, Faculty of Manufacturing Technologies, Technical University of Kosice, Presov 08001, Slovakia

Correspondence should be addressed to Vladimir Modrak; vladimir.modrak@tuke.sk

Received 22 April 2021; Revised 3 September 2021; Accepted 11 November 2021; Published 8 December 2021

Academic Editor: Mohammad Yaghoub Abdollahzadeh Jamalabadi

This study is aimed at exploring the problem of quantification of process modularity degree. Modularity as a system design principle is apprehended here as the extent to which processes can be decomposed into modules to be executed in parallel and/or in series. For this purpose, a new method is proposed to measure relative modularity of different assembly process structures. This method is compared with other relative modularity measures, namely singular value modularity index, degree of process module, and process module independence, in order to verify its effectiveness. For this purpose, selected representative types of assembly process structures are used. This testing proved that the proposed relative modularity indicator for manufacturing and/or assembly process structures reflects the expected system property in adequate way.

1. Introduction

In wider sense, system modularity can be characterized as the degree to which a system is made up of relatively independent parts, while each part is typically carrying an isolated set of functionality [1]. System modularity concept, similar to system complexity, is an important element of general systems theory, since one can apply it to different kinds of systems such as technical, social, or biological systems, respectively [2, 3]. Sako and Murray [4] identify three arenas of modularity, which are modularity-in-design (MID), modularity-in-use (MIU), and modularity-in-production (MIP). Manufacturing assembly processes that are of interest in this paper belongs to the third domain, where consequences of the MID have to be adapted to the factory floor. As MIP can be viewed from different aspects, here it is useful to introduce a working classification of system modularity as shown in Figure 1.

In line with this classification, process structure modularity is the subject of this paper. As known, final assembly lines especially in mass customization environment are faced with the greatest burden caused by product variability [5, 6]. Therefore, product components or modules under such conditions need to be assembled using work stations (process modules) with simple series of tasks instead of work stations integrating higher number of input components into one unit.

According to Ulrich [7], a product modular architecture is based on one-to-one mapping functional requirements to the design parameters. Such architecture follows the first axiom in the Axiomatic Design theory defined by Suh [8] specifying that each system function or functional requirement has to be satisfied by an independent design parameter. Subsequently, product design parameters are transformed into the production work order document determining the sequence of operations. An important feature of the system modularity is that complexity of technical systems can be effectively managed through their modular design [9–12]. Tate [13] categorized modularity from the Axiomatic Design theory perspective into three types: resource, operational, and interfacial. According to him, the resource modularity can be defined as "ease of manufacturing." This definition at least shows a certain connection between process modularity and complexity in

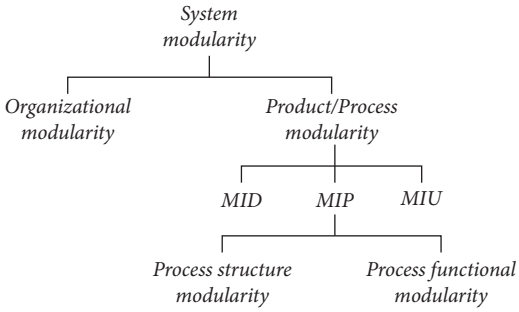

Figure 1: System modularity classification.

system design [14]. According to Mehrsai et al. [15], extension of modularity into processes and resources allows to generate alternative structures of organizations or supply chain networks by splitting their performances into modules and adjusting them as required. Mentioned works clearly show that product modularity and process modularity become increasingly important over the last decades, especially due to diffusion of mass customization. In this nexus, modularity measurement plays a vital role in product and process design.

2. Literature Review and Related Works

The vast majority of studies on modularity deal with product and organizational modularity (see, e.g., [16–19]). One of them has been offered by Ulrich [20] who provided a comprehensive overview of product modular design approaches in engineering. But there is considerable lack of studies on manufacturing process modularity. However, a few of them brought a partial insight into modularity in production. For instance, Starr [21] in his pioneering work on mass customization depicted that modular production is a very useful concept utilizing standardized and interchangeable parts and allowing to produce the so-called combinatorial outputs. Later, he emphasized how mass customization is related to modularity issues [22]. Calcagno [23] argued that there is a need to measure a degree at which a manufacturing system is modular. According to him, formalized concepts of process modularity should attract researchers' more and more attentions. In this context, one can identify research studies focused on the operational/functional process modularity metrics [24–28]. Although, there is some relation between functional modularity and structural modularity [29], they differ in their nature. It is because that operational modularity measures aim to improve performance characteristics [30], and the goal of process structure modularity is the ease of changing from one product variant to another through layout design optimization [31].

Process modularity for mass customization was defined by Abdelkafi [32] as "the degree to which the production process on the shop floor can be broken down into independent subprocesses called process modules." This definition fully corresponds with a view on process structure modularity used in this paper. Langlois [33] identifies modularity as a very general set of principles for managing complexity. This statement is in line with the approach taken for development of the proposed indicator in this work. Other authors [34, 35] in their research discussed the possible relationship between product and process modularity. Nevertheless, one can claim that product modularity and process modularity differ in several respects. One of them is that expectations regarding process modularity are significantly different depending on preferred production strategy, while product modularity is the inherent part of product design. Another important issue regarding system modularity is its optimal level. As it is known, optimal modularity does not equate to maximal modularity [36–39]. Efatmaneshnik and Ryan [40] proved that optimal modularity can be achieved through balanced modularization by using a concept of structural symmetry in the distribution of the module sizes. The presented work was also inspired by methods focused on optimal assembly sequence generation and multistation assembly sequence planning [41–44]. The most relevant works to this research include works [32, 45, 46], which will be analyzed in detail in a separate section of this paper.

3. Methodological Framework

First, have a look at the simplest structural model of manufacturing assembly process (MAP). As shown in Figure 2, its structure consists of the three obligatory element types which are input elements—at least two and more; one and more process operations; and minimum one output element.

As the topology of assembly process structures varies case by case and depends upon specific factors, it seems to be useful to create an initial classification framework of MAPs in order to model real processes more adequately (see Figure 3).

For this purpose, assembly process structures can be divided into the following classes:

(1) Single layer multiproduct (SLMP) assembly network: this class of MAP structures includes all single-step assembly networks with different numbers of input components, parallel single assembly operations, and output components. Selected alternative MAP structures, when the number of input components equals four and the number of output components equals six, are shown in Figure 3. Modularization followed here is based only on vertical fragmentation of the network modules into submodules.

(2) Multilayer single-product (MLSP) assembly network: all possible alternative MAP structures when the number of input components equals four and the number of output components equals one are shown in Figure 3. These networks are modelled as single-rooted tree graphs. The numbers of all possible process structures when a number of input elements are given can be exactly determined through the integer sequence A000669 [47] by using the formula:

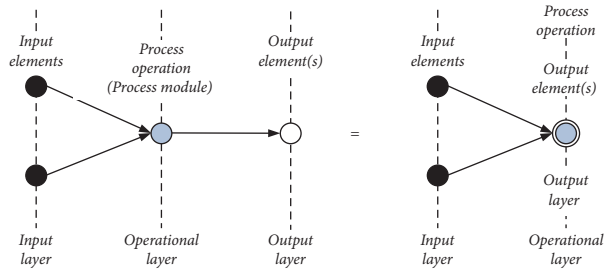

Figure 2: The generic model of manufacturing assembly process.

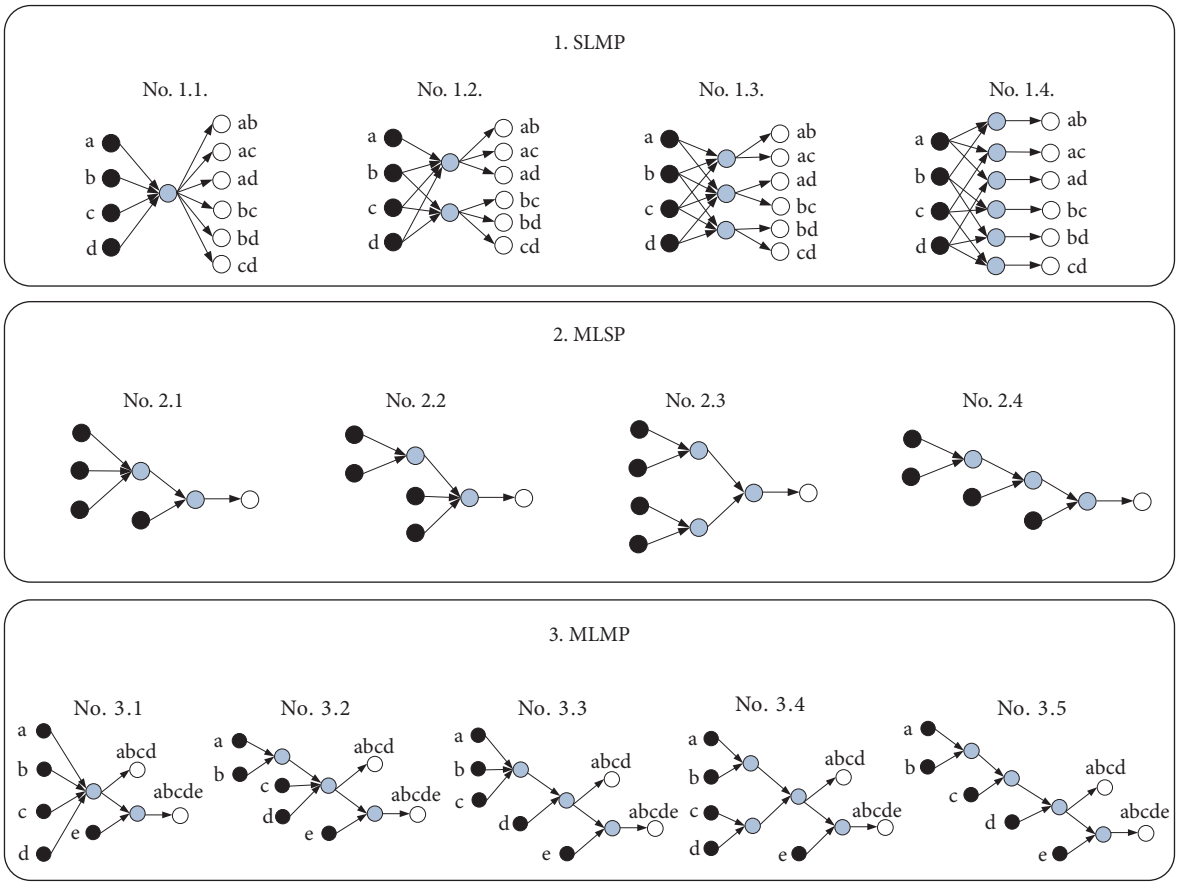

Figure 3: The assembly process networks classification. (a) SLMP. (b) MLSP. (c) MLMP.

$$a(i) = A000669(i) - 1. \quad (1)$$

(3) Multilayer multiproduct (MLMP) assembly network: this class of MAP structures is important especially in terms of mass customization. Examples of such process alternative structures are shown in Figure 3.

Another purpose of this classification is to provide models of MAP structures with distinct assembly attributes that can influence computation of relative modularity in different ways.

4. Description of the Modularity Measures

4.1. Existing Modularity Measures. In the first part of this section, the following existing modularity indicators will be described: singular value modularity index (SMI), degree of process module (M(P)), and process module independence (PMI).

4.1.1. Singular Value Modularity Index. This index called singular value modularity index (SMI) quantifies the degree of modularity of a product on its internal structure, and it

measures the average weighted decay rate of sorted singular values in the system. The following equation for its enumeration has been proposed [45]:

$$\mathrm{SMI}\left(\Sigma_{\mathrm{DSM}}\right) = 1 - \frac{1}{N \cdot \sigma_1} \sum_{i=1}^{N-1} \sigma_i \left(\sigma_i - \sigma_{i+1}\right), \tag{2}$$

where N is the number of components of the system and σ_i represents singular values, $i = 1,2, \ldots, N-1$, ordered in decreasing magnitude.

This method is based on performing singular value decomposition on the binary design structure matrix (DSM), while singular values and corresponding orthogonal eigenvectors are expressed by the following equation:

$$\mathrm{DSM} = U \cdot \Sigma_{\mathrm{DSM}} \cdot V^T, \tag{3}$$

where

$$\Sigma_{\mathrm{DSM}} = \begin{bmatrix} \sigma_1 & 0 & 0 \\ 0 & \ddots & 0 \\ 0 & 0 & \sigma_N \end{bmatrix}. \tag{4}$$

The SMI index is theoretically bounded between 0 and 1. When SMI values are closer to 1, it indicates a maximum degree of modularity, while SMI values closer to 0 indicate a minimum product modularity or integral product architecture.

Even though this indicator was originally dedicated to quantify degree of product modularity, its applicability for process modularity has been already proved in the work of [48]. To demonstrate its applicability on MAP process structures, let us use the selected process structure shown in Figure 4.

The procedure to calculate the singular values consists of the following six steps:

Step 1. Create adjacency DSM A for the process structure from Figure 4.

$$A = \begin{bmatrix} 0 & 0 & 1 & 0 & 0 \\ 0 & 0 & 1 & 0 & 0 \\ 0 & 0 & 0 & 0 & 1 \\ 0 & 0 & 0 & 0 & 1 \\ 0 & 0 & 0 & 0 & 0 \end{bmatrix}. \tag{5}$$

Step 2. Compute its transpose A^T.

$$A^T = \begin{bmatrix} 0 & 0 & 0 & 0 & 0 \\ 0 & 0 & 0 & 0 & 0 \\ 1 & 1 & 0 & 0 & 0 \\ 0 & 0 & 0 & 0 & 0 \\ 0 & 0 & 1 & 1 & 0 \end{bmatrix}. \tag{6}$$

Step 3. Compute the A^TA matrix.

$$A^TA = \begin{bmatrix} 0 & 0 & 1 & 0 & 0 \\ 0 & 0 & 1 & 0 & 0 \\ 0 & 0 & 0 & 0 & 1 \\ 0 & 0 & 0 & 0 & 1 \\ 0 & 0 & 0 & 0 & 0 \end{bmatrix} * \begin{bmatrix} 0 & 0 & 0 & 0 & 0 \\ 0 & 0 & 0 & 0 & 0 \\ 1 & 1 & 0 & 0 & 0 \\ 0 & 0 & 0 & 0 & 0 \\ 0 & 0 & 1 & 1 & 0 \end{bmatrix} = \begin{bmatrix} 1 & 1 & 0 & 0 & 0 \\ 1 & 1 & 0 & 0 & 0 \\ 0 & 0 & 1 & 1 & 0 \\ 0 & 0 & 1 & 1 & 0 \\ 0 & 0 & 0 & 0 & 0 \end{bmatrix}. \tag{7}$$

Step 4. Determine the eigenvalues of A^TA. In the first substep, set matrix $|A^TA - \lambda I|$ to zero, in order to obtain the homogeneous equation:

$$\begin{vmatrix} 1-\lambda & 1 & 0 & 0 & 0 \\ 1 & 1-\lambda & 0 & 0 & 0 \\ 0 & 0 & 1-\lambda & 1 & 0 \\ 0 & 0 & 1 & 1-\lambda & 0 \\ 0 & 0 & 0 & 0 & -\lambda \end{vmatrix} = 0. \tag{8}$$

Then, solve the characteristic polynomial for the eigenvalues:

$$\begin{aligned} \left(2\lambda^2 - 5\lambda^3 + 4\lambda^4 - \lambda^5\right) + \left(-2\lambda^2 + \lambda^3\right)0 + 0 + 0 &= 0, \\ \left(-4\lambda^3 + 4\lambda^4 - \lambda^5\right) &= 0, \\ -\lambda^3 (\lambda - 2)(\lambda - 2) &= 0. \end{aligned} \tag{9}$$

The obtained eigenvalues of matrix A^TA are 2, 2, 0, 0, and 0.

Step 5. Sort the eigenvalues in the descending order, in the absolute sense.

The eigenvalues of A^TA in the descending order are given by $\lambda = 2, 2, 0, 0, 0$.

Step 6. Identify of the singular values of matrix A.

Then, the singular values of $A - \sigma_i$ are quantified as the square roots of the eigenvalues of A^TA:

$$\Sigma_{\mathrm{DSM}} = \begin{bmatrix} 1,414 & 0 & 0 & 0 & 0 \\ 0 & 1,414 & 0 & 0 & 0 \\ 0 & 0 & 0 & 0 & 0 \\ 0 & 0 & 0 & 0 & 0 \\ 0 & 0 & 0 & 0 & 0 \end{bmatrix}. \tag{10}$$

Subsequently, it is possible to calculate modularity using SMI index by equation (2). Then, the degree of modularity of the process structure equals 0.7172.

By applying this procedure, it is possible to quantify SMI values of the MAP process networks depicted in Figure 3. Enumerated values are available in Table 1.

4.1.2. Degree of Process Module. A concept of this indicator is based on assumption that a network is represented by directed graph $G(V, A)$, where V is a set of nodes and A is a set of interactions. A partition $P = \{V_1, V_2, \ldots, V_M\}$ is a set of

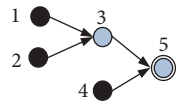

Figure 4: Selected example of assembly process structure.

Table 1: Process modularity values of MLSP type of MAPs.

	No. 2.1	No. 2.2	No. 2.3	No. 2.4
SMI	0.755	0.755	0.798	0.798
M(P)	0.417	0.417	0.245	0.245
PMI	0.17	0.17	0.29	0.29
RNM	0.157	0.157	0.21	0.21

nonempty and nonoverlapping subsets of V, which covers V (i.e., $V_i \cap V_j = \varnothing$, and $U_{i=1}^{M} V_i = V$). Then, the degree of process module extracted from the network is calculated by using formula [46]:

$$M(P) = \sum_{i=1}^{M} \left(\frac{w_{vivi}}{w} - \frac{w_{vi}^{\text{in}} * w_{vi}^{\text{out}}}{w^2} \right), \tag{11}$$

where

w_{ViVi} is the number of input and output edges of the individual module V_i

w_{vi}^{out} is the number of output edges of the individual module V_i

w_{vi}^{in} is the number of input edges of the individual module V_i

w is the total number of interactions in the network

Then, the modularity of the network is expressed as $M(G) = \max M(P)$. Modularity values close to zero mean maximal modularity, and modularity values close to 1 indicate minimal modularity.

As a *process operation*, according to the generic model of MAP (see Figure 2), which is not decomposable module, then formula (11) can be simplified as follows:

$$M(P) = \frac{w_{vi}}{w} - \frac{w_{vi}^{\text{in}} * w_{vi}^{\text{out}}}{w^2}, \tag{12}$$

where

w_{Vi} is the number of input edges into the individual module V_i

w_{vi}^{in} is the number of input edges of the individual module V_i

w_{vi}^{out} is the number of output edges of the individual module V_i

w is the total number of interactions in the network

To show applicability of this indicator, let us have process structure in Figure 5.

This process structure is firstly divided into two operational modules. Then, the modularity for operational module #1 and operational module #2 is calculated using equation (12) as follows:

$$M(P)_1 = \frac{2}{5} - \frac{2 * 1}{5^2} = 0.32,$$
$$M(P)_2 = \frac{2}{5} - \frac{2 * 1}{5^2} = 0.32. \tag{13}$$

As modularity of the network equals the largest module, it is needed to choose the largest modularity value. Accordingly, the modularity of this process structure equals 0.32.

4.1.3. Process Module Independence. Abdelkafi [32] adopted a cluster independence (CI) indicator for the measurement of product modularity developed by Newcomb et al. [49] in order to propose a modified indicator to measure module independence (MI). MI is defined as the ration of the sum of relations inside all modules to the sum of all relations:

$$MI = \frac{\text{the sum of the relations inside all modules}}{\text{the sum of all relations}}. \tag{14}$$

According to Abdelkafi [32] "cross-module independence (or degree of loose-couplings) is nothing else than (1 – *MI*)."

Then, this assertion can be transformed into a process module independence (PMI) indicator expressed as

$$\text{PMI} = 1 - \text{MI}. \tag{15}$$

4.2. Proposed Modularity Measure. In this section, the novel relative modularity indicator will be introduced using the following assumptions.

Assumption 1. Typical MAPs are modelled as MLSP type structures as it was proposed by Hu et al. ([50], page 48).

Assumption 2. There is certain correlation between structural network complexity and network modularity [9, 10, 13].

Assumption 3. Under the previous assumption, it is expected that if MAP modularity increases, then the average complexity of all the modules of MAP decreases, and vice versa.

Proposition 1. *To measure average complexity of all the modules (AMC) of any MAP, the following formula is proposed:*

$$\text{AMC} = \frac{\sum_{i=1}^{V} \deg(v)_i \log_2 \deg(v)_i}{m}, \tag{16}$$

where

$\deg(v)_i$ *is the degree of vertex of* $(v)_i$ *in graph G, while G consists of a set of V vertices* $\{V\} = \{v_1, v_2, \ldots, v_V\}$

m *is the number of modules in the network*

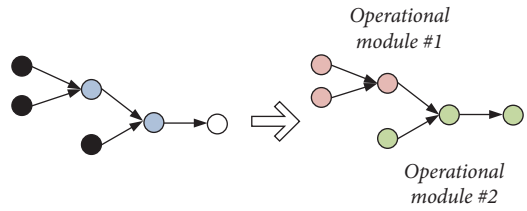

Figure 5: Example of process structure with two operational modules.

Proof. This proposition can be proved on SLMP networks from Figure 3, where one can see that MAP structure No. 1.1 is minimally modular or nonmodular, while No. 1.4 is maximally modular, and structure No. 1.3 is more modular than structure No. 1.2. When applying the AMC indicator for the selected networks, the following values are obtained and summarized in Table 2.

Now, it can be seen that the most modular network No. 1.4 has the lowest complexity, and the structure No. 1.1 which is minimally modular has the highest complexity. This relation also applies to the networks No. 1.2. and No. 1.3. This proves that AMC reflects complexity of the selected MAPs according to Assumption 3. □

Proposition 2. *Relative network modularity (RNM) of any MAP can be measured through the inverse function of formula (16):*

$$\mathrm{RNM} = \frac{m}{\sum_{i=1}^{V} \deg(v)_i \log_2 \deg(v)_i}. \tag{17}$$

Proof. The assertion of this proposition will be proved on MLSP networks from Figure 3. The proof is based on the deduction principle to show that if the order of degree of modularity of alternative MAPs is known, then modularity values of the MAPs using RNM should confirm the same order. By applying all the three existing modularity indicators, the order of degree of modularity of the MAPs can be achieved as highlighted in grey in Table 1.

Subsequently, the same order of degree of modularity of the MAPs is obtained using the RNM indicator. One can see that all the four indicators map modularity in the same way. This proves that RNM quantifies relative modularity of the selected MAPs in the same way as the three alternative indicators. □

5. Comparison of the Proposed Relative Modularity Indicator with the Existing Ones

In this section, the abovementioned four indicators will be mutually benchmarked on SLMP and MLMP types of MAP models depicted in Figure 3. The obtained relative modularity values are shown in Table 3.

The groups of MAP models in Table 3 are arranged in the ascending order in terms of the relative modularity. The order of SLMP type of MAPs has been already explained (see the proof of Proposition 1). The order of MLMP type of MAPs has been obtained by applying the three of the four indicators, namely, SMI, PMI, and RNM measures. All the three indicators brought the same degree of modularity tendency.

Table 2: Process complexity values of the selected assembly process networks.

	No. 1.1	No. 1.2	No. 1.3	No. 1.4
AMC	33,22	20,58	17,42	7,93

Nevertheless, according to the mutual comparison of values in Table 3, it can be seen that some values do not reflect the increasing order (see values **in the boxes**). It implies that SMI is not suitable for SLMP type of the MAPs, and M(P) is not suitable for MLMP type of the MAPs. Moreover, PMI is not applicable for SLMP type of the MAPs since it generates for all the four MAP structures zero values.

In addition, it is also evident that the RNM indicator can distinct small modularity differences between similar structures (see pair of structures No. 3.2 and No. 3.3), while the indicators SMI and PMI consider this pair of structures as identical in terms of modularity (see the values highlighted in grey).

In order to verify Proposition 2, all the indicators will be further comprehensively assessed on more complex examples of MAPs and compared according to the four criteria specified in Table 4.

As it can be seen from the Table 4, all the three existing indicators show at least one significant drawback, while RNM reflects all the criteria in positive way. This fact justifies to provisionally estimate this indicator as the most appropriate to evaluate structural relative modularity of manufacturing assembly processes.

In order to validate suitability of the proposed indicator and to test alternative indicators on more complex realistic cases, MAPs of MLSP type with six input components will be also used for this purpose (see Figure 6). The exact number of the alternative MAP structures is determined through formula (1) as follows:

$$a(6) = A000669(6) - 1 = 32. \tag{18}$$

After generating of the all MAP structures for $i = 6$ (see Figure 6), RNM, SMI, $M(P)$, and PMI values are calculated. The obtained values which are graphically presented in Figure 7 are arranged in ascending order according to the RNM values.

The following findings resulting from the computational data analysis employing evaluation criteria EC2 and EC3 can be summarized:

(i) SMI indicator does not satisfy EC2 and EC3

Table 3: The obtained SMI, M(P), PMI, and RNM values.

Selected MAP structures		Obtained modularity values by using the indicators			
		SMI	$M(P)^*$	PMI	RNM
SLMP	No. 1.1	0.811	0.76	N/A	0.03
	No. 1.2	**0.857**	0.468	N/A	0.046
	No. 1.3	**0.837**	0.344	N/A	0.057
	No. 1.4	0.895	0.161	N/A	0.126
MLMP	No. 3.1	0.86	0.5	0.125	0.099
	No. 3.2	**0.892**	**0.259**	**0.22**	0.142
	No. 3.3	**0.892**	**0.296**	**0.22**	0.145
	No. 3.4	0.906	0.18	0.3	0.18
	No. 3.5	0.906	0.18	0.3	0.18

$^*M(P)$ values range between 0 and 1, while values close to 0 means maximal modularity and values close to 1 indicates minimal modularity.

Table 4: Assessment of the modularity indicators according to the four evaluation criteria.

Process structure modularity indicators	Evaluation criteria (EC)			
	EC1: applicability for all the MAP types	EC2: ability to differ between better and worse degrees of modularity of MAPs	EC3: ability to recognize small modularity changes in between two or more MAPs with the proper tendency	EC4: simplicity of calculation
SMI	✓	X	X	X
$M(P)$	✓	X	X	✓
PMI	X	✓	X	✓
RNM	✓	✓	✓	✓

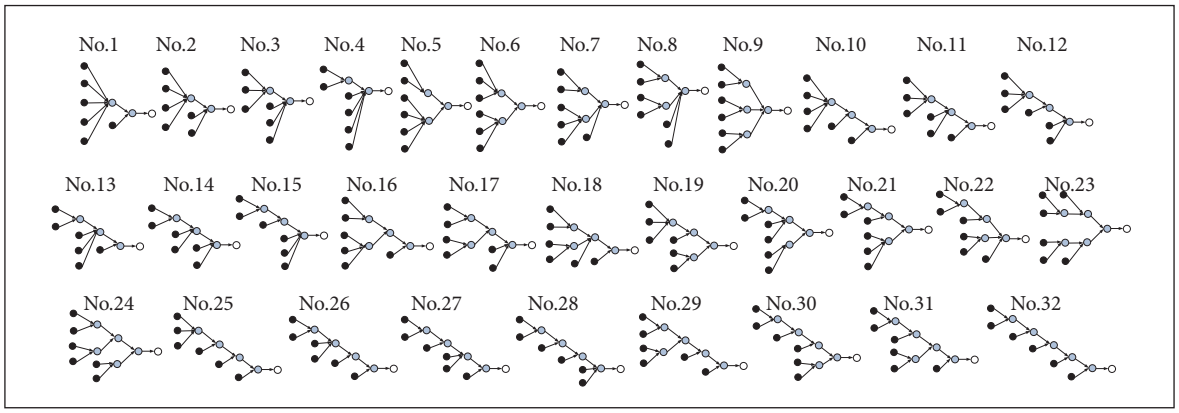

Figure 6: The all possible MLSP MAP structures with six input components.

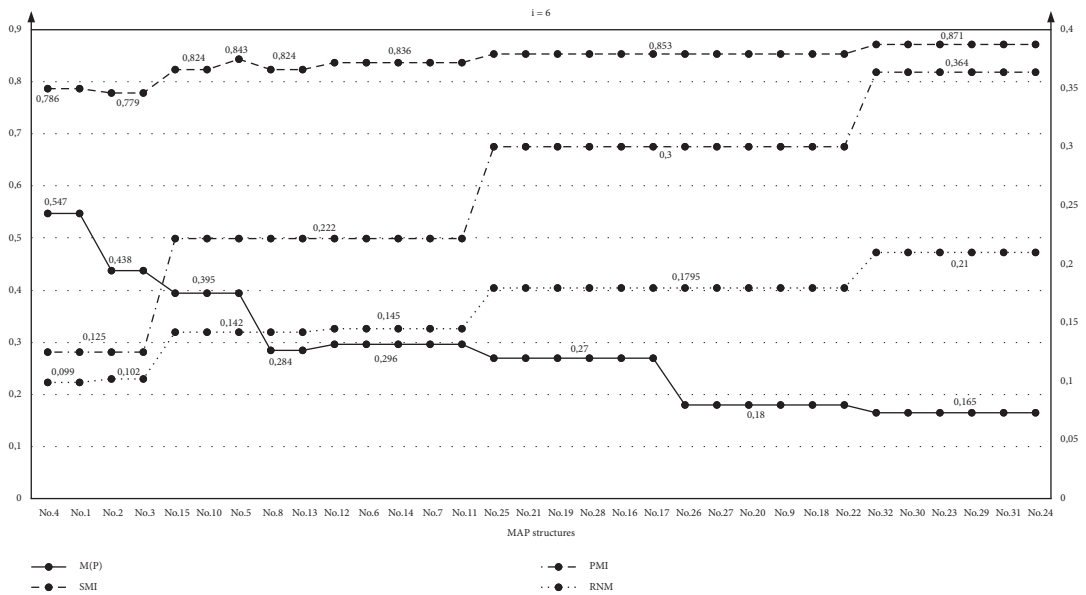

Figure 7: All possible MLSP process structures with six input components.

(ii) M(P) indicator does not satisfy EC2 and EC3

(iii) PMI indicator satisfies EC2, but does not satisfy EC3

(iv) RNM indicator satisfies the both criteria EC2 and EC3

These four findings correspond in full scale with the results of the previous assessment of the four indicators shown in Table 4.

6. Conclusions

Building on the computational experiments, it can be stated that the RNM indicator reliably reflects the expected system attribute-relative structural modularity of the MAPs. Accordingly, this indicator can be considered as the most appropriate modularity measure from the compared ones because it is fully suitable for all the types of MAPs. Moreover, it does not require time-consuming calculation.

In addition, this paper offers the new assembly process networks classification which can help in further possible testing of modularity indicators. In this context, further research can be focused on testing more complex MAPs and verifying proposed indicator through real-case examples. The follow-up research could also be oriented towards analysing additional different assembly attributes that contribute to the relative modularity computation.

Data Availability

The data used to support the findings of this study are included within the article.

Disclosure

This is an extended version of a preliminary conference paper that was presented in the 14th International Conference on Axiomatic Design (ICAD 2021) 23rd-25th June 2021, Lisbon, Portugal [51].

Conflicts of Interest

The authors declare that there are no conflicts of interest regarding the publication of this paper.

Acknowledgments

This research was funded by the KEGA project granted by the Ministry of Education of the Slovak Republic (no. 025TUKE-4/2020).

References

[1] K. Sinha, E. S. Suh, and O. de Weck, "Integrative complexity: an alternative measure for system modularity," *Journal of Mechanical Design*, vol. 40, no. 5, 2018.

[2] M. A. Schilling, "Toward a general modular systems theory and its application to interfirm product modularity," *Academy of Management Review*, vol. 25, no. 2, pp. 312–334, 2000.

[3] C. Y. Baldwin and K. B. Clark, "Managing in an age of modularity," *Managing in the modular age: Architectures, networks, and organizations*, vol. 149, pp. 84–93, 2003.

[4] M. Sako and F. Murray, "Modules in design, production and use: implications for the global auto industry," in *Proceedings of the IMVP Annual Sponsors Meeting*, Cambridge, MA, USA, 1999.

[5] V. Modrak and Z. Soltysova, "Development of operational complexity measure for selection of optimal layout design alternative," *International Journal of Production Research*, vol. 56, no. 24, pp. 7280–7295, 2018.

[6] V. Modrak and Z. Soltysova, "Novel complexity indicator of manufacturing process chains and its relations to indirect complexity indicators," *Complexity*, vol. 2017, Article ID 9102824, 15 pages, 2017.

[7] K. Ulrich, "The role of product architecture in the manufacturing firm," *Research Policy*, vol. 24, no. 3, pp. 419–440, 1995.

[8] N. P. Suh, *The Principles of Design*, Oxford University Press, New York, NY, USA, 1990.

[9] S. K. Ethiraj and D. Levinthal, "Modularity and innovation in complex systems," *Management Science*, vol. 50, no. 2, pp. 159–173, 2004.

[10] D. B. Parker, "Modularity and complexity: an examination of the effects of product structure on the intricacy of production systems," *Michigan State University*, vol. 119, 2010.

[11] V. Modrak and D. Marton, "Configuration complexity assessment of convergent supply chain systems," *International Journal of General Systems*, vol. 43, no. 5, pp. 508–520, 2014.

[12] V. Modrak, S. Bednar, and Z. Soltysova, "Application of axiomatic design-based complexity measure in mass customization," *Procedia CIRP*, vol. 50, pp. 607–612, 2016.

[13] D. Tate, *A roadmap for decomposition: activities, theories, and tools for system design*, Ph.D. Thesis, Massachusetts Institute of Technology, Cambridge, MA, USA, 1999.

[14] V. Modrak and S. Bednar, "Using axiomatic design and entropy to measure complexity in mass customization," *Procedia CIRP*, vol. 34, pp. 87–92, 2015.

[15] A. Mehrsai, H. R. Karimi, and K.-D. Thoben, "Integration of supply networks for customization with modularity in cloud and make-to-upgrade strategy," *Systems Science & Control Engineering*, vol. 1, no. 1, pp. 28–42, 2013.

[16] C. Y. Baldwin and K. B. Clark, "Design rules: the power of modularity," *MIT press*, vol. 1, 2000.

[17] R. Sanchez and J. T. Mahoney, "Modularity, flexibility, and knowledge management in product and organization design," *Strategic Management Journal*, vol. 17, no. S2, pp. 63–76, 1996.

[18] V. Modrak V, *Mass Customized Manufacturing: Theoretical Concepts and Practical Approaches*, CRC Press, Boca Raton, FL, USA, 2017.

[19] K. Frenken and S. Mendritzki, "Optimal modularity: a demonstration of the evolutionary advantage of modular architectures," *Journal of Evolutionary Economics*, vol. 22, no. 5, pp. 935–956, 2012.

[20] K. Ulrich, *Fundamentals of Product Modularity Management of Design*, pp. 219–231, Springer, Dordrecht, Netherlands, 1994.

[21] M. K. Starr, "Modular production–a new concept," *Harvard Business Review*, vol. 43, no. 6, pp. 131–142, 1965.

[22] M. K. Starr, "Modular production-a 45-year-old concept," *International Journal of Operations & Production Management*, vol. 30, no. 1, pp. 7–19, 2010.

[23] M. Calcagno, "Dynamics of modularity: a critical approach," *Euram Conference*, vol. 9, no. 11, pp. 1–11, 2002.

[24] S. K. Vickery, X. Koufteros, C. Dröge, and R. Calantone, "Product modularity, process modularity, and new product introduction performance: does complexity matter?"

Production and Operations Management, vol. 25, no. 4, pp. 751–770, 2016.

[25] R. Duray, P. T. Ward, G. W. Milligan, and W. L. Berry, "Approaches to mass customization: configurations and empirical validation," *Journal of Operations Management*, vol. 18, no. 6, pp. 605–625, 2000.

[26] B.-W. Lin, "Cooperating for supply chain effectiveness: manufacturing strategy for Chinese OEMs," *International Journal of Manufacturing Technology and Management*, vol. 5, no. 3, pp. 232–245, 2003.

[27] Q. Tu, M. A. Vonderembse, T. S. Ragu-Nathan, and B. Ragu-Nathan, "Measuring modularity-based manufacturing practices and their impact on mass customization capability: a customer-driven perspective," *Decision Sciences*, vol. 35, no. 2, pp. 147–168, 2004.

[28] D. B. Parker, "Modularity and complexity: an examination of the effects of product structure on the intricacy of production systems," Unpublished doctoral dissertation, Michigan State University, East Lansing, MI, USA, 2010.

[29] Z. Toroczkai, "Functional vs. Structural Modularity: do they imply each other?" *APS March Meeting Abstracts*, vol. 9, no. 13, 2009.

[30] A. Muñoz Rios, Hexagonal Architecture in the Modernization of Corebanking Systems to Cloud, Transformation and Modernization, 2021, https://www.fintechna.com/articles/hexagonal-architecture-in-the-modernization-of-corebanking-systems-to-cloud/.

[31] J. M. Dasch and D. J. Gorsich, *Survey of Modular Military Vehicles: Benefits and Burdens*, Army Tank Automotive Research, Development and Engineering Center (TARDEC) Warren United States, Warren, MI, USA, 2016.

[32] N. Abdelkafi, "Variety induced complexity in mass customization: concepts and management," *Erich Schmidt Verlag GmbH & Co KG*, vol. 7, 2008.

[33] R. N. Langlois, "Modularity in technology and organization," *Journal of Economic Behavior & Organization*, vol. 49, no. 1, pp. 19–37, 2002.

[34] M. Jacobs, C. Droge, S. K. Vickery, and R. Calantone, "Product and process modularity's effects on manufacturing agility and firm growth performance," *Journal of Product Innovation Management*, vol. 28, no. 1, pp. 123–137, 2011.

[35] A. Kusiak, "Integrated product and process design: a modularity perspective," *Journal of Engineering Design*, vol. 13, no. 3, pp. 223–231, 2002.

[36] D. Standage, C. N. Areshenkoff, J. Y. Nashed et al., "Dynamic reconfiguration, fragmentation, and integration of whole-brain modular structure across depths of unconsciousness," *Cerebral Cortex*, vol. 30, no. 10, pp. 5229–5241, 2020.

[37] N. Kashtan and U. Alon, "Spontaneous evolution of modularity and network motifs," *Proceedings of the National Academy of Sciences*, vol. 102, no. 39, pp. 13773–13778, 2005.

[38] M. Kirschner and J. Gerhart, "Evolvability," *Proceedings of the National Academy of Sciences*, vol. 95, no. 15, pp. 8420–8427, 1998.

[39] G. P. Wagner, *Robustness and Evolvability in Living Systems*, Princeton University Press, Princeton, NJ, USA, 2005.

[40] M. Efatmaneshnik and M. j. Ryan, "On optimal modularity for system construction," *Complexity*, vol. 21, no. 5, pp. 176–189, 2016.

[41] Y. Yang, M. Yang, L. Shu, S. Li, and Z. Liu, "A novel parallel assembly sequence planning method for complex products based on PSOBC," *Mathematical Problems in Engineering*, vol. 2020, Article ID 7848329, 11 pages, 2020.

[42] M. R. Bahubalendruni, B. B. Biswal, M. Kumar, and R. Nayak, "Influence of assembly predicate consideration on optimal assembly sequence generation," *Assembly Automation*, vol. 35, no. 4, 2015.

[43] B. Wu, P. Lu, J. Lu, J. Xu, and X. Liu, "A hierarchical parallel multi-station assembly sequence planning method based on GA-DFLA," *Proceedings of the Institution of Mechanical Engineers-Part C: Journal of Mechanical Engineering Science*, vol. 203–210, Article ID 0954406220974065, 2020.

[44] M. R. Bahubalendruni and B. B. Biswal, "An intelligent approach towards optimal assembly sequence generation," *Proceedings of the Institution of Mechanical Engineers-Part C: Journal of Mechanical Engineering Science*, vol. 232, no. 4, pp. 531–541, 2018.

[45] K. Holtta K, E. S. Suh, and O. de Weck, "Tradeoff between modularity and performance for engineered systems and products," in *Proceedings of the ICED 05: 15th International Conference on Engineering Design: Engineering Design and the Global Economy (Engineers Australia)*, pp. 449-450, Melbourne, Australia, January 2005.

[46] T. D. Tran and Y. K. Kwon, "The relationship between modularity and robustness in signalling networks," *Journal of The Royal Society Interface*, vol. 10, no. 88, Article ID 20130771, 2013.

[47] The On-line Encyclopedia of Integer Sequences (OEIS), 2021, https://oeis.org/A000669.

[48] V. Modrak and Z. Soltysova, "Process modularity of mass customized manufacturing systems: principles, measures and assessment," *Procedia CIRP*, vol. 67, pp. 36–40, 2018.

[49] P. J. Newcomb, B. Bras, and D. W. Rosen, "Implications of modularity on product design for the life cycle," in *Proceedings of the International Design Engineering Technical Conferences and Computers and Information in Engineering Conference*, Irvine, CA, USA, August 1996.

[50] S. J. Hu, X. Zhu, H. Wang, and Y. Koren, "Product variety and manufacturing complexity in assembly systems and supply chains," *CIRP annals*, vol. 57, no. 1, pp. 45–48, 2008.

[51] V. Modrak and Z. Soltysova, "Modularity measurement as a crucial design element," in *Proceedings of the 14th International Conference on Axiomatic Design (ICAD 2021)*, Lisbon, Portugal, June 2021.

Hindawi
Mathematical Problems in Engineering
Volume 2021, Article ID 5531449, 9 pages
https://doi.org/10.1155/2021/5531449

Research Article

Diagnosis Index System Setup for Implementation Status Management in Large-Scale Construction Projects

Wan-Yu Wang and Yi Wang

School of Economy and Management, North China Electric Power University, Beijing 102206, China

Correspondence should be addressed to Wan-Yu Wang; wangwanyu@ncepu.edu.cn

Received 25 February 2021; Revised 8 May 2021; Accepted 27 May 2021; Published 10 June 2021

Academic Editor: Sudhakarapandian RanjithaRamasamy

In order to scientifically set up the diagnosis index system for the implementation state of large-scale construction projects, this paper proposed a new method which takes into account the indicators in all level states. Different from the index system constructed by other methods, the indexes/indicators established in this paper are more systematically correlated, with a better hierarchical progression in all levels of the index system. The particular diagnosis index parameters of the management objects are firstly analysed through the mathematic model based on the Rough Set. Then, the representation of the periodical management problems is taken as the study object, and the detailed establishing process to form the index system is presented based on the evidenced theory and the Rough Set extraction. Finally, a case study is presented to validate the proposed method. It is shown that the index system set up by the proposed method can not only represent the systematic hierarchical relationships among all corresponding indexes but also diagnose the macroscopic, the mesostates, and the microstates effectively.

1. Introduction

The establishing method of the index system for the construction projects is essential to scientific management [1]. Previous studies have validated the significance of the proper index system for sustainability in the highway construction projects [2, 3], and for the comprehensive assessment in the cross-border power grid interconnection projects [4].

However, the current frame of the index system is far from qualified in engineering applications. It is found that the traditional plan-driven model sometimes is not the most appropriate approach to complex construction projects subject to successive changes, while more agile approaches might be more adequate [5]. For instance, the internal audit effectiveness measurement index system in architecture construction projects faces the problems of large losses and waste, ineffective audit rectification, and lagging audit innovation [6], while the gas pipeline projects follow the issue of energy security and the need to diversify suppliers [7]. The key reason is that the index system for different projects needs too many efforts to concretize and verify the indexes/indicators. Consequently, how to scientifically pick the sensitive parameters to form the effective index system has become the key point.

The index parameters refer to many factors. Taking the modular integrated construction (MiC) project as an example, Wuni et al. identified and evaluated 22 potential critical failure factors (CFFs) for such MiC projects [8]. In addition, these parameters and factors correspond to varied project index types with different highlights and targets. Most commonly, the factors refer to the costs and waste [9, 10], the risk and safety [11–17], the procedure delay [18–20], the decision-making [21], and so forth. People have tried various methods to select the proper parameters and indicators for different index systems. Typically, Elfahham employed Neural Networks, Linear Regression, and Autoregressive Time Series to obtain the Construction Cost Index [9], while Okudan et al. proposed a knowledge-based risk management tool for the construction projects by using the case-based reasoning method [12]. To reduce the risk, the BIM-integrated safety assessment is widely used at the design stage in building projects [13]. For the construction

projects which need to deal with multisource information, such as the tunnel construction [14] and the subway construction [16], the analytic network process and the extension cloud models are frequently employed to assess the safety and the risk of the project.

The aforementioned research developed varied indicators to form the index system by multifarious methods and models. However, most of them primarily selected the most related indicators, while the correlation of these indicators in different level stages was not finely taken into account. It has been shown that the systematic and dynamics model which considers the factors that affect the behaviour of the study object will be more scientific to form the qualified index system [22].

In this paper, we proposed a new approach which takes into account the indicators in all level states to set up the diagnosis index system for the implementation status management in large-scale construction projects. Different from the index system constructed by other methods, the indexes/indicators established in this paper are more systematically correlated, with a better hierarchical progression in all levels of the index system. The remainder of this paper is constructed as follows: the methodology to determine the diagnosis indicators and to construct the index system is proposed in Section 2, while the case study and the validation of the established index system are presented in Section 3. Finally, the primary conclusions are drawn up in Section 4.

2. Methodology

2.1. Basic Method Theory. In order to realize the effective management of large-scale construction projects through the diagnosis system, how to ensure the scientificity as well as the systematicness and completeness of the diagnosis indicators in the system is the primary issue.

Currently, there are many methods to analyse and determine the diagnosis index parameters of the implementation state of a project from many sources, such as the expert experience method, the homologous reference method, and the Rough Set (RS) extraction method [23–25]. Among these methods, the RS extraction method is the most effective one in practice. This method generally relies on the evidence-based theory and begins with the relative representation analysis.

In our proposed approach, we primarily employ the Rough Set (RS) extraction method based on the evidence-based theory. The evidence-based theory is the most effective method to obtain the problem representation of the project implementation state [26]. It takes the actual environment and the practical data of the management object to obtain the information and complete the description of the management object. Therefore, it has become the most popular problem representation method.

The application of the aforementioned RS extraction method based on the evidence-based theory requests three work steps, as illustrated in Figure 1.

As shown in Figure 1, to construct the index system, the problem representation of the management object needs to be obtained firstly. Second, the characteristic parameters need to be obtained by analysing the problem representation. Third, the characteristic parameters need to be transformed into the corresponding diagnosis index. Based on these three steps, the index system can be constructed. Among the three steps, the second one is the most important. During this step, it determines the representation features from the core of the problem by removing the redundant information and then obtains the characteristic parameters.

2.2. Determination of Diagnosis Indicators. In order to obtain the problem representations of the management objects in the practical large-scale construction projects, we obtained 5,738 pieces of information that effectively reflected the problems at various stages of the project through a survey of 276 managers.

By analysing the information obtained, we found that there are 258 common and typical problem representations, which are of 20 categories in total. Among these representations, 17 are for the decision-making stage belonging to 3 categories, 66 are for the preparation stage referring to 5 categories, 143 are for the construction stage belonging to 8 categories, and the other 32 are for the completion stage referring to 4 categories. Taking the decision-making stage as an example, the representations and the referring categories are listed in Table 1.

When dealing with the specific problems, the simplified information needs to be determined according to the project management rules, and the mathematical model can be written as [27]

$$\mathrm{RED}(R) = \mathrm{RED}(R - (r)), \tag{1}$$

where $\{r\}$ is the redundant information of the problem representation, and the kernel set $\mathrm{CORD}(R)$ is the rest of {KX} after the reduction. All of the representations x of the problems in all stages of the project K should be equivalent to the original set {KX} in R degree [28].

Assuming that T is the feature set of x element in {KX}, P is the parameter set corresponding to T, and I is the mapping index set with the same set potential as P; then, according to the RS theory, the kernel formed after reduction can be expressed as

$$\mathrm{CORD}(R) = \mathrm{KX} - \mathrm{Kr}, \tag{2}$$

where

$$\mathrm{Kr} \notin I\{\mathrm{CORD}(R)\colon \mathrm{CORD}(R) \in \mathrm{RED}(\mathrm{KX})\}. \tag{3}$$

Since $\mathrm{CORD}(\mathrm{R}) \in R\colon \mathrm{RED}(\mathrm{KX})$, all the objects contained in $\mathrm{CORD}(R)$ are related [29], and there is

$$\mathrm{CORD}(R) \in \mathrm{RED}\{(\mathrm{KX}) \subseteq \Lambda(\mathrm{KX})\}, \tag{4}$$

$$(\mathrm{KT})_R \subseteq \mathrm{IND}\{\mathrm{CORD}(R) \subseteq \Lambda(\mathrm{KX})\}, \tag{5}$$

$$(\mathrm{KP})_R \subseteq \mathrm{IND}\{(\mathrm{KT}) \subseteq \Lambda(\mathrm{KX})\}. \tag{6}$$

According to the coprime mapping, the parameters and the indicators have the same set potential, and we have

$$f\colon \mathrm{dom}(R) \longrightarrow^{\mathrm{injec}} \mathrm{ran}(R) \Rightarrow \{\mathrm{KP}\} \longrightarrow^{\mathrm{injec}} \{\mathrm{KI}\}, \quad (7)$$

where KX, KT, and KP are problem-depend parameters and need to be specified and symbolized according to the detailed topics. These characteristic parameters can be extracted through the analysis of all problem representations in each stage of the system, and then the diagnosis indicators can be obtained to establish a complete index system. The key issue of the RS method is to obtain the problem representations.

To determine the diagnosis index after obtaining the problem representations of the management object, an analysis on the characteristic parameters of the problem representation is needed. Taking the decision-making stage A as an example, the 17 representations of the 3 categories, namely, the project planning AX1, the feasibility study analysis AX2, and the decision-making approval AX3, have the relations as

$$\begin{aligned}\{\mathrm{AX}\} &\supseteq \{\mathrm{AX1}, \mathrm{AX2}, \mathrm{AX3}\}\\ &= \left\{\cup Ax_i \in \mathrm{AX}, \left(x_i, i = 1-17\right)\right\}\\ &= \{A1, A2, \cdots A1\}.\end{aligned} \quad (8)$$

Based on the analysis on the problem representations, it is shown that the decision-maker's unawareness of the current status ($A1$), the developing tendency ($A2$), or the relative policy ($A3$) during the project planning stage will lead to the miss of the construction scale and investment intention ($A4$) and cause divergence and disputation ($A5$). Consequently, the inefficient project proposal ($A6$) and the delay of the approval to higher departments ($A7$) will be produced. Therefore, the primary problems focus on the project conception and the construction proposal. To solve these problems, it needs to carry out the subject indexing and the problem symbolizing, as shown in Table 2.

Then, according to the RS method, the characteristic parameters in AX1 can be extracted, and meanwhile, the diagnosis indicators can be obtained. The whole process can be expressed as

$$\{\mathrm{AX1}\} = \left\{\cup Ax_i\left(x_i\colon i = 1-7\right)\right\} = \{A1, A2, \cdots, A7\}, \quad (9)$$

$$\mathrm{CORD}(\mathrm{AR}) \in \mathrm{RED}\{(\mathrm{AX1}) \subseteq \Lambda\left(\cup Ax_i\left(x_i\colon i = 1-7\right)\right)\}. \quad (10)$$

Specifically,

$$\begin{aligned}&\because \mathrm{CORD}(\mathrm{AR1}) \in \mathrm{RED}\left\{\cup Ax_i\left(x_i\colon i = 1-3\right)\right\}, \mathrm{CORD}(\mathrm{AR2}) \in \mathrm{RED}\left\{\cup Ax_i\left(x_i\colon i = 4-5\right)\right\},\\ &\quad \mathrm{CORD}(\mathrm{AR3}) \in \mathrm{RED}\left\{\cup Ax_i\left(x_i\colon i = 6-7\right)\right\}\\ &\therefore \mathrm{CORD}(\mathrm{AR}) \supseteq \cup\{\mathrm{AR1}, \mathrm{AR2}, \mathrm{AR3}\}, (\mathrm{AT111})_R \subseteq \mathrm{IND}\{\mathrm{CORD}(\mathrm{AR1}) \subseteq \Lambda(\mathrm{AX1})\},\\ &\quad (\mathrm{AT112})_R \subseteq \mathrm{IND}\{\mathrm{CORD}(\mathrm{AR2}) \subseteq \Lambda(\mathrm{AX1})\}, (\mathrm{AT121})_R \subseteq \mathrm{IND}\{\mathrm{CORD}(\mathrm{AR3}) \subseteq \Lambda(\mathrm{AX1})\},\\ &\quad (\mathrm{AT11})_R \supseteq \cup\{\mathrm{AT111}, \mathrm{AT112}\}, (\mathrm{AT12})_R \supseteq \cup\{\mathrm{AT121}\}, (\mathrm{AT})_R \supseteq \{\mathrm{AT11}, \mathrm{AT12}\} \subseteq \Lambda(\mathrm{AX1})\\ &\quad \because (\mathrm{AP})_R \subseteq \mathrm{IND}\{(\mathrm{AT}) \subseteq \Lambda(\mathrm{AX})\}\\ &\therefore (\mathrm{AP111})_R \subseteq \mathrm{IND}\{\mathrm{AT111} \subseteq \Lambda(\mathrm{AX1})\}, (\mathrm{AP112})_R \subseteq \{(\mathrm{AT112}) \subseteq \Lambda(\mathrm{AX1})\}\\ &\quad (\mathrm{AP121})_R \subseteq \mathrm{IND}\{(\mathrm{AT121}) \subseteq \Lambda(\mathrm{AX1})\}, (\mathrm{AP})_R \supseteq \cup\{\mathrm{AP111}, \mathrm{AP112}, \mathrm{AP121}\}.\end{aligned} \quad (11)$$

Further, based on the same set potential of the parameters and the indicators, there is

$$\begin{aligned}&f\colon \mathrm{dom}(\mathrm{AR}) \xrightarrow{\mathrm{injec}} \mathrm{ran}(\mathrm{AR}) \Rightarrow \{\mathrm{AP}\} \xrightarrow{\mathrm{injec}} \{\mathrm{AI}\},\\ &\because (\mathrm{AP})_R \supseteq \mathrm{U}\{\mathrm{AP111}, \mathrm{AP112}, \mathrm{AP121}\},\\ &\therefore \{\mathrm{AI}\}_R \supseteq \mathrm{U}\{\mathrm{AI111}, \mathrm{AI112}, \mathrm{AI121}\}.\end{aligned} \quad (12)$$

Then, the diagnosis indicators of the management objects at all levels in the project planning stage are obtained. Similarly, the diagnosis indicators for the feasibility study stage and the decision approval stage can be determined as well; more details are shown in Table 3.

By employing the aforementioned method, the diagnostic indicators of the management objects at various levels in other stages of large construction projects can be also obtained. Limited by space, this paper mainly focuses on the establishing method of the problem indicators, while the detailed processes which can be found in [30] are not presented.

2.3. Construction of Index System. As previously analysed, since the diagnosis indicators that are proposed based on the RS theory are particularly aiming at the problem representations, they are the most direct indexes to diagnose the practical problems in construction projects.

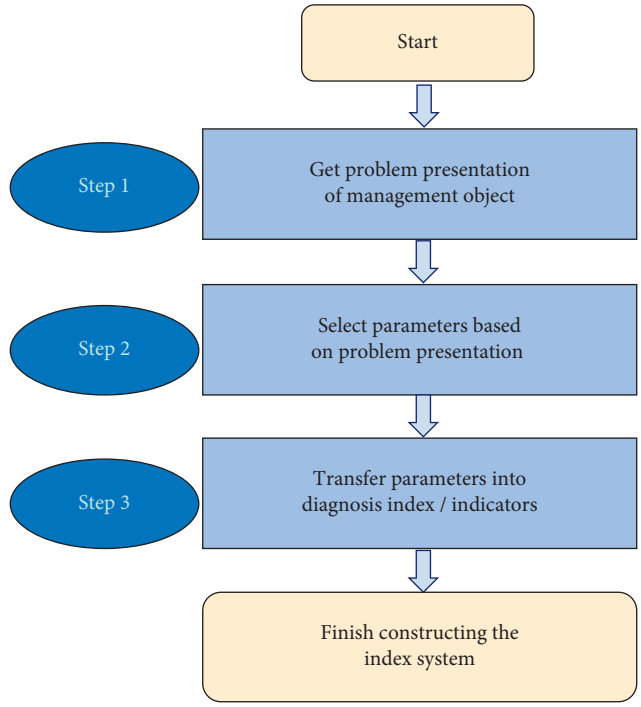

Figure 1: Index system construction steps.

Table 1: Problem representations in decision-making stage.

Category	Problem representation	Problem symbolization
Project planning	Current status unknown	$A1$
	Developing trend unknown	$A2$
	Policies not grasped	$A3$
	Project positioning unclear	$A4$
	Project decisions controversial	$A5$
	Report inefficiently prepared	$A6$
	Report delayed	$A7$
Feasibility analysis	Survey not actually performed	$A8$
	Survey scope incomprehensive	$A9$
	Information not true	$A10$
	Method incorrect	$A11$
	Content not comprehensive	$A12$
Decisions and approvals	Decision reference not reliable	$A13$
	Decision process incorrect	$A14$
	Decision-making inefficient	$A15$
	Approval process not standard	$A16$
	Approval inefficient	$A17$

Specifically, the indicators have the relationships as

$$\begin{aligned} (\mathrm{AI111} \cup \mathrm{AI112}) &\in \mathrm{AI11}, \\ (\mathrm{AI121}) &\in \mathrm{AI12}, \\ (\mathrm{AI11} \cup \mathrm{AI12}) &\in \mathrm{AI1}. \end{aligned} \tag{13}$$

According to the above formulas, AI11 can be derived through AI11 and AI12, while AI12 can be inferred from AI121, and AI1 and be derived through AI11 and AI12. Similarly, AI21, AI22, and AI2 can be derived through AI121, AI211, AI212, AI213, AI221, and AI222, while AI31, AI32, and AI3 can be inferred from AI311, AI321, and AI322.

Further, the overall situation of the project in the decision-making stage can be obtained through the derivation of AI1, AI2, and AI3. And the manager is able to obtain the systematic analysis and assessment on the managing objects in the decision-making stage from the microlayer to the macrolayer.

By using the same method, the indicators as well as their membership function in the preparation stage, the construction stage, and the completion stage can be derived,

Table 2: Subject indexing and representation symbols.

Category and indexing	Feature and indexing	Problem representation indexing	Representation features and indexing	Characteristic parameters and indexing
Plan project AX1	Project idea AT11	$A1$	Incomplete information AT111	Request information AP111
		$A2$		
		$A3$		
		$A4$	Imperfection of planning AT112	Plan and analysis AP112
		$A5$		
	Submit advice AT12	$A6$	Inefficient report AT121	Work efficiency AP121
		$A7$		

Table 3: Diagnosis index of management objects in the decision-making stage.

Diagnosis index	Index code
Project plan	AI1
Feasibility analysis	AI2
Decision approval	AI3
Conception	AI11
Proposal	AI12
Condition	AI21
Analysis	AI22
Decision	AI31
Approval	AI32
Information acquire rate	AI111
Analysis improving rate	AI112
Work-effect ratio of report	AI121
Reliability rate	AI211
Satisfaction rate	AI212
Work-effect ratio of report	AI213
Correctness rate	AI221
Comprehensive rate	AI222
Work-effect ratio	AI311
Disobeying rate	AI321
Work-effect ratio	AI322

respectively. Then, according to the system structure of the diagnosis index presented in the scientific theories, the general diagnosis index system for the implementation state of each management object can be set up both in micro- and macroaspects, as illustrated in Figure 2.

3. Case Study and Validation

3.1. Case Study. In order to verify the scientificity and the effectiveness of the index system constructed by the aforementioned method, the index system was applied to a construction project for the implementation state diagnosis. The decision-making stage was taken as the specific detection object. The required information of the related 11 microdiagnosis indicators was input into the system to obtain the diagnosis value *TN*. Then, the diagnosis values of the macro- and the mesomanagement objects were calculated as well.

Meanwhile, six senior engineers, who were in charge of the project and had more than 15 years' experience, were invited to evaluate the actual status of the management objects in macro-, meso-, and microaspects. Scores were given by these engineers with the same criterion of the index system. Then, the test RN value can be obtained after the normalized performance on the scores. Finally, the error rate VR between TN and RN can be calculated, as shown in Table 4.

As indicated in Table 4, the maximum value of VR of the microstate diagnosis result is 10.8%, while the minimum value is 1.05%. The maximum and the minimum VR values of the median state diagnosis results are 10.4% and 1.12%, respectively. The maximum VR value of the macrostate diagnosis is 7.40%, while the minimum value is 0.81%.

Since the maximum allowable test deviation of the Chinese large-scale construction project implementation status diagnosis system is ±15% [31], the macro- and mesoresults by the proposed diagnosis index system can fully meet the requirements. Consequently, the ongoing macro and mesostatus of the project can be reflected rapidly with a qualified accuracy.

3.2. Discussion

3.2.1. About Determination of Indicators. The established diagnosis index system, which has been applied in the practical construction projects, includes many kinds of diagnosis indicators. Generally, there are three types of diagnosis indicators.

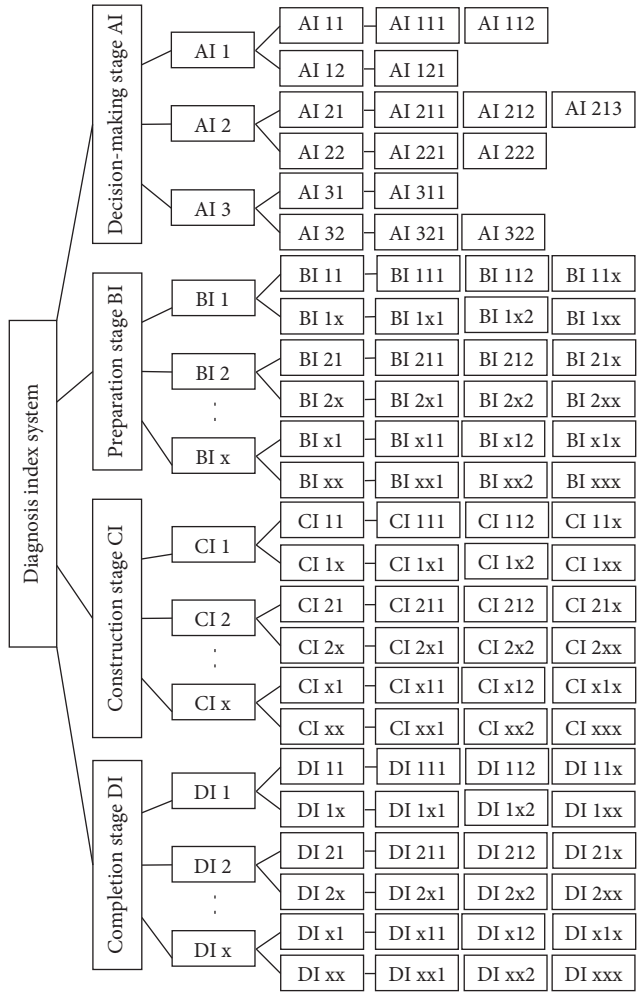

Figure 2: Diagnosis index system for implementation state of large-scale construction projects.

The first type is that which has clarified indicators. Taking the project quality as an example, the national standard named *Unified Standards for Acceptance of Construction Quality* has clear items about the assessment method as well as the specific parameters such as the dimensions, the flatness, the perpendicularity, and the mechanical mechanics' properties of the materials.

The second type is the indicators which have already been attached to the project, such as the project investment, the construction scale, the construction area, the completion time, and the concerned regulations that have been already made in advance. Once the project is carried out, the exact limitations will be applied to these indicators such as the money, the period, the materials, and the sites. Consequently, the corresponding indicators can be set up according to the exact limitations.

The third type is the indicators without specific and clear standards, such as the work efficiency of the staff and the coordination efficiency. Due to the diversity of the project, the management contents will be adjusted and revised according to varied project requirements. However, there are still two common characteristics for these indicators. First, these indicators are often determined in a qualitative or semiquantitative form. Second, although these indicators satisfy all the specific requirements and rules of an actual project, most contents of these indicators are still universal.

In practical engineering, to make full use of the established standards and regulations, the project managers often carry out the evaluation by means of giving an exact score to the implementation effect. This method has been widely used in practice and has received common acceptance. This kind of method provides a good reference for the indicator establishing in construction projects. To make this method not only satisfy all of the requirements of the projects but also practically applied in actual engineering, the detailed contents of the standards and rules are divided into different items which can be evaluated by varied scores. Consequently, the quantitative indicators are brought into the

Table 4: Effectiveness comparison of the diagnosis index system.

Macrostate	Medium state				Microstate							
	Diagnosis index	*TN*	*RN*	*VR* %	Diagnosis index	*TN*	*RN*	*VR* %	Diagnosis index	*TN*	*RN*	*VR* %
Decision-making stage *TN*: 0.87 *RN*: 0.81 *VR*: 7.40	Project plan	0.82	0.77	6.49	Conception value	0.77	0.72	6.94	Information acquire rate	0.85	0.80	6.25
									Improved rate	0.71	0.65	9.23
					Suggestion value	0.88	0.89	1.12	Work-efficiency ratio of report	0.88	0.89	1.12
	Feasible process	0.93	0.87	6.89	Feasible condition	0.94	0.86	9.30	Data reliable rate	0.96	0.87	10.3
									Condition satisfied rate	0.92	0.83	10.8
									Work-efficiency ratio of report	0.95	0.92	3.26
					Feasible analysis	0.93	0.89	4.49	Method correctness rate	0.96	0.95	1.05
									Feasibility content comprehensive rate	0.89	0.82	8.53
	Decision for approval	0.86	0.79	8.86	Project decision	0.87	0.80	8.75	Work-efficiency ratio of decision	0.87	0.80	8.75
									Rule disobeying rate	0.00	0.00	0.00
					Project approval	0.85	0.77	10.4	Work-efficiency ratio of approval	0.85	0.77	10.4

original qualitative management items, and all of the diagnosis indicators of the index system can be fully determined.

3.2.2. About Standardization of Indicators. During the assessment of the project implantation status, the analytical results obtained based on different standards include both qualitative indicators and quantitative indexes. Hence, the diagnosis results of the indexes are diversified. For the sake of the normalized evaluation, all of the diagnosis results need to be quantified. Generally, there are three types of diagnosis results, namely, the qualitative results, the quantitative results, and the semiquantitative results.

For the first type, the exact values can be obtained according to the national and departmental standards. For the second type, the detailed evaluation values can be obtained based on the difference comparison between the actual and the planned ones. For the third type, the evaluation values can be adaptively obtained based on the comparison between the standard ones and the diagnosis index values given by means of table indexes.

The other issue about the diagnosis standardization is caused due to the diversity of the diagnosis contents. Some of the diagnosis results may be a percentage value, some may be a binarization value which is either zero or one, and some may be numerical values. Therefore, the indicators need to be standardized as well when they are transformed into quantitative forms. In this paper, all of the indicator values are transformed into decimal forms which are in the range of [0, 1] based on the practical experiment experience and experts' professional suggestions.

3.2.3. About the Effect of Index System. In our method, the maximum error rates of the microstate, the median state, and the macrostate are 10.8%, 10.4%, and 7.40%, respectively, while the minimum error rates are pretty satisfied. More details about the results can be found in Table 4.

Obviously, the implementation state of the large-scale construction project can be finely diagnosed based on an exact quantitative index value. Other scholars have also presented other methods to deal with the implementation state diagnosis for large-scale constructions. For instance, Hou Xueliang et al. employed the Kernel Principal Component Analysis (KPCA) and Bayesian Inference to carry out the diagnosis on the construction quality [30, 31]. Comparatively, such a method is more suitable for the qualitative analysis on the implementation state, while our method is able to further obtain the exact index values and therefore seems more refined.

4. Conclusions

This paper proposed a new method to construct the diagnostic index system in large-scale construction projects and carries out the application of the proposed method into a case study for validation. The primary conclusions based on the study can be drawn up as follows:

(1) The establishing method of the index system for the construction projects is essential to the scientific management. However, the current frame of the index system is far from qualified in engineering applications, since the index system for different projects needs too many efforts to concretize and verify the indexes/indicators.

(2) How to scientifically pick the sensitive parameters to form the effective index system is the key point. Since the index parameters refer to many factors, it is significant to select the proper indicators in all-level stages. The Rough Set method based on the evidence theory is an effective approach to determine the appropriate indicators.

(3) It is shown that the diagnostic index system constructed by the proposed method is able to meet the actual management needs of large-scale construction

projects, with qualified scientificity, systematicness, and completeness. Different from the index system constructed by other methods, the indexes/indicators established in this paper are more systematically correlated, with a better hierarchical progression in all levels of the index system.

Particularly, to solve the problem of the large number of indicators referring to the diversity of the diagnosis contents, the proposed method needs to transform the indicator values into the standardized decimal forms which are in the range of [0, 1]. This procedure requests large amount of work and requires qualified experience of the operators. Therefore, there is a limitation of the proposed method which sometimes relies on the practical experiment experience and the experts' professional suggestions. In our next step work, we will carry out a specific study to improve this issue.

Data Availability

The data used to support the findings of this study are available from the corresponding author upon request.

Conflicts of Interest

The authors declare that there are no conflicts of interest regarding the publication of this paper.

Acknowledgments

This work was supported by the National Natural Science Foundation of China (71171081) and the Beijing Natural Science Foundation (9162014).

References

[1] J. Zhu, Z. Chen, and L.-j. Sun, "A method of construction of index system for highway maintenance management," *Procedia - Social and Behavioral Sciences*, vol. 96, pp. 1593–1602, 2013.

[2] A. H. Ibrahim and M. A. Shaker, "Sustainability index for highway construction projects," *Alexandria Engineering Journal*, vol. 58, no. 4, pp. 1399–1411, 2019.

[3] S. Hendiani and M. Bagherpour, "Developing an integrated index to assess social sustainability in construction industry using fuzzy logic," *Journal of Cleaner Production*, vol. 230, pp. 647–662, 2019.

[4] T. Zhao, Y. Jiang, H. Jiang et al., "Index system and methods for comprehensive assessment of cross-border power grid interconnection projects," *Global Energy Interconnection*, vol. 3, no. 6, pp. 532–544, 2020.

[5] A. Lalmi, G. Fernandes, and S. B. Souad, "A conceptual hybrid project management model for construction projects," *Procedia Computer Science*, vol. 181, pp. 921–930, 2021.

[6] Q. Gaosong and Y. Leping, "Measurement of internal audit effectiveness: construction of index system and empirical analysis," *Microprocessors and Microsystems*, vol. 21, p. 104046, 2021.

[7] Z. Dubský, L. Tichý, and D. Pavliňák, "A quantifiable approach to the selection of criteria and indexation for comparison of the gas pipeline projects leading to the EU: diversification rationality against securitisation?" *Energy*, vol. 225, Article ID 120238, 2021.

[8] I. Y. Wuni and G. Q. Shen, "Fuzzy modelling of the critical failure factors for modular integrated construction projects," *Journal of Cleaner Production*, vol. 264, Article ID 121595, 2020.

[9] Y. Elfahham, "Estimation and prediction of construction cost index using neural networks, time series, and regression," *Alexandria Engineering Journal*, vol. 58, no. 2, pp. 499–506, 2019.

[10] P. T. I. Lam, A. T. W. Yu, Z. Wu, and C. S. Poon, "Methodology for upstream estimation of construction waste for new building projects," *Journal of Cleaner Production*, vol. 230, pp. 1003–1012, 2019.

[11] M. Urbański, A. U. Haque, and I. Oino, "The moderating role of risk management in project planning and project success: evidence from construction businesses of Pakistan and the UK," *Engineering Management in Production and Services*, vol. 11, no. 1, pp. 23–35, 2019.

[12] O. Okudan, C. Budayan, and I. Dikmen, "A knowledge-based risk management tool for construction projects using case-based reasoning," *Expert Systems with Applications*, vol. 173, Article ID 114776, 2021.

[13] Y. Lu, P. Gong, Y. Tang, S. Sun, and Q. Li, "BIM-integrated construction safety risk assessment at the design stage of building projects," *Automation in Construction*, vol. 124, 2021.

[14] H. Zhou, Y. Zhao, Q. Shen, Y. Liu, and H. Cai, "Risk assessment and management via multi-source information fusion for undersea tunnel construction," *Automation in Construction*, vol. 111, 2020.

[15] G. Andrea Peñaloza, T. Abreu Saurin, and C. Torres Formoso, "Monitoring complexity and resilience in construction projects: the contribution of safety performance measurement systems," *Applied Ergonomics*, vol. 82, 2020.

[16] Q. Guo, S. Amin, H. Qianwen, and O. Haas, "Resilience assessment of safety system at subway construction sites applying analytic network process and extension cloud models," *Reliability Engineering & System Safety*, vol. 201, 2020.

[17] U. H. Issa, S. A. A. Mosaad, and M. S. Hassan, "Evaluation and selection of construction projects based on risk analysis," *Structures*, vol. 27, pp. 361–370, 2020.

[18] H. O. Elhusseiny, I. Nosair, and A. S. Ezeldin, "Systematic processing framework for analyzing the factors of construction projects' delays in Egypt," *Ain Shams Engineering Journal*, vol. 13, 2021.

[19] J. Boon Hui Yap, P. L. Goay, Y. Bee Woon, and S. Martin, "Revisiting critical delay factors for construction: analysing projects in Malaysia," *Alexandria Engineering Journal*, vol. 60, no. 1, pp. 1717–1729, 2021.

[20] A. Adeboye Fashina, M. Abdillahi Omar, A. Abdullahi Sheikh, and F. F. Fakunle, "Exploring the significant factors that influence delays in construction projects in Hargeisa," *Heliyon*, vol. 7, no. 4, 2021.

[21] I. M. Mahdi, M. E. Ahmed, and R. Khallaf, "Decision support system for optimum soft clay improvement technique for highway construction projects," *Ain Shams Engineering Journal*, vol. 11, no. 1, pp. 213–223, 2020.

[22] M. Abdul Nabi, I. H. El-adaway, and C. Dagli, "A system dynamics model for construction safety behavior," *Procedia Computer Science*, vol. 168, pp. 249–256, 2020.

[23] A. Banakar, "Combined application of decision tree and fuzzy logic techniques for indexes," *Journal of Process Engineering*, vol. 40, no. 3, pp. 1212–1218, 2017.

[24] K. Liu and Q. I. Song, "Application of index weighting system in large-scale construction project management," *Architecture, Building Materials and Engineering Management*, vol. 75, pp. 390–394, 2015.

[25] X. Hou and Y. Li, "Research on meticulous collection methods of construction information for engineering projects," in *Proceedings of the 3rd International Conference on Engineering Technology and Application*, pp. 321–326, Aizu-Wakamatsu Japan, November 2016.

[26] H. Qiao, "Evidence science from evidence based perspective," *Evidence Science*, vol. 21, no. 2, pp. 566–573, 2013.

[27] R.-l. Pan, L. Yuan-qin, and H.-l. Zhang, "Fuzzy-rough attribute redecution algorithm based on α information entropy," *Control and Decision*, vol. 32, no. 12, pp. 340–348, 2016, in Chinese.

[28] Z. Xu and Y. Hu, "The diagnosis of aero-engine's state based on rough set," in *Proceedings of the 6th Workshop on Rough Set Theory*, pp. 301–307, Santiago, Chile, December 2016.

[29] S. Hu and X. Xie, "Research on dynamic topological relationship between area and area based rought set," *Journal of Henan Polytechnic University (Natural Science)*, vol. 34, no. 3, pp. 356–366, 2015, in Chinese.

[30] X. Hou, *Method to Pick Management Index of Construction Project and its Application*, China Electric Power Press, Beijing, China, 2014, in Chinese.

[31] X. Hou and Y. Wang, "On-line diagnosis model of construction project quality status and its simulation based on KPCA and bayesian inference," *Journal of System & Management*, vol. 24, no. 4, pp. 472–479, 2015, in Chinese.

Hindawi
Mathematical Problems in Engineering
Volume 2021, Article ID 6616037, 14 pages
https://doi.org/10.1155/2021/6616037

Research Article

Performance Analysis of Tyre Manufacturing System in the SMEs Using RAMD Approach

K. Velmurugan[1], **P. Venkumar**[1] and **R. Sudhakarapandian**[2]

[1]*Department of Mechanical Engineering, Kalasalingam Academy of Research and Education, Krishnankoil-626126, Tamil Nadu, India*
[2]*School of Mechanical Engineering, Vellore Institute of Technology VIT, Vellore-632014, Tamil Nadu, India*

Correspondence should be addressed to R. Sudhakarapandian; sudhame@gmail.com

Received 31 December 2020; Revised 8 April 2021; Accepted 13 May 2021; Published 28 May 2021

Academic Editor: Abdullahi Yusuf

In the recent trends, production plants in the automobile industries all over the world are facing a lot of challenges to achieve better productivity and customer satisfaction due to increasing the passenger's necessity and demand for transportation. In this direction, the belt, tyre, and tube manufacturing plants act as vital roles in the day-to-day life of the automobile industries. Tyre production plant comprises five major units, namely, raw material selection, preparation, tyre components, finishing, and inspection. The main purpose of this research is to implement the new method to predict the most critical subsystems in the tyre manufacturing system of the rubber industry. As mathematically, any one maintenance parameter among reliability, availability, maintainability, and dependability (RAMD) parameters is evaluated to identify the critical subsystems and their effect on the effectiveness of the tyre production system. In this research, the effect of variation in maintenance indices, RAMD, is measured to identify the critical subsystem of the tyre production system based on the mathematical modeling Markov birth-death approach (MBDA), and the equations of the subsystems are derived by using the Chapman–Kolmogorov method. Besides, it also calculates the performance of certain maintenance parameters concerning time such as mean time between failures (MTBF), mean time to repair (MTTR), and dependability ratio for each subsystem of the tyre production system. Finally, RAMD analysis of the tyre production systems has been executed for predicting the most critical subsystem by changing the rates of failure and repair of individual subsystems with the utilization of MATLAB software. RAMD analysis reveals that the subsystem bias cutting is most critical with the minimum availability of 0.8387, dependability 5.19, dependability ratio 0.8701, and maximum MTTR 38.46 hours of the subsystem. In this implementation of the proposed method, a real-time case study of the industrial repairable system of tyre manufacturing system has been taken for evaluating RAMD indices of the production plant of rubber industry cited in the southern region of Tamil Nadu, India.

1. Introduction

In the recent trends, in the last few decades, logistics and transportation have rapidly increased throughout the world due to the customers or passenger's necessity, and the population explosion. In that situation, the demand for the automobile industrial product (tyre, tube, and belt) manufacturing also maximized. The manufacturing process of the automobile industry consists of lots of subsystems and components. The effectiveness of the entire production system closely depends on the availability of the individual machines and their critical components [1]. The better productivity and availability of the manufacturing system can be achieved through the utilization of the proper maintenance strategy. Hence, the prediction of the critical subsystems, machines, and their components is an essential activity for a better maintenance management system in the industry. The effectiveness and performance of the production system can easily be obtained by identifying the critical subsystems, machines, and components earlier. The important maintenance parameters, RAMD, of the manufacturing system are evaluated with different selections and combinations of repair, failure rates of the individual manufacturing machines, and their components in the shop

floor area with the utilization of the mathematical modeling and analysis. From the mathematical analysis results, significant changes in the availability of the individual subsystems, the most critical subsystem, and its components are identified. Besides, other maintenance parameters (MTBF, MTTR, dependability, and dependability ratio) are also evaluated and analyzed to identify the critical subsystems in the manufacturing system of industry. This section also presents the critical overview of the various published research articles based on the RAMD analysis of the different manufacturing systems, applications, challenges, and opportunities of mathematical modeling in the industries.

Performance evaluation of the milk production industry is described, and the reliability and availability of the milk production systems are analyzed through the application of the MINITAB software package with the different mathematical analysis techniques of RAM engineering. Also, the RAM of all individual workstations in the dairy industry is evaluated [2, 3]. RAM analysis of the reciprocating compressor in the oil and gas refinery industry has been described, and the operational performance of the compressor has been identified based on the genetic failure database with the application of the mathematical method tools and engineering techniques such as MTBF and availability of the equipment in the oil and gas industry. This research has been analyzed to develop a new model maintenance strategy to address real-time challenges in the industry's maintenance management system [4]. Reliability-centred maintenance (RCM) and redundancy allocation problem (RAP) have been discussed, and the maintenance scheduling of the repairable subsystems is analyzed through the application of three different metaheuristic algorithms such as nondominated sorting genetic algorithm (NSGA-II), multiobjective particle swarm optimization (MOPSO), and multiobjective firefly algorithm (MOFA) for implementing the novel integrated model to optimize the RCM and RAP in the industrial applications [5].

A real case study of planning the tunnel construction problems is described, and the suitable and optimal planning of the tunnel evacuation process is predicted through the simulation techniques such as Markov chain and Monte Carlo simulation techniques. With this proposed model, the optimal planning model has been implemented with reduced total cycle time of the tunnel evacuation process [6]. Implementation of the optimal Six Sigma strategy in the bag production systems through the utilization of the Define, Measure, Analyze, Improve, and Control (DMAIC) approach and RAM analysis was illustrated. This analysis estimates the nature of the downtime pattern of the bag production system concerning the RAM changes [7]. The real-time case study of the transport systems has been discussed, and the optimal travel routes are predicted based on the utilization of the three different mathematical models such as hidden Markov model, K-means algorithm, and Laplace smoothing techniques. The effectiveness of the route prediction is increased by organizing the optimal train model of this proposed research result [8]. Optimal maintenance and production planning for a deteriorating production system are advised using joint optimization and Monte Carlo simulation techniques. The proposed results organize the best and optimal scheduling framework with the minimum expected cost per unit time of the production [9]. Two objectives such as addressing the uncertainty in maintenance budgeting and rehabilitation problems in the pavement have been analyzed with an application of the two stages of stochastic models in integer programming [10].

Conditional maintenance strategy simulation and sensitivity analysis model with energy consumption and carbon dioxide emissions of the production system are explained to the reduction of the total maintenance cost, environmental impact, and improvement of maintenance plan [11]. The significant issues of the real-world problems in fault detection in the industrial manufacturing process have been explained. We resolve these problems by the application of the novel method combination of the Markov Chain and generalized projection nonnegative matrix factorization (MCM GPNMF) for diagnosing the faults in the industry [12]. Reliability index analysis of the rock tunnels with the utilization of the high-dimensional model representation (HDMR) function is conducted through combining the response surface method (RSM) and first-order reliability method (FORM). The proposed model reveals the stability of the horseshoe tunnel concerning the reliability index [13]. The mathematical modeling analysis of the impact of the maintenance strategy based on the service life of the flexible pavements concerning the International Roughness Index values of the quarter heavy vehicles has been demonstrated [14]. Performance of the star repairable system with spatial dependence has been discussed, and the reliability of the systems is analyzed with the utilization of the vector Markov process and Laplace transformation methods [15].

The reliability analysis of the milk powder production system is conducted in dairy plants with the application of the Markov process and RAMD approach. The proposed results identified the critical subsystem in the milk powder production system with concerning variation in the values of major maintenance parameters [16]. Identifying the utmost critical operation in the tunnel boring systems in mixed ground conditions has been illustrated, and the RAMD of the individual tunnel boring operations in mixed ground conditions is obtained with the application of the Markov chain process [17]. Performance modeling of the refined systems in the sugar plant has been presented through the application of the Markov birth-death approach. This proposed analysis predicts the most important and sensitive subsystems in the refined system of sugar mills regarding the impact of variations on the reliability of subsystems [18]. Mathematical modeling and performance analysis of the pan crystallization system in sugar plants have been described with the application of the fuzzy reliability analysis and Markov birth-death model. The mathematical models obtain exponential distribution and differential equations of failure, and repair rates in the pan crystallization system of the sugar plant [19]. The performance and analysis of the cooking oil production plant by the application of the Markov mathematical method have been described. Besides, the most critical subsystems of the cooking oil production have been revealed concerning the shift-wise workforce in the industry [20].

We investigate the availability and profit of the power generation in the sewage treatment plant through the application of the MBDA with exponential distribution mathematical technique. It reveals the effect of variations in the availability changes of sewage treatment plants [21]. Performance and evaluation of channel bonding in the wireless local area network have been described. We proposed the better and optimal channel bonding with the utilization of the Markov decision model and modulation and coding scheme technology to the access point analysis of local area wireless network connection [22]. The systematic literature review of the reliability, availability, maintainability, and security/safety (RAMS) for critical infrastructure protection is explained. Identify the emerging field of research in the RAMS and critical infrastructure production technology through this critical overview research [23]. The reliability of centralized traffic control systems in the autonomous station computer system has been described. Besides, the proposed reliability analysis framework can easily predict the failure rate and fault detection probability of autonomous computer stations with the application of the Markov model and fuzzy dynamic fault tree analysis approach [24]. Variable reliability measures (RAMD) of the cloud computing technology have been explained through the application of the reliability, availability, and cost analysis approach [25]. We investigate the different types of fractional modeling problems such as falling body problems and the temperature (heating and cooling) dynamic problem in the building with the application of the Laplace transformation and Atangana–Baleanu fractional derivative in the sense of Caputo (ABC) technologies [26–28]. We investigate the transmission dynamics of pine wilt disease infections by the application of the Caputo fractional operators to analyze the biological observable behavior of the diseases. We provide more efficient and flexible information about the complexity model through the comparative analysis of the previously build integer model [29]. We identify the most critical subsystems during the conceptual designing operation in the industry through the utilization of the Markov analysis for measuring the various parameters such as failure and repair rate. This RAM analysis proposed the optimal result for predicting the sensitive subsystem in the industry concerning the variations of the parameters [30]. They have explained the evaluation of supplier selection in the industry using the hybrid fuzzy decision model for achieving the better customer satisfaction and higher productivity [31].

This research consists of an overview of the research approaches, applications, and challenges mentioned above. This research paper is based on the performance analysis and mathematical model of the tyre manufacturing system in the rubber industry to predict the most critical subsystems in the work environment using the RAMD and Markov birth-death approach. This research technique is widely used for RAM engineering because the upcoming behaviors of a particular machine can be easily predicted by analyzing the current variables of the machine. The main motive of this research analysis is to minimize unnecessary breakdown of machines and production delay due to sudden failure of machines. Furthermore, we enhance the availability, productivity, and efficiency of the maintenance workforce through this research analysis in the rubber industry.

This research article has been organized into seven sections. The first section presents the introductory maintenance, a critical overview of the existing literature, and the motivation of this research. In Section 2, materials and methods of the proposed research have been appended. In Section 3, we deal with the assumptions, notations, and transition state diagrams of the RAMD analysis. In Section 4, we present a detailed description of the tyre manufacturing system in the rubber industry. In Section 5, numerical and graphical results of the RAMD variations are discussed through the table and graph. Section 6 presents the discussions about the RAMD findings of the tyre manufacturing system. Finally, the conclusion and future scope of this research have been illustrated in Section 7.

2. Materials and Methods

2.1. Markov Birth-Death Process. It is the most widely used mathematical and stochastic process to measure the maintenance parameters (RAMD) of the production systems concerning three different state conditions. This mathematical approach was introduced by the Russian mathematician Andrey Andreyevich Markov to solve sequential problems. It analyzed the present state behavior of the system to identify the future state condition of that particular system [32]. It is the best and optimal tool for the RAMD analysis because of the redundancy management of sequential arrangement problems, and it can easily predict the repairable production systems. The steady-state and transition state of the subsystems can be analyzed through the application of stochastic modeling approaches such as the Markov process and quenching process. This approach, also called Markov decision process (MDP), is further classified into the discrete and continuous state transition process (Markov process and Markov chain).

2.2. Reliability. Reliability is the most important maintenance parameter; it simply denotes "$R(t)$" which means the probability that failure of the systems may not occur in the given specific time interval in the working environment [33]. The $R(t)$ of individual systems and subsystems concerning the rate of failure can be expressed as follows:

$$R(t) = e^{-\lambda t}. \tag{1}$$

2.3. Availability. Availability of the repairable systems simply defined as the ratio of the uptime to the total lifetime of the particular production system is denoted as "Av," or it integrates both reliability and maintainability parameters concerning the number of failures occurring and how quickly that fault will be rectified. The Av of the systems can be expressed as follows:

$$Av = \frac{X}{X+Y} \Rightarrow \frac{\lambda}{\lambda+\mu}, \tag{2}$$

where X = uptime or lifetime, Y = downtime or repair time, and $X + Y$ = total life time.

The uptime of the systems is represented by the mean time to failure (MTTF) which can be measured through the failure analysis of the systems [33]. The mean time to repair (MTTR) can be evaluated through the maintenance analysis of the given system. The estimation of repair time is represented as follows:

$$Av = \frac{MTTF}{MTTF + MTTR}, \tag{3}$$

$$MTTF = \int R(t)\mathrm{d}t \Rightarrow \int_0^{\alpha} e^{-\lambda t}\mathrm{d}t \Rightarrow \frac{1}{\lambda}, \tag{4}$$

$$MTTR = \left(\frac{1 - Av}{Av}\right)MTTF. \tag{5}$$

Equation (3) expressed the availability measuring, equation (4) expressed the MTTF measuring, and equation (5) expressed the MTTR measuring of the manufacturing systems.

2.4. Maintainability. Defined as the probability function of that failed system, subsystems and their components are restored into the original or operative condition in the given specific time interval (downtime) that is denoted as "$M(t)$" [34]. The $M(t)$ of the industrial repairable systems can be expressed as follows:

$$M(t) = 1 - e^{-\mu t}. \tag{6}$$

2.5. Dependability. Dependability is another most important maintenance parameter measure; it is simply defined as the system's ability to deliver the service with a specific time interval concerning the assumption of the rate of failure and repair of the production system [35]. The dependability and its ratio "D_{Min}" of the repairable industrial system can be expressed as follows:

$$d = \frac{MTTF}{MTTR}, \tag{7}$$

$$D\mathrm{min}_i = \left[1 - \left(\frac{1}{d-1}\right)\left(e^{-\ln d/(d-1)} - e^{-d\ln d/(d-1)}\right)\right]. \tag{8}$$

3. Notations and Assumptions

The notations and assumptions used for RAMD analysis of the tyre manufacturing model are provided. The tyre manufacturing system of the rubber industry is described briefly, and maintenance problems of this system are discussed. Achieving better availability of production machinery and its equipment at this shop floor is one of the major problems of the rubber industry. The transition state diagram of the tyre manufacturing machines is illustrated in Figure 1.

3.1. Notations. The various notations used for this RAMD analysis research in the tyre manufacturing system of the rubber industry are given as follows:

SBM, SBB, SCL, SBC, SEX, SBD, and SCU working state of the machines

SBM, SBB, SCL, SBC, SEX, SBD, and SCU under maintenance state of the machines

∗SBM, ∗SBB, ∗SCL, ∗SBC, ∗SEX, ∗SBD, and ∗SCU repair state of the machines

BM: Banbury mixing subsystem

BB: bead and belt cord manufacturing subsystem

CL: calendaring subsystem

BC: bias cutting subsystem

EX: extruding subsystem

BD: building subsystem

CU: curing subsystem

λ_i: failure rate of the subsystems (i = BM, BB, CL, BC, EX, BD, and CU)

μ_i: repair rate of the subsystems

ϕ_i: transition rate of the subsystems

η_i: PM rate of the subsystems

b: constant (0 for ideal and 1 for faulty)

$P_0(t)$: the probability function of subsystems is in the original state

$P_1(t)$: the probability functions of the respective subsystems are in the under maintenance state

$P_2(t)$: the probability functions of the respective subsystems are in the repair state

3.2. Assumptions. Here, the RAMD analysis of the tyre manufacturing system maintenance model in this research article confirms the following assumptions:

(i) Initially, every subsystem is in the original state or good (BM, BB, CL, BC, EX, BD, and CU)

(ii) The rate of repair and failure of every subsystem is constant and statistically independent (λ_i, μ_i = constant) (i = BM, BB, CL, BC, EX, BD, and CU)

(iii) Every repaired system is considered as good as new

(iv) The single maintenance team to handle the PM of the subsystem

(v) Every subsystem has three state conditions such as original, under maintenance, and repair (e.g., S, S, and ∗S)

(vi) The simultaneous failures of the subsystems are not considered

(vii) The rate of PM and transition of the critical systems are taken as constant (ηi, ϕ_i = constant)

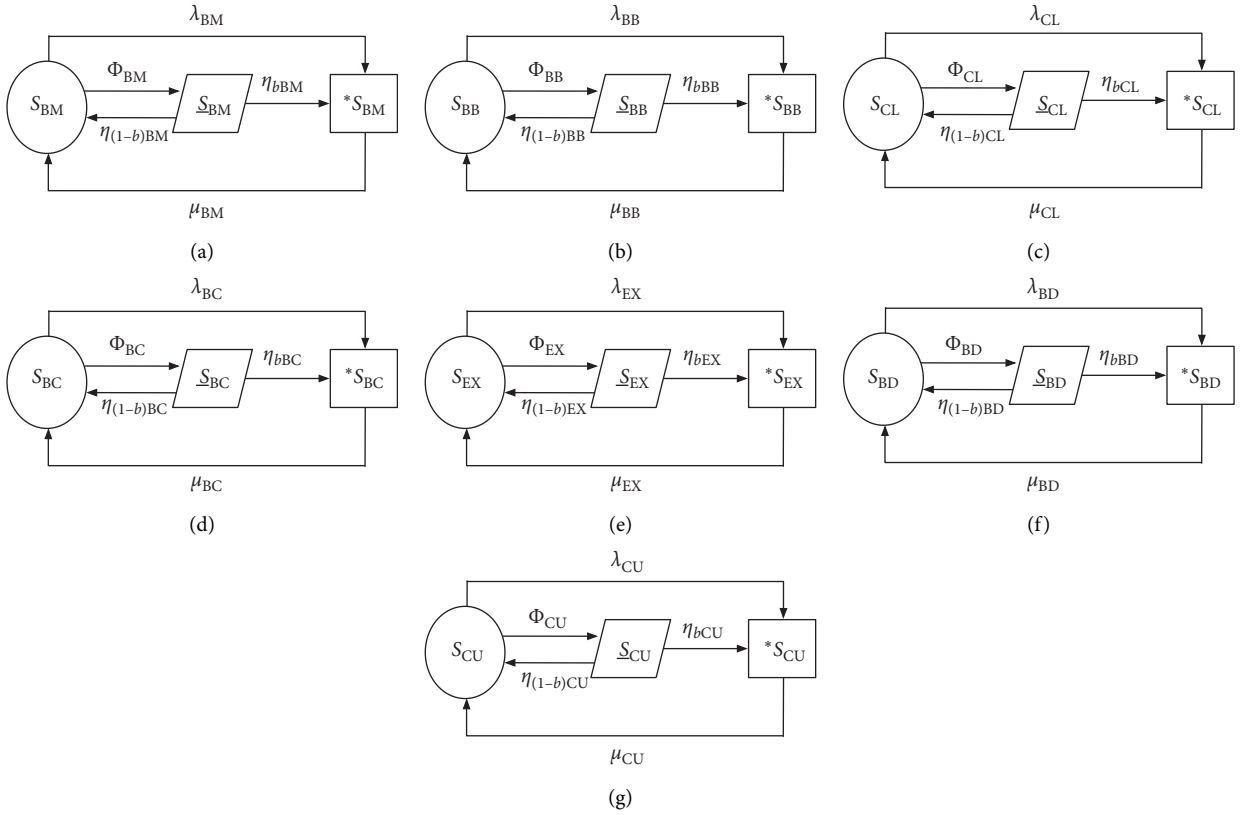

Figure 1: Transition state diagram of tyre production systems.

4. Description of Tyre Manufacturing System

In this research, all the maintenance parameters measured are derived on the subsystem wise. The rate of failure and repair of all the subsystems are considered exponentially distributed. In this section, a detailed description of the tyre manufacturing plant has been presented. The tyre manufacturing plant has five major systems such as material selection, initial preparation, tyre component preparation, finishing, and inspections. The graphical representation of the tyre manufacturing system is illustrated in Figure 2. These systems majorly considered several subsystems such as Banbury mixing, bead and belt cord manufacturing, calendaring, bias cutting, extruding, building, and curing. All the subsystems are arranged in the series operation architecture, and these subsystems have internal redundancy. A detailed explanation of the tyre production systems is given as follows.

4.1. System A (Raw Materials). The tyre production system consists of these major materials such as rubber, textiles, carbon black, sulfur, and other chemical additives. Rubber is the major raw material (natural and synthetic rubber), and it has been collected from various places such as Kerala. The other ingredient is carbon black which is in a fine powder form. It has been added to the raw rubber for the softening process in the tyre production system. Then, sulfur and some chemical additives are added into the raw rubber to achieve the required tyre characteristics such as friction and ultraviolet radiation.

4.2. System B (Preparation). The tyre manufacturing process preparation is the initial operation, and it has some series operating subsystems such as Banbury mixing and bead and belt cord manufacturing. A detailed description of the subsystems is given below.

4.2.1. Banbury Mixing (Subsystem BM). It is the initial process of the tyre manufacturing system, the mixing of raw materials (natural and synthetic rubber, carbon black, sulfur, and other chemical additives), and forming the rubber compound through the application of the computer control system. That controls the composition of rubber, and chemical mixing automatically depends upon the required tyre parts.

4.2.2. Bead and Belt Cord Manufacturing (Subsystem BB). In this section, the mixed rubber compounds are further heated for softening the mix and evenly distributing the chemical additives. Once it is completed, that mixed compound feeds into the two sets of rollers and rotates the different directions of the powerful rolling mill that presses and squeezes the mixed rubber compound and makes the thick sheet. Those sheets are utilized to produce the specific part (bead and belt cord) of the tyre components covered

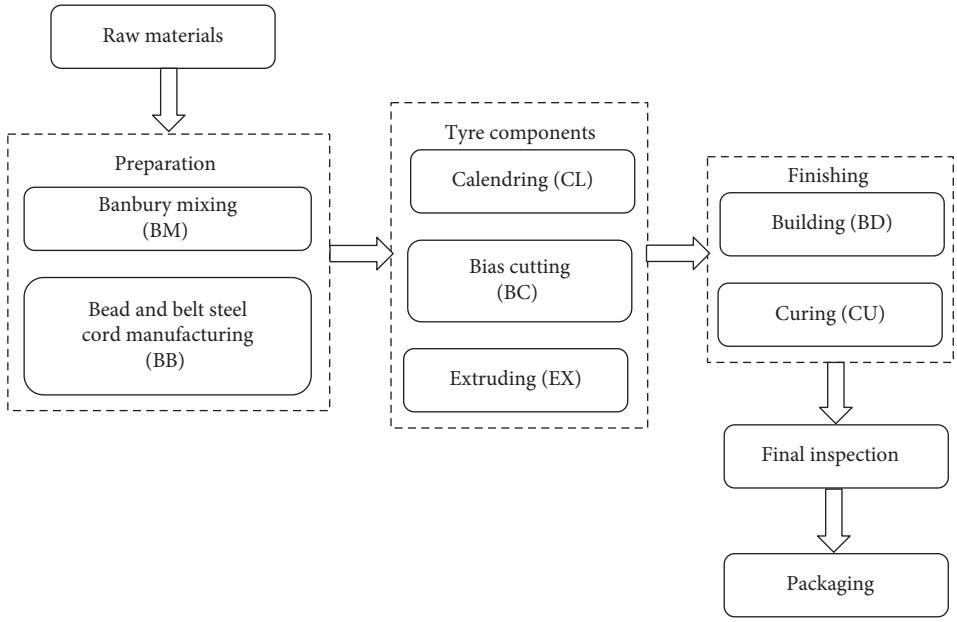

Figure 2: Manufacturing process of a tyre production system.

with a combination of textile and fabric. This final rubberized fabric was used to build the layer of the tyre called a ply.

4.3. System C (Tyre Components). This section consists of the three different subsystems that the manufacturing process applied to produce the tyre components. The detailed description of the tyre component production subsystems is explained below.

4.3.1. Calendaring (Subsystem CL). After completing the mixed rubber compounds that will feed into the calendering operation for reducing the thickness of the rubber-mixed compound, we released the porous gases and gravidities in the rubber-mixed compounds through the application of the powerful rolling operation. This calendaring subsystem has some major activities such as (1) to create the mixed rubber compound as a uniform thick sheet with specific dimensions and (2) to prepare the initial coats of rubber on the textile fabric, to insert the steel or textile fabric in the rubber compound through friction.

4.3.2. Extruding (Subsystem EX). In the extruding operations, the mixed rubber compound feeds into the extruder machine and then forced out through the die with the required shape of an orifice to produce the required size and shape of the tyre components. The large, flat sheet of the tyre treads is developed by the extruding process.

4.3.3. Bias Cutting (Subsystem BC). After the calendaring and extruding operations are completed, flat rubber sheets move into the conveyor to the bias cutting operation. In that situation, we cut the required shape and size of the flat rubber sheets with the application of the grating blade.

4.4. System D (Finishing). This section consists of the two subsystems of the final operation in the tyre manufacturing process. The detailed demonstration of the subsystems is given as follows.

4.4.1. Building (Subsystem BD). This system is also called the tyre assembly process after the bias cutting process that stripped textile fabric rubber compound sheets, and other tyre components (bread, plies, sidewall, and treads) are assembled on the drum of the building machine to form the "green tyre" through this operation.

4.4.2. Curing (Subsystem CU). Finally, that green tyre goes to the vulcanizing process that is placed on the large mold of the curing machine that is called the bladder. That bladder filled with the high pressure and temperature steams during this operation green tyre is vulcanized up to 280° within the specified time limit. After completing the curing operation, the finished tyre will go to the cooling process and then quality checking activity.

4.5. System E (Inspection). After the vulcanizing process is completed, the finished tyre is moved into the quality and inspection process. In that situation, each tyre is thoroughly inspected with the application of various techniques such as visual inspection, destructive, and nondestructive inspection techniques, and based on these techniques, the flaws are identified such as bubbles and voids in the tyres. Once they completed the inspection and satisfy the required quality, the final product is moved into the packaging section and then stored in the warehouse for customer distribution.

5. Numerical and Graphical Result

The real-time case study of the RAMD analysis in the tyre manufacturing system of the rubber industry has been evaluated by applying the last five-year maintenance record data of the individual subsystems in the tyre manufacturing system [36, 37]. The input numerical values of RAMD analysis for applying the mathematical modeling are illustrated in Table 1.

5.1. RAMD Indices of the Tyre Manufacturing Subsystems. This research analyzed the performance of the tyre production systems in the rubber industry. The description of the tyre production system is presented in the previous section. That production system has seven numbers of subsystems to achieve tyre production. All the subsystems are arranged in the series configuration production process in the manufacturing plant. Hence, the maintenance parameters (RAMD) of all the subsystems are measured through the utilization of the Markov birth-death process and the mathematical equations are derived by using the differential-difference equations [36, 37]. The basis of the Markov birth-death approach sample transition state diagram and the mathematical modeling of the reference subsystems is graphically represented in Figure 3. The recurrence relationship of subsystems with derived mathematical equations is as follows:

$$P_0'(t) = \eta_{i(1-b)}P_0(t) + \mu_i P_{2(t)} - \varphi_i P_{0(t)} - \lambda_i P_{0(t)}, \quad (9)$$

$$P_1'(t) = \varphi_i P_0(t) - \eta_{i(1-b)}P_{1(t)} - \eta_{ib}P_{1(t)}, \quad (10)$$

$$P_2'(t) = \eta_{ib}P_{1(t)} + \lambda_i P_0(t) - \mu_i P_{2(t)}. \quad (11)$$

In initial state conditions, apply time $t = 0$ in equations (1) to (3). We get

$$\eta_{i(1-b)}P_0 + \mu_i P_2 - \varphi i P_0 - \lambda_i P_0 = 0, \quad (12)$$

$$\varphi i P_0 - \eta_{i(1-b)}P_1 - \eta_{ib}P_1 = 0, \quad (13)$$

$$\eta_{ib}P_1 + \lambda_i P_0 - \mu_i P_2 = 0. \quad (14)$$

Now, applying the normalizing state conditions where $j = 0$, 1, and 2,

$$\sum_{j}^{n} Pj = 1 \Rightarrow P_0 + P_1 + P_2 = 1. \quad (15)$$

Derive equations (1) to (3), and substitute the values of P_0, P_1, and P_2 in equation (8). The availability of the tyre manufacturing subsystems is as follows:

$$AV_i = \left[1 + \left(\frac{\varphi_i}{\eta_{i(1-b)} + \eta_{ib}}\right) + \left(\frac{\varphi_i \times \eta_{ib} + \lambda_i}{\mu_i\left(\eta_{i(1-b)} + \eta_{ib}\right)}\right)\right]^{-1}, \quad (16)$$

where i = BM, BB, CL, BC, EX, BD, and CU, t = time, and if $b = 1$ for faulty state condition and if $b = 0$ for ideal state condition, availability of the tyre manufacturing subsystem in fault state condition is $S_{\mathrm{BM}} = 0.8827$. Availability of the tyre manufacturing subsystem in ideal state condition is $S_{\mathrm{BM}} = 0.9206$. Reliability of the tyre manufacturing subsystems is derived as follows:

$$R_i(t) = e^{-\lambda_i t}, \qquad RBM(t) = e^{-0.008t}. \quad (17)$$

Maintainability of the tyre manufacturing subsystems is derived as follows:

$$M_i(t) = 1 - e^{-\mu_i t}, \qquad M_{\mathrm{BM}}(t) = 1 - e^{-0.150t}. \quad (18)$$

Other maintenance performance parameter measures of the tyre manufacturing subsystems are as follows:

$$MTBF_i = \frac{1}{\lambda_i};$$

$$MTTR_i = \frac{MTBF_i\left(1 - Av_i\right)}{Av_i},$$

$$d_i = \frac{MTBF_i}{MTTR_i};$$

$$D\min_i = \left[1 - \left(\frac{1}{d-1}\right)\left(e^{-\ln d/(d-1)} - e^{-d\ln d/(d-1)}\right)\right], \quad (19)$$

where $MTBF_{\mathrm{BM}} = 125.00$; $MTTR_{\mathrm{BM}} = 16.16$; $d_{\mathrm{BM}} = 7.52$; and $D_{\min\ (\mathrm{BM})} = 0.9025$.

Similarly, we measured the all other individual subsystem maintenance parameters through the application of equations (8) to (18) and the transition state diagram of the individual subsystems are illustrated in Figure 1 for analyzing the total performance of the tyre manufacturing system in the rubber industry.

5.2. Reliability of the System. Since the seven subsystems are arranged in the series configuration of the tyre manufacturing system and if failed, any one of the subsystems causes the entire production system to fail. The reliability of the tyre production system is equal to the product of each subsystem's reliability. Hence, the overall reliability of the tyre production systems is achieved by using the following equation:

$$\begin{aligned} R_{\mathrm{Sys}}(t) &= R_{BM}(t) \times R_{BB}(t) \times R_{CL}(t) \times R_{BC}(t) \times R_{EX}(t) \\ &\quad \times R_{B\,D}(t) \times R_{CU}(t), \\ R_{\mathrm{Sys}}(t) &= e^{-0.008t} \times e^{-0.007t} \times e^{-0.004t} \times e^{-0.005t} \times e^{-0.007t} \\ &\quad \times e^{-0.003t} \times e^{-0.002t}, \\ R_{\mathrm{Sys}}(t) &= e^{-0.036t}. \end{aligned} \quad (20)$$

The effect of changes of all the subsystems and total system reliability concerning the time between 30 and 75 days are analyzed, and results are illustrated in Table 2. The

Table 1: Input numerical values of the RAMD analysis.

Subsystem	Failure rate	Repair rate	Transition rate	PM rate
Banbury mixing	0.008	0.150	0.007	0.70
Bead and belt cord making	0.007	0138	0.005	0.60
Calendaring	0.004	0.290	0.006	0.40
Bias cutting	0.005	0.158	0.003	0.20
Extruding	0.007	0.144	0.008	0.50
Building	0.003	0.244	0.004	0.30
Curing	0.002	0.310	0.002	0.20

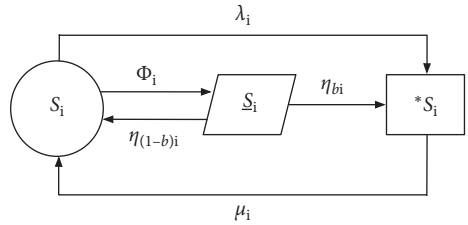

Figure 3: Sample transition state diagram of the subsystem.

reliability variation of the tyre production system pictorial representation is presented in Figure 4. In the graphical representation, horizontal axis denotes the time in days and the vertical axis refers to the reliability of the individual subsystem and entire tyre production system. The reliability of the individual subsystems in the tyre production system has gradually decreased concerning the working time.

5.3. Availability of the System. The availability of the individual subsystems will affect the entire production system because of the series configuration of the manufacturing process in the industry. The availability of the tyre production system equals the product of the individual subsystem's availability. Hence, the overall availability of the tyre production system is demonstrated in the following equation:

The effect of changes of all the subsystems and total system availability concerning the specific rate of failure and repair of the subsystems are analyzed, and results are illustrated in Table 3. The availability variation of the tyre production system graphical representation is presented in Figure 5. In the pictorial representation, the horizontal line denotes the subsystem of the tyre production and the vertical line refers to the availability of the particular subsystem. The spline curve denotes the two different states (faulty and ideal) of availability variations of the individual subsystems in the tyre production system.

$$\begin{aligned} AV_{\text{sys}} &= AV_{\text{BM}} \times AV_{\text{BB}} \times AV_{\text{CL}} \times AV_{\text{BC}} \times AV_{\text{EX}} \\ &\quad \times AV_{\text{BD}} \times AV_{\text{CU}}, \\ AV_{\text{sys}} \text{ at Faulty} &= 0.8827 \times 0.8859 \times 0.9344 \times 0.8387 \\ &\quad \times 0.8555 \times 0.9339 \times 0.9535 = 0.4668, \\ AV_{\text{sys}} \text{ at Faulty} &= 0.9206 \times 0.9153 \times 0.9528 \times 0.8523 \\ &\quad \times 0.8982 \times 0.9485 \times 0.9495 = 0.5535. \end{aligned} \tag{21}$$

5.4. Maintainability of the System. The overall maintainability of the tyre production system can be obtained by utilizing the following equation:

$$\begin{aligned} M_{\text{sys}}(t) &= M_{\text{BM}}(t) \times M_{\text{BB}}(t) \times M_{\text{CL}}(t) \times M_{\text{BC}}(t) \\ &\quad \times M_{\text{EX}}(t) \times M_{\text{BD}}(t) \times M_{\text{CU}}(t), \\ M_{\text{sys}}(t) &= \left(1 - e^{-0.150t}\right) \times \left(1 - e^{-0.138t}\right) \times \left(1 - e^{-0.290t}\right) \\ &\quad \times \left(1 - e^{-0.158t}\right) \times \left(1 - e^{-0.144t}\right) \times \left(1 - e^{-0.244t}\right) \\ &\quad \times \left(1 - e^{-0.310t}\right) = \left(1 - e^{-1.43t}\right). \end{aligned} \tag{22}$$

The effect of changes of all the subsystems and total system maintainability concerning the time between 30 and 75 days are analyzed, and results are illustrated in Table 4.

Table 2: Effect of changes in the reliability of tyre production system.

T (days)	R_{BM}	R_{BB}	R_{CL}	R_{BC}	R_{EX}	R_{BD}	R_{CU}	R_{Sys}
30	0.7866	0.8106	0.8869	0.8607	0.8106	0.9139	0.9418	0.3396
35	0.7558	0.7827	0.8694	0.8395	0.7827	0.9003	0.9324	0.2837
40	0.7261	0.7558	0.8521	0.8187	0.7558	0.8869	0.9231	0.2369
45	0.6977	0.7298	0.8353	0.7985	0.7298	0.8737	0.9139	0.1979
50	0.6703	0.7047	0.8187	0.7788	0.7047	0.8607	0.9048	0.1653
55	0.6440	0.6805	0.8025	0.7596	0.6805	0.8479	0.8958	0.1381
60	0.6188	0.6570	0.7866	0.7408	0.6570	0.8353	0.8869	0.1153
65	0.5945	0.6344	0.7711	0.7225	0.6344	0.8228	0.8781	0.0963
70	0.5712	0.6126	0.7558	0.7047	0.6126	0.8106	0.8694	0.0805
75	0.5488	0.5916	0.7408	0.6873	0.5916	0.7985	0.8607	0.0672

The maintainability variation of the tyre production system graphical representation is presented in Figure 6. The horizontal axis denotes the working time in days, and the vertical axis represents the maintainability of the entire tyre production system in the industry.

5.5. Dependability of the System. The overall dependability of the series configured tyre production system can be obtained by utilizing the following equation:

$$\begin{aligned} D_{\mathrm{Sys(min)}}(t) &= D_{\mathrm{BM(min)}}(t) \times D_{\mathrm{BB(min)}}(t) \times D_{\mathrm{CL(min)}}(t) \\ &\quad \times D_{\mathrm{BC(min)}}(t) \times D_{\mathrm{EX(min)}}(t) \times D_{\mathrm{BD(min)}}(t) \\ &\quad \times D_{\mathrm{CU(min)}}(t), \\ D_{\mathrm{Sys(min)}} &= 0.9025 \times 0.9049 \times 0.9429 \times 0.8701 \\ &\quad \times 0.8823 \times 0.9422 \times 0.9582 = 0.53370. \end{aligned} \tag{23}$$

5.6. Mean Time to Repair. The MTTR of repairable tyre production subsystems concerning the specific availability changes in the subsystems of the tyre production systems is derived through the application of equations (5) or (9). The graphical representation of the MTTR variation is shown in Figure 7. In the pictorial representation, the horizontal axis denotes the individual subsystem of the tyre production and the vertical axis refers MTTR of that particular subsystem. The individual subsystem's MTTR variation can be obtained by applying the following equation:

$$\begin{aligned} MTTR_{\mathrm{BM}} &= \frac{MTBF_{\mathrm{BM}}\left(1 - Av_{\mathrm{BM}}\right)}{Av_{\mathrm{BM}}}, \\ MTTR_{\mathrm{BM}} &= \frac{125\,(1 - 0.8827)}{0.8827} \Rightarrow 16.16\,\mathrm{Hr}. \end{aligned} \tag{24}$$

The summary of all the subsystem maintenance parameters of the tyre production system in the rubber industry is appended in Table 5.

6. Discussion

The RAMD analysis of the numerous subsystems and tyre production systems has been carried out for a real-time case study of the small- and medium-scale rubber industry by assigning the numerical values of the maintenance parameters of the tyre production system as shown in Table 1. The $R(t)$, Av, $M(t)$, D_{Min}, and MTTR of the individual subsystems of the tyre production plant have been revealed in Tables 2–4, and 6. The overall RAMD indices of the tyre production systems concerning the numerical values and the mathematical modeling results have been illustrated in Table 5. The maintenance parameters availability, dependability, and dependability ratio values of the subsystem BM (Banbury mixing) are lower than those of the other subsystems in the overall tyre production system while the MTTR of the particular subsystem is higher than that of all other subsystems. Hence, the more attention is needed to the subsystem BM compared to all other subsystems for achieving the better performance and availability of the tyre production system in the rubber industry. The effect of rate of failure and repair of the subsystem BM on the availability of that particular subsystem is revealed by varying the repair rate of the subsystem BC $\mu_{\mathrm{BC}} = 0.128$ to 0.188, a failure rate of the subsystem BC $\lambda_{\mathrm{BC}} = 0.002$ to 0.008, and other maintenance parameters such as transition rate and preventive maintenance rate of the subsystem BC are taken as a constant value $\eta_{\mathrm{BC}} = 0.003$ and $\phi_{\mathrm{BC}} = 0.2$. The availability of the subsystem BC has been calculated through the application of these values, and results are illustrated in Table 7.

That result shows the availability of the subsystem BC approximately decreases from 3.03 to 2.21% with an increased repair rate of the particular subsystem. However, the availability of the subsystem will increase from 0.59 to 1.36% with an increased failure rate of the subsystem, and the MTTR will decrease by 4.87% approximately. The graphical representation of the availability changes in the subsystem BC concerning the rate of failure and repair is shown in Figure 8. The Av variation of the subsystem BC is entirely different from all other subsystems due to the sudden up and down values of (up to normal) Av changes. Other

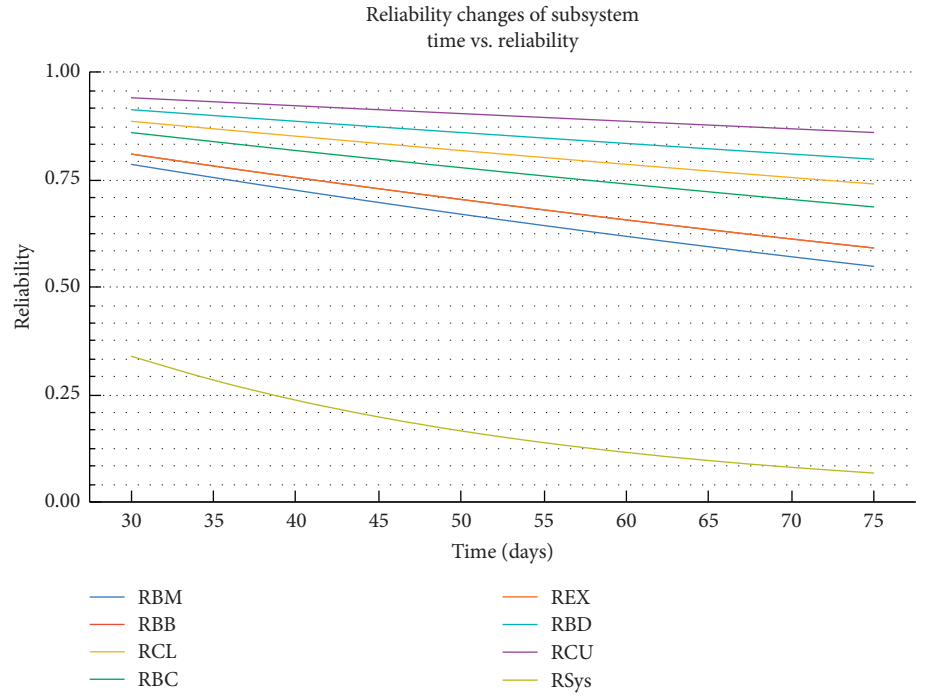

Figure 4: Reliability changes of the tyre production system.

Table 3: Effect of changes in the availability of tyre production system.

Subsystem	Availability at faulty state	Availability at ideal state
Banbury mixing	0.8827	0.9206
Bead and belt cord making	0.8859	0.9153
Calendaring	0.9344	0.9528
Bias cutting	0.8387	0.8523
Extruding	0.8555	0.8982
Building	0.9339	0.9485
Curing	0.9535	0.9594

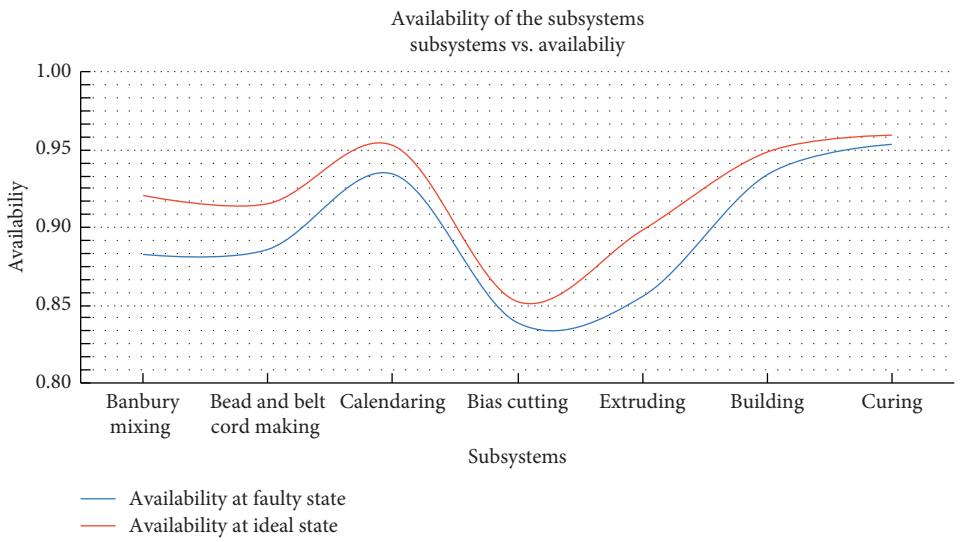

Figure 5: Availability variation of the tyre production system.

Table 4: Effect of changes in the maintainability of a tyre production system.

T (days)	M_{BM}	M_{BB}	M_{CL}	M_{BC}	M_{EX}	M_{BD}	M_{CU}	M_{Sys}
30	0.9889	0.9841	0.9998	0.9913	0.9867	0.9993	0.9999	1.0000
35	0.9948	0.9920	1.0000	0.9960	0.9935	0.9998	1.0000	1.0000
40	0.9975	0.9960	1.0000	0.9982	0.9968	0.9999	1.0000	1.0000
45	0.9988	0.9980	1.0000	0.9992	0.9985	1.0000	1.0000	1.0000
50	0.9994	0.9990	1.0000	0.9996	0.9993	1.0000	1.0000	1.0000
55	0.9997	0.9995	1.0000	0.9998	0.9996	1.0000	1.0000	1.0000
60	0.9999	0.9997	1.0000	0.9999	0.9998	1.0000	1.0000	1.0000
65	0.9999	0.9999	1.0000	1.0000	0.9999	1.0000	1.0000	1.0000
70	1.0000	0.9999	1.0000	1.0000	1.0000	1.0000	1.0000	1.0000
75	1.0000	1.0000	1.0000	1.0000	1.0000	1.0000	1.0000	1.0000

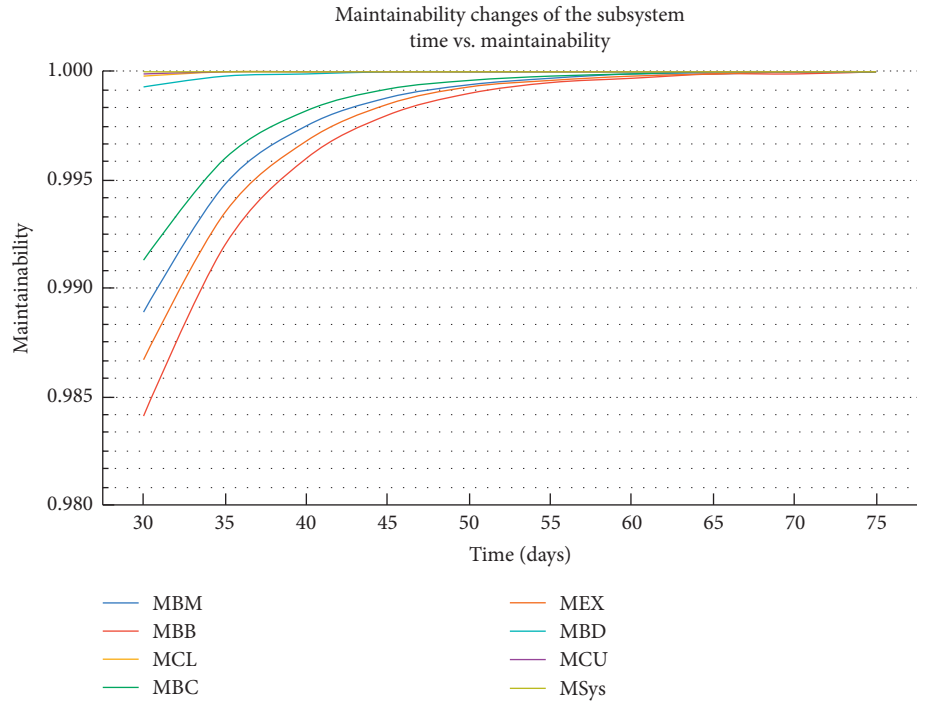

Figure 6: Maintainability changes of a tyre production system.

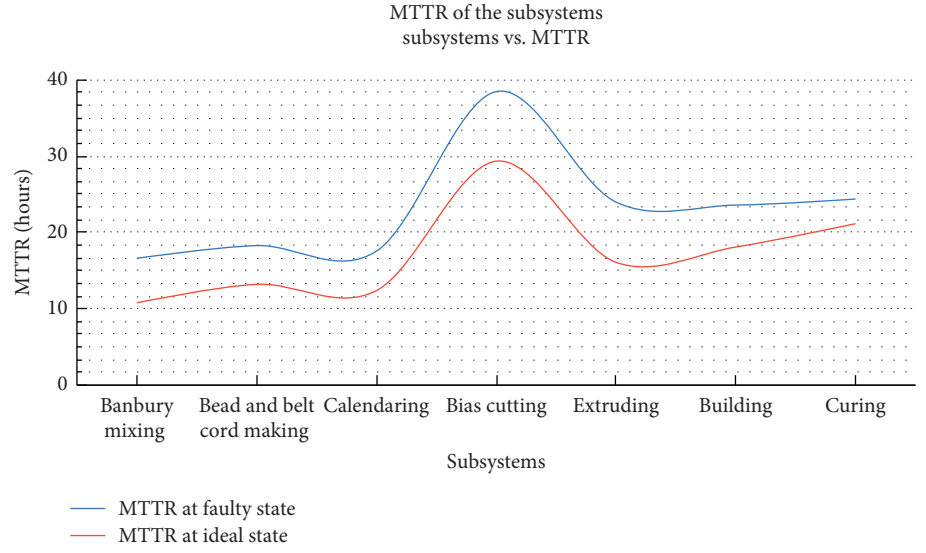

Figure 7: MTTR changes in the tyre production system.

Table 5: RAMD indices for the tyre production system.

RAMD indices	S_{BM}	S_{BB}	S_{CL}	S_{BC}	S_{EX}	S_{BD}	S_{CU}
Reliability	$e^{-0.008t}$	$e^{-0.007t}$	$e^{-0.004t}$	$e^{-0.005t}$	$e^{-0.007t}$	$e^{-0.003t}$	$e^{-0.002t}$
Maintainability	$1-e^{-0.150t}$	$1-e^{-0.138t}$	$1-e^{-0.290t}$	$1-e^{-0.158t}$	$1-e^{-0.144t}$	$1-e^{-0.244t}$	$1-e^{-0.310t}$
Availability (faulty)	0.8827	0.8859	0.9344	0.8387	0.8555	0.9339	0.9535
Availability (ideal)	0.9206	0.9153	0.9528	0.8523	0.8982	0.9485	0.9594
Dependability	7.52	7.76	14.24	5.19	5.92	14.12	20.5
MTTR (faulty)	16.61h	18.28h	17.55h	38.46h	23.98h	23.59h	24.38h
MTTR (ideal)	10.78h	13.21h	12.38h	29.34h	16.09h	18.09h	21.15h
MTBF	125.0h	142.8h	250.0h	200.0h	142.0h	333.3h	500.0h
Dep. ratio D_{Min}	0.9025	0.9049	0.9429	0.8701	0.8823	0.9422	0.9582

Table 6: Effect of changes in the MTTR of a tyre production system.

Subsystem	MTTR at faulty state (hours)	MTTR at ideal state (hours)
Banbury mixing	16.16	10.78
Bead and belt cord making	18.28	13.21
Calendaring	17.55	12.38
Bias cutting	38.46	29.34
Extruding	23.98	16.05
Building	23.59	18.09
Curing	24.38	21.15

Table 7: Availability variations of the subsystem BC concerning the rate of failure and repair.

λ_{BC} / μ_{BC}	0.002	0.003	0.004	0.005	0.006	0.007	0.008
0.128	0.8956	0.9015	0.9068	0.9113	0.9154	0.9191	0.9224
0.138	0.8653	0.8730	0.8798	0.8858	0.8912	0.8960	0.9003
0.148	0.8370	0.8463	0.8544	0.8616	0.8681	0.8740	0.8792
0.158	0.8105	0.8211	0.8304	0.8388	0.8463	0.8530	0.8592
0.168	0.7857	0.7974	0.8078	0.8171	0.8255	0.8331	0.8400
0.178	0.7623	0.7750	0.7863	0.7965	0.8057	0.8140	0.8216
0.188	0.7402	0.7538	0.7660	0.7769	0.7868	0.7958	0.8040
MTTR	**70.197**	**65.322**	**61.096**	**57.433**	**54.194**	**51.319**	**48.756**

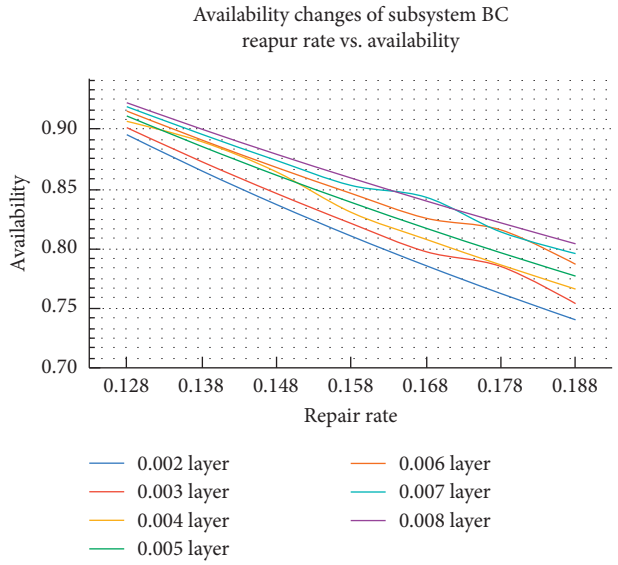

Figure 8: Availability variation of the subsystem BC.

subsystems are having gradual and uniform Av variation while increasing repair and failure rate values of the specific subsystem in the tyre production plant. Figures 5 and 7 reveal the Av and MTTR changes of individual subsystems in the tyre production system of the rubber industry. Table 5 consists of the RAMD indices of the entire subsystem, and based on these results, the subsystem BC has been classified as the most critical subsystem in tyre production. Because of that subsystem BC having the lowest Av, dependability, dependability ratio, and highest MTTR are compared to other subsystems of the tyre production system in the rubber industry.

7. Conclusion

In this RAMD analysis of research, the utilization of the MBDA in measuring the $R(t)$, Av, $M(t)$, d, and $D_{\min}$ of subsystems to the tyre production plant has been demonstrated. The transition state diagram reveals the relationship between the subsystems in the tyre production plant. From the results of the proposed mathematical modeling and analysis, the most important subsidiary system in the tyre manufacturing system in the rubber industry was identified. The subsystem bias cutting is classified as more sensitive and critical than all other subsystems as it has the lowest Av 0.8387, d 5.19, D_{Min} 0.8701, and maximum MTTR of 38.46 hours compared to other subsystems in the tyre manufacturing system. Therefore, it is advisable to monitor the failure and repair rate change of that particular bias cutting subsystem and conclude that the subsystem is very sensitive and highly critical. Then, it is suggested that the maintenance engineer's team of the tyre production plant in the rubber industry should take utmost care and higher attention to maximize the availability, productivity, and effectiveness of the tyre production system of the real-time manufacturing shop floor area of the industry. It is suggested that controlling the maintenance parameter (failure and repair rate) of a more sensitive subsystem through proper maintenance strategy can increase the efficiency of the overall tyre production system in the industry. Finally, the results of this RAMD research are discussed with the maintenance management of the tyre manufacturing plant, as well as to confirm that these proposed structures are highly beneficial to the production and maintenance sectors in the rubber industry.

In the future, this proposed mathematical technology will be used to establish the predictive maintenance management process of smart machines and the health prediction system of its vital components. We intend to implement it with the help of the latest industrial revolution (Industry 4.0) technologies such as Industrial Internet of Things, Cyber-Physical Production Systems, and Internet Communication Technology.

Data Availability

The detailed input numerical data used in this RAMD analysis of the real-time industrial case study are available from the corresponding author upon request. Due to the actual fact that data were collected from the industry, it is used for research purposes only.

Conflicts of Interest

The authors declare that there are no conflicts of interest regarding the publication of this research article.

Acknowledgments

The authors wish to thank the Management of Kalasalingam Academy of Research and Education (KARE), Krishnankovil, Tamil Nadu, India, and Vellore Institute of Technology (VIT), Vellore, Tamil Nadu, India, for their support in this research.

References

[1] G. Sharma and R. Khanduja, "Performance evaluation and availability analysis of feeding system in a sugar industry," *International Journal of Engineering and Applied Sciences*, vol. 3, no. 9, pp. 38–50, 2013.

[2] P. Tsarouhas, "Evaluation of reliability, availability and maintainability of a milk production line," *International Journal of Industrial and Systems Engineering*, vol. 31, no. 3, pp. 324–342, 2019.

[3] P. Tsarouhas, "Statistical techniques of reliability, availability, and maintainability (RAM) analysis in industrial engineering," in *Diagnostic Techniques in Industrial Engineering*, pp. 207–231, Springer, Berlin, Germany, 2018.

[4] F. Corvaro, G. Giacchetta, B. Marchetti, and M. Recanati, "Reliability, Availability, Maintainability (RAM) study, on reciprocating compressors API 618," *Petroleum*, vol. 3, no. 2, pp. 266–272, 2017.

[5] S. Mohammad Zadeh Dogahe and S. J. Sadjadi, "A new biobjective model to optimize integrated redundancy allocation and reliability-centered maintenance problems in a system using metaheuristics," *Mathematical Problems in Engineering*, vol. 2015, Article ID 396864, 16 pages, 2015.

[6] J. P. Vargas, J. C. Koppe, S. Pérez, and J. P. Hurtado, "Planning tunnel construction using Markov chain Monte Carlo (MCMC)," *Mathematical Problems in Engineering*, vol. 2015, Article ID 797953, 8 pages, 2015.

[7] P. Tsarouhas, "Reliability, availability and maintainability analysis of a bag production industry based on the six sigma DMAIC approach," *International Journal of Lean Six Sigma*, vol. 12, 2020.

[8] N. Ye, Z.-Q. Wang, R. Malekian, Q. Lin, and R.-C. Wang, "A method for driving route predictions based on hidden Markov model," *Mathematical Problems in Engineering*, vol. 2015, Article ID 824532, 12 pages, 2015.

[9] X.-Z. Ma and W.-Y. Lv, "Joint optimization of production and maintenance using Monte Carlo method and metaheuristic algorithms," *Mathematical Problems in Engineering*, vol. 2019, Article ID 3670495, 22 pages, 2019.

[10] M. Ameri, A. Jarrahi, F. Haddadi, and M. H. Mirabimoghaddam, "A two-stage stochastic model for maintenance and rehabilitation planning of pavements," *Mathematical Problems in Engineering*, vol. 2019, Article ID 3971791, 15 pages, 2019.

[11] A. Jiang, N. Dong, K. L. Tam, and C. Lyu, "Development and optimization of a condition-based maintenance policy with sustainability requirements for production system,"

Mathematical Problems in Engineering, vol. 2018, Article ID 4187575, 19 pages, 2018.

[12] N. Yuguang, S. Wang, and M. Du, "A combined Markov chain model and generalized projection nonnegative matrix factorization approach for fault diagnosis," *Mathematical Problems In Engineering*, vol. 2017, Article ID 7067025, 7 pages, 2017.

[13] H. Zhao, "High dimension model representation-based Response Surface for reliability analysis of tunnel," *Mathematical Problems in Engineering*, vol. 2018, Article ID 8049139, 10 pages, 2018.

[14] M. Ruiz, L. Ramirez, F. Navarrina, M. Aymerich, and D. López-Navarrete, "A mathematical model to evaluate the impact of the maintenance strategy on the service life of flexible pavements," *Mathematical Problems in Engineering*, vol. 2019, Article ID 9480675, 10 pages, 2019.

[15] L. Wang, Q. Yang, and Y. Tian, "Reliability analysis of 6-component star Markov repairable system with spatial dependence," *Mathematical Problems in Engineering*, vol. 2017, Article ID 9728019, 7 pages, 2017.

[16] A. Aggarwal, S. Kumar, and V. Singh, "Performance modeling of the skim milk powder production system of a dairy plant using RAMD analysis," *International Journal Of Quality & Reliability Management*, vol. 32, 2015.

[17] A. Kr Aggarwal, S. Kumar, and V. Singh, "Performance modeling of the serial processes in refining system of a sugar plant using RAMD analysis," *International Journal Of System Assurance Engineering And Management*, vol. 8, pp. 1910–1922, 2018.

[18] A. K. Agrawal, V. M. S. R. Murthy, and S. Chattopadhyaya, "Investigations into reliability, Maintainability and availability of tunnel boring machine operating in mixed ground condition using Markov chains," *Engineering Failure Analysis*, vol. 105, pp. 477–489, 2019.

[19] O. Dahiya, A. Kumar, and M. Saini, "Mathematical modeling and performance evaluation of A-pan crystallization system in a sugar industry," *SN Applied Sciences*, vol. 1, p. 339, 2019.

[20] A. Yaghoubi, S. Rahimi, R. Soltani, and S. T. Akhavan Niaki, "Availability analysis of a cooking oil production line," *Journal of Optimization in Industrial Engineering*, vol. 14, no. 1, pp. 1–9, 2021.

[21] M. Saini, D. Goyal, A. Kumar, and D. Sinwar, "Investigation of performance measures of power generating unit of sewage treatment plant," *Journal of Physics: Conference Series*, vol. 1714, no. 1, 2021.

[22] M. Stojanova, T. Begin, and A. Busson, "A Markov model for performance evaluation of channel bonding in IEEE 802.11," *Ad Hoc Networks*, vol. 115, p. 102449, 2021.

[23] S. Pirbhulal, V. Gkioulos, and S. Katsikas, "A systematic literature review on RAMS analysis for critical infrastructures protection," *International Journal of Critical Infrastructure Protection*, vol. 33, p. 100427, 2021.

[24] L. Yan, T. Zhang, Y. Gao, R. Wang, and S. Ding, "Reliability analysis of station autonomous computer system based on fuzzy dynamic fault tree and Markov model," *Engineering Reports*, p. 12376, 2021.

[25] M. Manglik, N. Rawat, and M. Ram, "Reliability and Availability analysis of a cloud computing transition system under multiple failures," *International Journal of Quality & Reliability Management*, vol. 37, no. 6/7, pp. 823–835, 2020.

[26] B. Acay, R. Ozarslan, R. Ozarslan, and E. Bas, "Fractional physical models based on falling body problem," *AIMS Mathematics*, vol. 5, no. 3, pp. 2608–2628, 2020.

[27] B. Acay and M. Inc, "Fractional modeling of temperature dynamics of a building with singular kernels," *Chaos, Solitons & Fractals*, vol. 142, p. 110482, 2021.

[28] B. Acay and M. Inc, "Electrical circuits RC, LC, and RLC under generalized type non-local singular fractional operator," *Fractal and Fractional*, vol. 5, no. 1, p. 9, 2021.

[29] A. Yusuf, B. Acay, U. T. Mustapha, M. Inc, and D. Baleanu, "Mathematical modeling of pine wilt disease with Caputo fractional operator," *Chaos, Solitons & Fractals*, vol. 143, p. 110569, 2021.

[30] A. Al-Douri, V. Kazantzi, F. T. Eljack, M. S. Mannan, and M. M. El-Halwagi, "Mitigation of operational failures via an economic framework of reliability, availability, and maintainability (RAM) during conceptual design," *Journal of Loss Prevention in the Process Industries*, vol. 67, p. 104261, 2020.

[31] P. Pandian, P. Venkumar, and S. Rajakarunakaran, "Fuzzy hybrid decision model for supplier evaluation and selection," *International Journal of Production Research*, vol. 51, pp. 3903–3919, 2013.

[32] E. R. Barlow and P. Frank, "Mathematical theory of reliability," *Society for Industrial and Applied Mathematics*, SIAM, Philadelphia, PA, USA, 1996.

[33] K. L. Cavalca, "Availability optimization with genetic algorithm," *International Journal of Quality & Reliability Management*, vol. 20, 2003.

[34] R. K. Sharma and S. Kumar, "Performance modeling in critical engineering systems using RAM analysis," *Reliability Engineering & System Safety*, vol. 93, no. 6, pp. 913–919, 2008.

[35] J. G. Wohl and G. Joseph, "System operational readiness and equipment dependability," *IEEE Transactions on Reliability*, vol. R-15, no. 1, pp. 1–6, 1966.

[36] K. Velmurugan, P. Venkumar, and R. Sudhakarapandian, "Design of optimal maintenance policy using Markov model," *International Journal of Engineering and Advanced Technology*, vol. 9, pp. 907–917, 2019.

[37] K. Velmurugan, P. Venkumar, and R. Sudhakarapandian, "Reliability availability maintainability analysis in forming industry," *International Journal of Engineering and Advanced Technology*, vol. 9, pp. 822–828, 2019.

Hindawi
Mathematical Problems in Engineering
Volume 2020, Article ID 8843657, 11 pages
https://doi.org/10.1155/2020/8843657

Research Article

Layout Design of Stiffened Plates for Large-Scale Box Structure under Moving Loads Based on Topology Optimization

Zhaohua Wang[1], **Chenglong Yang**[1], **Xiaopeng Xu**[2], **Dezhuang Song**[1] and **Fenghe Wu**[1,3]

[1]*School of Mechanical Engineering, Yanshan University, Qinhuangdao 066004, China*
[2]*School of Mechanical Engineering, Luoyang Institute of Science and Technology, Luoyang 471023, China*
[3]*Heavy-Duty Intelligent Manufacturing Equipment Innovation Center of Hebei Province, Qinhuangdao 066004, China*

Correspondence should be addressed to Fenghe Wu; risingwu@ysu.edu.cn

Received 1 October 2020; Revised 27 October 2020; Accepted 28 October 2020; Published 10 November 2020

Academic Editor: Ponnusamy Venkumar

As the main load-bearing structure of heavy machine tools, cranes, and other high-end equipment, the large-scale box structures usually bear moving loads, and the results of direct topology optimization usually have some problems: the load transfer skeleton is difficult to identify and all working conditions are difficult to consider comprehensively. In this paper, a layout design method of stiffened plates for the large-scale box structures under moving loads based on multiworking-condition topology optimization is proposed. Based on the equivalent principle of force, the box structures are simplified into the main bending functional section, main torsional functional section, and auxiliary functional section by the magnitude of loads and moments, which can reduce the structural dimension and complexity in topology optimization. Then, the moving loads are simplified to some multiple position loads, and the comprehensive evaluation function is constructed by the compromise programming method. The mathematical model of multiworking-condition topology optimization is established to optimize the functional sections. Taking a crossbeam of superheavy turning and milling machining center as an example, optimization results show that the stiffness and strength of the crossbeam are increased by 17.39% and 19.9%, respectively, while the weight is reduced by 12.57%. It shows that the method proposed in this paper has better practicability and effectiveness for large-scale box structures.

1. Introduction

The large-scale box structures are widely used in heavy equipment such as machine tools, cranes, and so on. They usually bear the moving loads with the continuous change of position and its stiffness, strength, and weight directly affect the mechanical performance of the equipment. For example, the crossbeam of a machine moves on the gantry and bears the loads from the cutting components. The stiffness directly affects the machining accuracy [1]. The main beam of a large bridge crane bears the moving loads when carrying goods, it moves on the end beam (fixed on the wall), and the strength directly affects the safety of the lifting process [2]. At present, the experience analogy method is mainly used in the design of the large-scale box structures, but the structures are always cumbersome because of the large safety factor, which causes large inertial loads and affects the operation sensitivity. Therefore, the design of large-scale box structures with high stiffness, high strength, and low weight is the long-term goal of engineers.

The box structures are composed of external skin and internal stiffened plates, and the essence of lightweight design is to optimize the layout and size parameters of the internal stiffened plates [3]. At present, the researches on the layout optimization of two-dimensional (2D) stiffened plates have been widely concerned by many scholars [4–6], while the research on the large-scale three-dimensional (3D) box structures is very few. Some scholars try to realize the lightweight design of the box structures by means of structural bionics. Gao et al. [7, 8] studied the distribution law of the main vein and the secondary vein in the leaf vein, and the bionic design of the internal stiffened plates of a

machine tool column was carried out to improve the structural performance based on the principle of similarity. But the design idea is subjective in the selection of the biological prototype as well as structural design, which lacks a theoretical basis. In references [9–12], a method for optimizing the layout of stiffened plates in the box structures is proposed according to the growth mechanism of the biological branching system in nature. The stiffened plates grow, bifurcate, and degenerate towards the direction of the maximum total stiffness under the given loads and constraints, and the layout with an effective load path is obtained. However, the layout calculated is complex; the processing cost is very high, especially for the large-scale box structures with the moving loads.

Topology optimization is a method that is used to seek an optimal configuration for the hollow location and number in some certain and continuous regions. It has been widely used in structural lightweight design [13–15], and some scholars apply topology optimization to the layout optimization of 3D box structure. Qin and Zhu [16] established a topology optimization model based on the method of moving asymptotes for the bridge crane girder structures, and some satisfying results were obtained. However, the method is only suitable for the discrete box girder structures and cannot be applied to the continuum structures studied in this paper. Konstantinos et al. [17] focused on the application of structural topology optimization to design steel perforated I-sections to replace the traditional cellular beams, and an optimum web opening configuration was suggested. But the applied load is uniform and invariable, and the beam section can be equivalent to the 2D structures, which cannot be applied to the 3D box structures. Young-Sop et al. [18] proposed a reliability-based topology optimization for the 3D structures using bidirectional evolutionary structural optimization and the standard response surface method. The results show that the optimal topology obtained for the 2D and 3D cantilever beams is very similar, and the thickness of the optimal topology gradually increased from the free end to the fixed end. However, due to the large aspect ratio of the large-scale box structures, the 3D topology optimization directly is easy to generate material aggregation [19, 20] and the inclined beam [21], resulting in the problems of difficult identification of the optimization results, which cannot be manufactured by traditional machining. The Additive Manufacturing (AM) can manufacture the structures with complex features, but it is still limited by the size and technology [22] and cannot be applied to the large-scale 3D box structures. On the other hand, the large-scale box structures usually bear the moving loads with the continuous change of position. The optimizations of extreme working conditions are easy to cause the problem of load sickness [23, 24].

Based on the above problems, this paper proposes a layout design method for the large-scale box structures under moving loads based on multiworking-condition topology optimization, which transforms the 3D topology optimization with moving loads of the large-scale box structures into the 2D topology optimization with multiple position loads. Section 2 describes the existing problems of topology optimization for large-scale box structures. The design method of structural decomposition process based on the functional sections and multiworking-condition topology optimization are introduced, respectively, in Section 3. Then, a crossbeam of a superheavy turning and milling machining center is taken as a case study and optimized by the proposed method.

2. Problem

2.1. SIMP Topology Optimization. SIMP topology optimization [25, 26] is a common method for topology optimization of the continuum structures, which introduces a material with a hypothetical relative density varying between 0 and 1 and uses a penalty factor to disperse the intermediate density value to 0/1, so as to eliminate the elements with intermediate density. In this paper, the optimal topology with maximum stiffness is calculated under the constraint of a certain material removal rate based on the theory of SIMP topology optimization. A topology optimization problem with the maximum stiffness as the objective can be expressed as follows:

$$\begin{cases} \text{find } x = (x_1, \ldots, x_n), \\ \min c(x) = \mathrm{U}^T \mathbf{K} \mathrm{U} = \sum_{e=1}^{n} (x_e)^p \mathbf{u}_e^T \mathbf{K}_e \mathbf{u}_e, \\ \text{subject to } \mathbf{K}(x)\mathbf{u} = F, \\ V(x) \le f \cdot V_0, \\ 0 < x_{\min} \le x_e \le 1, \end{cases} \tag{1}$$

where x is the relative density, $c(\mathrm{x})$ is the structural compliance; p is the penalty factor, $p > 1$. $\mathbf{U}$ and $\mathbf{F}$ are the displacement vector and the force vector. $\mathbf{K}(x)$ is the stiffness matrix of FEM. $\mathbf{u}_e$ and $\mathbf{K}_e$ are the displacement vector and stiffness matrix corresponding to the eth element. $V(x)$ is the objective volume value and V_0 is the initial volume value. $x_{\min}$ and x_e represent the minimum of relative density and the relative density of eth element, respectively, f is the prescribed volume fraction.

The optimization problem could be solved using several different approaches, such as Optimality Criteria (OC) methods, Sequential Linear Programming (SLP) methods, or the Method of Moving Asymptotes (MMA) and others [27]. For simplicity, we will here use a standard OC-method in this paper. Following Bendsøe [28], a heuristic updating scheme for the design variables can be formulated as follows:

$$x_e^{\text{new}} = \begin{cases} a, & \text{if } x_e B_e^{\eta} \le a, \\ x_e B_e^{\eta}, & \text{if } a < x_e B_e^{\eta} < b, \\ b, & \text{if } b \le x_e B_e^{\eta}. \end{cases} \tag{2}$$

where $a = \max(x_{\min}, x_e - m)$, $b = \min(1, x_e + m)$, m is a positive move-limit, η is a numerical damping coefficient, and B_e is found from the optimality condition as follows:

$$B_e = \frac{-(\partial c / \partial x_e)}{\lambda (\partial V / \partial x_e)}, \tag{3}$$

where λ is a Lagrangian multiplier that can be found by a bisectioning algorithm. The sensitivity of the objective function is found as follows:

$$\frac{\partial c}{\partial x_e} = -p\left(x_e\right)^{p-1} \mathrm{u}_e^T \mathrm{k}_0 \mathrm{u}_e. \tag{4}$$

2.2. Topology Optimization of a Box Structure. A large number of stiffened plates are usually arranged in the large-scale box structures to improve the stiffness and strength, so the essence of lightweight is to optimize the layout of stiffened plates. Taking a typical box structure with $1000 \times 200 \times 200$ mm shown in Figure 1 as an example, the left and right ends are fixed, and a vertical downward load F is applied on the left side of the upper face in Case 1, while F is applied in the middle of the upper face in case 2. The SIMP method (equations (1)–(4)) is used to calculate the load transfer skeleton in the box structure under two working conditions, and the results are shown in Figure 2.

Due to the large aspect ratio of the structure shown in Figure 1, the results show that there is a serious material deposition after topology optimization of two working conditions, and the result of case 2 appears inclined rib plates in three dimensions, which brings great trouble to the manufacturing. In addition, it can be seen from the comparison between Figures 2(a) and 2(b) that the load transfer skeletons under two working conditions are completely different because of the applied load in a different position. So, it is difficult to guarantee the safety of other working conditions if only the extreme working condition is considered, which may result in the problem of load sickness [29].

Therefore, we can get a conclusion: the direct topology optimization of the large-scale box structures has some problems: the load transfer skeletons are difficult to identify and all working conditions are difficult to consider comprehensively, which cannot provide guidance for the rational layout design of the internal stiffened plates. So, it is necessary to develop new design ideas to optimize large-scale box structures.

3. Method

According to the above problems, we assume that the material redundancy problem may be solved if we convert the 3D topology optimization problem into a 2D problem. The moving loads can be simplified to multiple position loads, which will restore the actual working condition of the box structures.

3.1. Decomposition of the Functional Section. The decomposition method of the functional sections refers to a method of decomposing the complex 3D structure into 2D sections by analyzing loads of complex working conditions. For the structures with complex working conditions, the loads can be simplified according to the equivalent principle of force in theoretical mechanics. As shown in Figure 3, the Cartesian coordinate system is established by selecting a

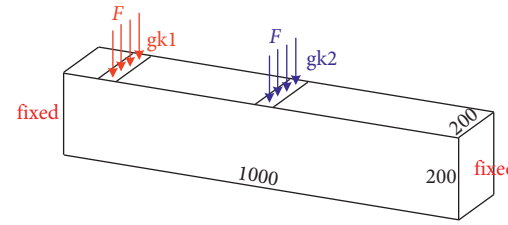

Figure 1: Diagram of a large-scale box structure.

point on the structure (such as the center of mass) as the origin, and then the spatial force system is simplified to this point so that the loads (F_x, F_y, F_z) and moments (M_x, M_y, M_z) are decomposed into three coordinate axes.

For the convenience of calculation, the XY plane, XZ plane, and YZ plane are defined as 2D functional sections, and the loads corresponding to each functional section are calculated and sorted. Take the plane with the largest load as the main bending functional section and the plane with the largest moment as the main torsional functional section. For example, if $F_x > F_y > F_z$, the XY plane is defined as the main bending functional section and the XZ plane as the secondary bending functional section. If $M_x > M_y > M_z$, the YZ plane is defined as the main torsional functional section and the XZ plane as the secondary torsional functional section. The last plane is the auxiliary functional section.

After determining the functional sections, the bearing types and boundary conditions of each functional section are analyzed and simplified. The Finite Element Model (FEM) is established, and topology optimization can be carried out by equation (1). So, the topology optimization of the large-scale box structures is transformed into the topology optimization of 2D functional sections. Finally, the 3D reconstruction of the topology optimization results of each functional section is carried out to obtain a lightweight 3D box structure.

3.2. Topology Optimization under the Moving Load. In this paper, the moving loads on the large-scale box structures are equivalent to several working conditions according to the position of loads. It is necessary to unify the optimization objectives of each working condition to consider the load transfer skeletons at any position in the process of topology optimization, which is a problem of multiobjective topology optimization.

A comprehensive evaluation function is needed to transform the multiobjective problem into a single objective problem. The linear weighting method is usually used to make it in the traditional multiobjective topology optimization. But it is to calculate weight average value for all functions and cannot reflect the prominent influence from some certain functions, which does not guarantee that all functions obtain the relative optimal solutions. The compromise programming method [30] can get a group of a better relative optimal solution by calculating the sensitivity of all functions to design variables and adjusting each objective to balance each other.

So, the objective function of the static multiworking-condition stiffness is established by the compromise

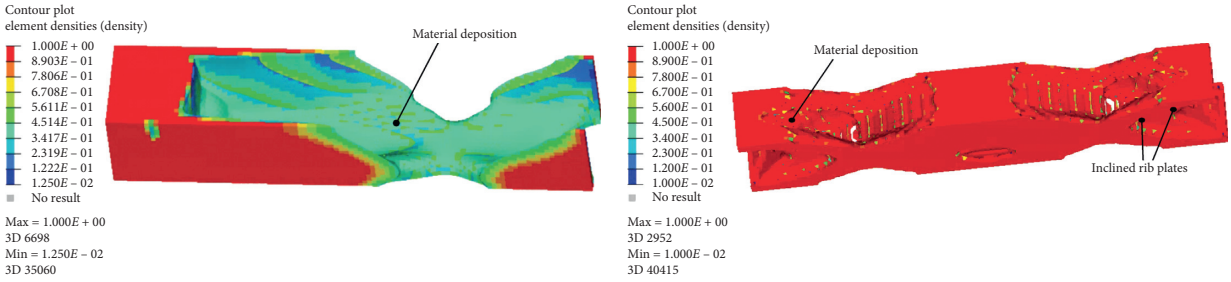

Figure 2: Optimization results. (a) Case 1, (b) case 2.

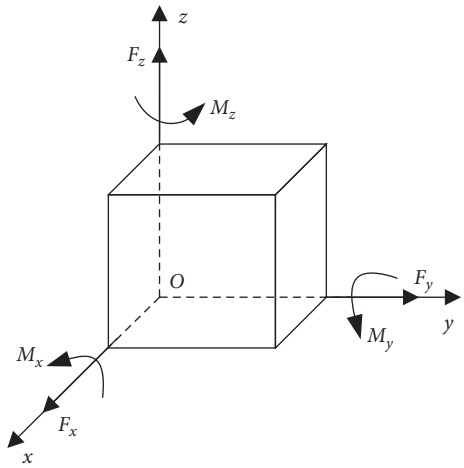

Figure 3: Diagrammatic sketch of load equivalent.

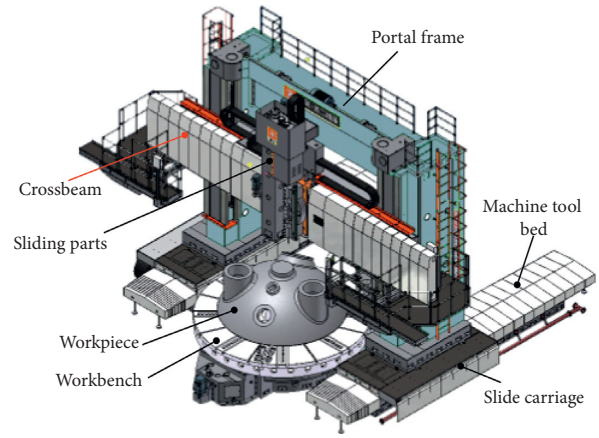

Figure 4: Superheavy turning and milling machining center.

programming method, as shown in equation (5). $C(x)$ is the comprehensive evaluation value of the static stiffness, and the smaller the value, the larger the structural overall stiffness.

$$\min_x C(x) = \left\{ \sum_{i=1}^{n} \omega_i^q \left[\frac{C_i(x) - C_i^{\min}}{C_i^{\max} - C_i^{\min}} \right]^q \right\}^{(1/q)}, \quad (5)$$

where n is the total number of working conditions. w_i is the weight coefficient of the ith working condition while q is the penalty coefficient ($q \geq 2$). $C_i(\rho)$ is the structural compliance of the ith working condition. $C_i^{\max}$ and $C_i^{\min}$ are the maximum and minimum compliance of the ith working-condition, respectively.

4. Topology Optimization of Crossbeam

In this paper, a large-scale crossbeam of superheavy turning and milling machining center is taken as an example to verify the proposed method. The turning and milling machining center is composed of crossbeam, sliding parts, workbench, slide carriage, machine tool bed, portal frame, and other components, as shown in Figure 4.

The crossbeam is installed on the portal frame, which is the supporting part of the sliding parts and also the main part bearing the cutting forces. Its static and dynamic performance directly affects the accuracy of the machine tool. The crossbeam is 10.4 m long, 7.5 m span, 1.28 m wide, 1.8 m high, and 40058 kg weight, and it is welded by a Q235 steel plate. It belongs to a typical box structure because of its large volume and mass, large inertia load in the process of moving up and down. To improve the overall mechanical performance of the crossbeam, the decomposition method of functional sections and multiworking-condition topology optimization are used to optimize the layout of the internal stiffened plates.

4.1. Finite Element Analysis. The crossbeam and sliding parts not only contain many parts but also have complex features. The efficiency and accuracy of the Finite Element Analysis (FEA) for all parts are very low, which is easy to lead to errors in simulation analysis. In order to improve the calculation efficiency, the features such as small holes, small corners, small gaps, and welds on the crossbeam are ignored, and a simplified model is established, as shown in Figure 5. According to the moving range of the sliding parts on the guide rail (0~7400 mm), taking the distance from the slider to the right boundary of the crossbeam as reference distance, 11 positions of the sliding parts along Y-direction are selected for FEA. When the sliding parts are in 3700 mm along Y direction, they are located at the middle of the crossbeam.

The boundary condition of the crossbeam can be equivalent to a simply supported beam. The sliding parts

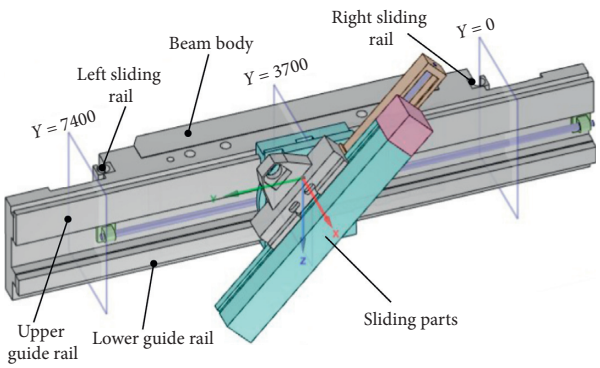

Figure 5: Simplified model of the crossbeam.

slide on one side of the crossbeam, and the crossbeam bears offset moving loads. Therefore, the loads that cause deformation of the crossbeam include self-gravity, gravity of the sliding parts, distortion caused by offset loads, and cutting forces. The cutting forces of the turning and milling machining center under a typical working condition are shown in Table 1. Since the cutting forces are much smaller than the self-gravity (400580 N), only the deformation caused by gravity is regarded as the static characteristics of the crossbeam. In addition, the rotation of the sliding parts is not considered because it has little influence on the static response of the crossbeam. The displacement constraints are applied to the crossbeam: X-direction constraint is applied to the large guide rail surface of the crossbeam and the portal frame (DOF_ X in Figure 6), Y-direction constraint is applied to the small guide rail surface of the crossbeam and the portal frame (DOF_ Y in Figure 6), and Z-direction constraint is applied to the left and right screw holes (DOF_ Z in Figure 6).

The model is imported into the FEA software ANSYS. The tetrahedral element is used to divide the parts with complex features, while the hexahedral element (hexdominant method) is used to divide other parts. The loads and constraints shown in Figure 6 are applied and the FEM is shown in Figure 7 (Y = 3700 mm).

As the sliding parts move to different positions on the crossbeam, the static response is different. 11 key positions are selected along the Y-direction for FEA, and the response curve of static maximum displacement is shown in Figure 8. The curve clearly reflects that the displacement of the crossbeam increases first, then decreases, and then increases from 0 to 7400 mm in Y-direction. When the sliding parts move to the middle of the crossbeam ($Y = 3700$ mm), the maximum deformation is 0.1289 mm, and the corresponding displacement distribution is shown in Figure 9(a). At this position, the stress distribution is shown in Figure 9(b), and the maximum stress is 12.77 MPa, which is less than the material yield strength (235 MPa). Therefore, it can be seen that the overall stress value of the crossbeam is relatively small, and there is a large lightweight space.

4.2. Establish Functional Sections. In this section, the decomposition method of functional sections is used to reduce

Table 1: Cutting forces under a typical working condition.

	Main cutting force F_c	Feeding force F_f	Radial force F_r
Value (N)	74760	41118	29904

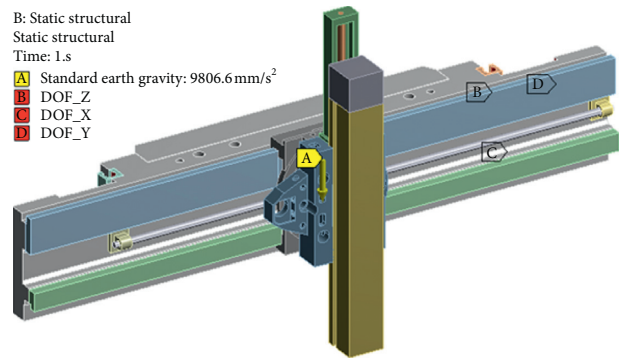

Figure 6: Simplified boundary conditions of the crossbeam.

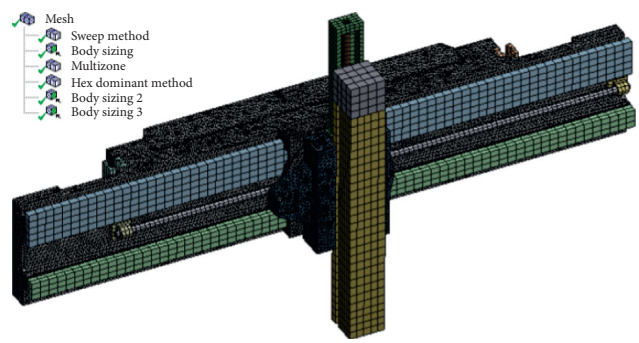

Figure 7: Finite element model ($Y = 3700$ mm).

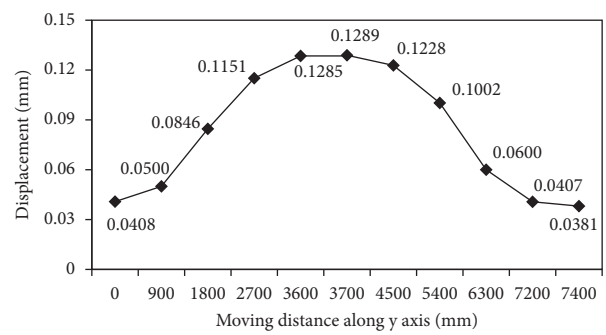

Figure 8: The response curve of the static maximum displacement.

the dimension of the crossbeam in topology optimization. Firstly, the coordinate system (shown in Figure 10) is established with the center of mass of the crossbeam as the origin.

According to the equivalent principle of force, loads of the crossbeam under the typical cutting condition mainly include self-gravity G_1, gravity G_2 of the sliding parts, cutting forces (main cutting force F_c, radial force F_r, feeding force

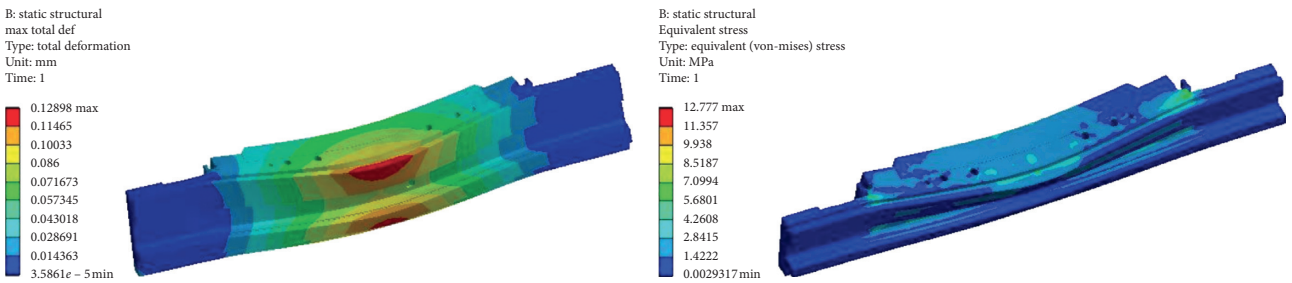

Figure 9: The results of FEA ($Y = 3700$ mm). (a) Displacement distribution. (b) Stress distribution.

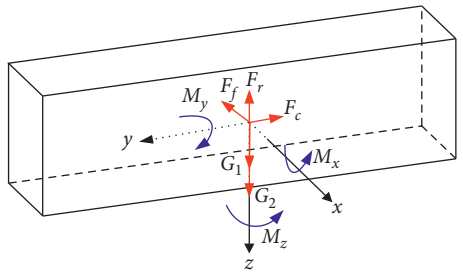

Figure 10: Equivalent loads at the center of mass of the crossbeam.

F_f), and moments $M_x \backslash M_y \backslash M_z$ from above loads on the center of mass. It can be seen from Section 4.1 that the gravity of the crossbeam and the sliding parts is far greater than the cutting forces and $F_c > F_f > F_r$ (Table 1). Therefore, it is obvious from Figure 10 that the equivalent loads at the center of mass have a relationship as follows:

$$\begin{cases} F_z > F_y > F_x, \\ M_y > M_x > M_z. \end{cases} \tag{6}$$

Based on the principle of determining functional sections proposed in Section 3, the YZ plane is defined as the main bending functional section, the XZ plane is defined as the main torsional functional section (also the secondary bending functional section), and the XY plane is defined as the auxiliary functional section. As the main function of the crossbeam is to resist overall bending deformation and torsional deformation caused by the offset loads, the main bending functional section and the main torsional functional section are only selected for topology optimization.

The main bending functional section is shown in Figure 11(a). As the sliding parts slide on the guide rail of the crossbeam, and the guide rail is not taken as the optimization object. So, the length that can be optimized is less than the length of the guide rail, and the size is set as $6850 \times 1580 \times 10$ mm. The moving load is equivalent to nine working conditions with the same distance, as shown in Figure 11(b). When the load is at different positions of the section, there are significant differences in the load transfer skeleton by topology optimization. So, it is necessary to carry out multiworking-condition topology optimization for the main bending functional section.

The main torsional functional section is shown in Figure 12(a). The torsional load mainly comes from the pressure exerted by the sliding parts on the guide rail, and the section shape is complex. So, the sectional size is simplified to a cube of $1000 \times 1000 \times 20$ mm, and the equivalent working condition is shown in Figure 12(b).

4.3. Topology Optimization

4.3.1. Main Bending Functional Section. In this section, topology optimization of the main bending functional section under nine working conditions ($n = 9$ in fd5(5)) is carried out. It is necessary to first determine the weight coefficient w_i of nine working conditions when establishing the comprehensive evaluation function of the crossbeam. According to the deformation law of the simply supported beams in theoretical mechanics, the closer the concentrated force is to the middle position, the larger the deformation is. In this paper, the response curve of displacement shown in Figure 8 is taken as the index, and the weight coefficients of each working condition are set as 0.07, 0.08, 0.1, 0.15, 0.2, 0.15, 0.1, 0.08, 0.07.

In addition, $C_i^{\max}$ and $C_i^{\min}$ in equation (5) are the maximum and minimum compliance of the ith working-condition, respectively, which can be obtained from the single-working-condition topology optimization. Therefore, the FEM of nine working conditions are established, respectively, and the single-working-condition topology optimization is carried out with equation (1). The results of $C_i^{\max}$ and $C_i^{\min}$ are shown in Table 2.

Taking the relative density as the design variable and a material removal rate of 30% as the constraint condition, aiming at the minimum comprehensive evaluation value of the static stiffness under multiple working conditions, the mathematical model of multiworking-condition topology optimization is established as shown in the following equation:

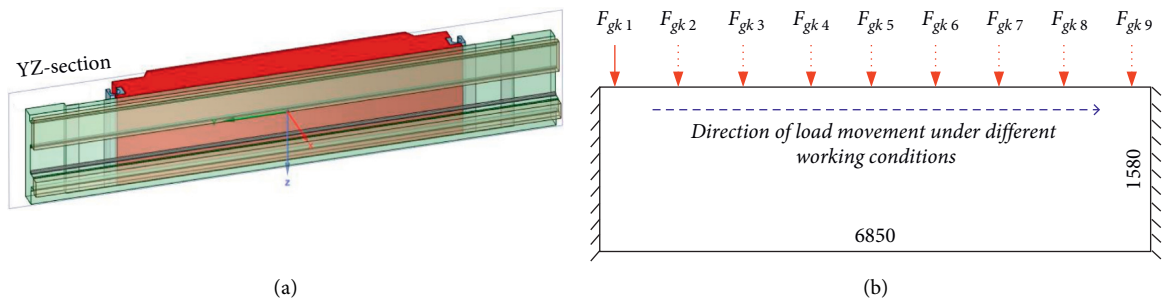

Figure 11: Main bending functional section. (a) YZ plane. (b) Equivalent working condition.

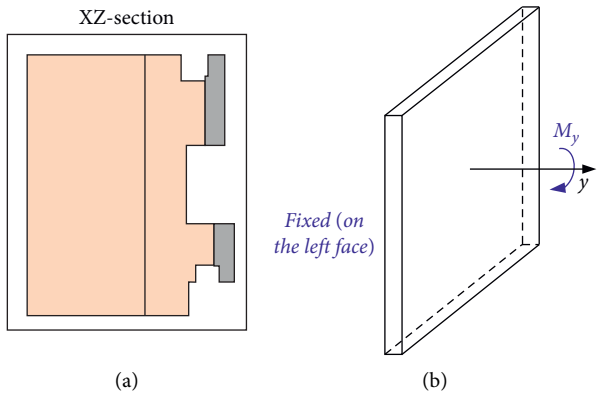

Figure 12: Main torsional functional section. (a) XZ plane, (b) equivalent working condition.

Table 2: The compliance of the ith working condition (Nmm).

No.	1	2	3	4	5	6	7	8	9
$C_k^{\min}$ (Nmm)	2.66	4.07	6.14	8.69	9.82	8.69	6.14	4.08	2.67
$C_k^{\max}$ (Nmm)	10.39	14.23	18.26	21.38	22.55	21.38	18.26	14.23	10.39

$$\begin{cases} \text{find } x = (x_1, \ldots, x_n), \\ \min C(\rho) = \left\{ \sum_{i=1}^{9} \omega_i^2 \left[\dfrac{C_i(\rho) - C_i^{\min}}{C_i^{\max} - C_i^{\min}} \right]^2 \right\}^{(1/2)}, \\ \text{subject to } \mathbf{K}(x)\mathbf{u} = \mathrm{F}, \\ V(x) \le 0.7 \cdot V_0, \\ 0 < x_{\min} \le x_e \le 1. \end{cases} \tag{7}$$

The optimization result is shown in Figure 13, and the importance degree of each region is decreasing when the color changes from red to blue. The load transfer skeleton of the YZ section is clearly given and the stiffened plates are established as shown in Figure 14.

In order to show the advantages of multiworking-condition topology optimization, the topology optimization of the fifth working condition (F_{gk5} in Figure 11(b)) is calculated. The result (Figure 15) shows that the load transfer skeleton can well bear the loads under the fifth working condition, but it is obvious that the layout of the stiffened

Figure 13: The optimization result.

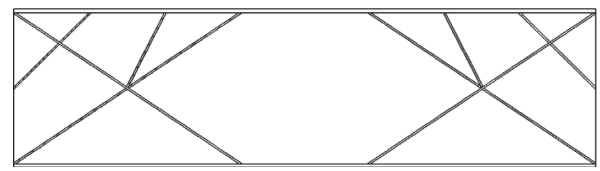

Figure 14: The layout of internal stiffened plates.

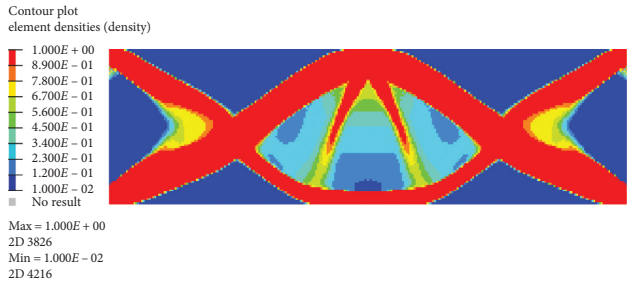

Figure 15: Optimization result of the fifth working condition.

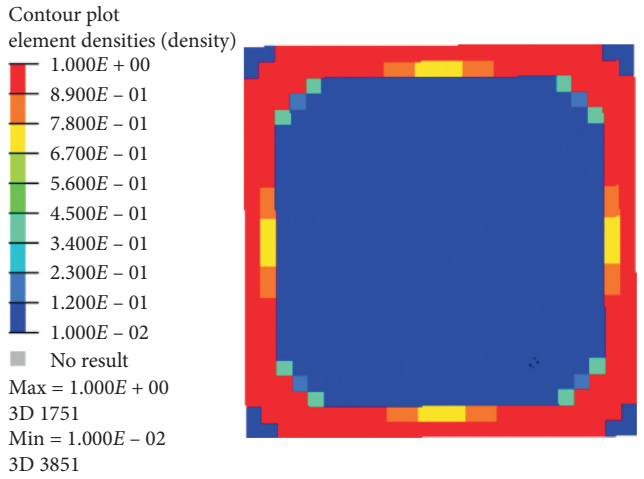

Figure 16: The optimization result of the XZ section.

plates is not suitable for other working conditions. On the contrary, the result of Figure 13 shows multiple stiffened plates at the location where the load is applied at the upper boundary of the functional section, which can meet the loads generated by the sliding parts at different locations of the crossbeam. Therefore, the result of Figure 13 is better than that of Figure 15.

4.3.2. Main Torsional Functional Section. The results of topology optimization for a main torsional functional section are shown in Figure 16, which shows that the best shape of a rectangular section is hollow and the corners are chamfered. So, the feature of chamfer is added to the cross section of the crossbeam in XZ plane, as shown in Figure 17.

Based on the above results, the new model of the crossbeam is established as shown in Figure 18.

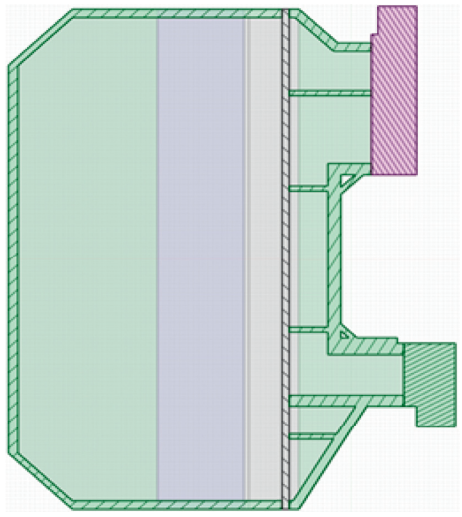

Figure 17: New cross section of the crossbeam.

4.4. Verification of Optimization Result. In order to verify the effect of multiworking-condition topology optimization of the crossbeam, taking the new model as the research object and applying the same boundary conditions (the same as Figure 6), the displacement of 11 working conditions is analyzed by FEA again. The total displacement response is shown in Table 3, and the comparison curve is shown in Figure 19.

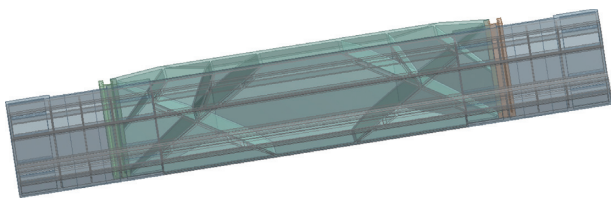

Figure 18: The new model of the crossbeam.

Table 3: The displacement of 11 working conditions.

No.	1	2	3	4	5	6	7	8	9	10	11
Location Y (mm)	0	0.04083	0.03227	2700	3600	3700	4500	5400	6300	7200	7400
Initial model (mm)	900	0.04998	0.04182	0.11514	0.12850	0.12898	0.12279	0.10020	0.06001	0.04068	0.03808
New model (mm)	1800	0.08456	0.07074	0.09542	0.10642	0.10655	0.09726	0.07365	0.04323	0.03319	0.03259

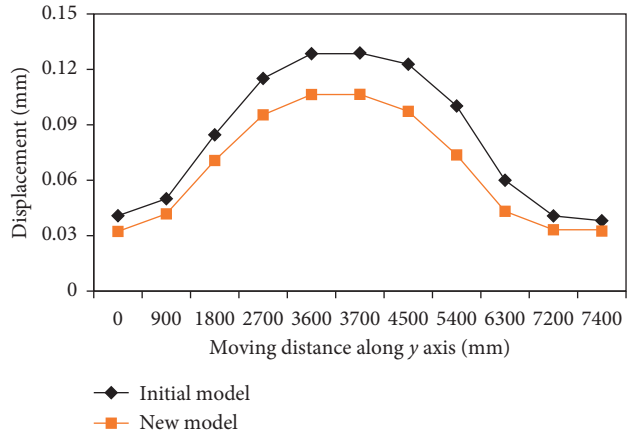

Figure 19: The comparison of the displacement response.

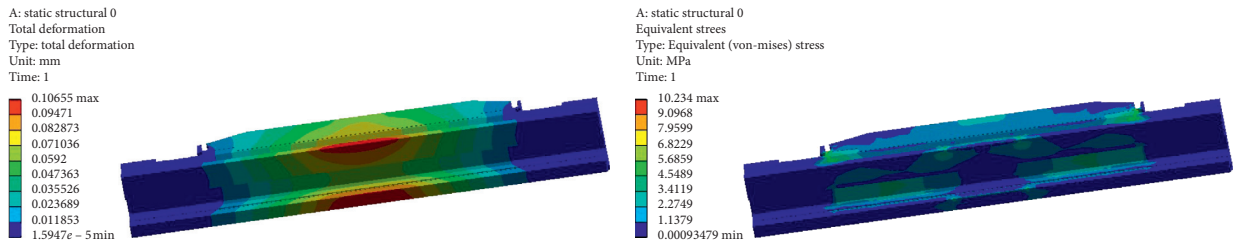

(a) (b)

Figure 20: The results of FEA for the new model. (a) Displacement distribution. (b) Stress distribution.

The results show that the overall displacements of the crossbeam become smaller than the initial model, which indicates that the structural stiffness is strengthened. Figure 19 also shows that the total deformation of the new model is largest when the sliding parts are at the middle of crossbeam ($Y = 3700$ mm). The displacement and stress distribution under extreme working conditions are shown in Figure 20. The maximum displacement is 0.10655 mm, which is 17.39% lower than the initial model, indicating that the static stiffness of the crossbeam has been significantly improved. The maximum stress is 10.234 MPa, which is smaller than the material yield strength (235 MPa), meeting the strength requirements.

Compare the static mechanical performances when the sliding parts are in the middle of crossbeam ($Y = 3700$ mm), as shown in Table 4. It can be seen that the maximum displacement value of the new crossbeam is reduced by 17.39%, the maximum stress value is reduced by 19.9%, and the mass is changed from 40058 kg to 35023 kg, which is reduced by 12.57%, indicating that the lightweight effect is very good.

Table 4: Comparison of mechanical performances.

	Max displacement (mm)	Max stress (MPa)	Mass (kg)
Initial model	0.12898	12.777	40058
New model	0.10655	10.234	35023
Variation	−17.39%	−19.9%	−12.57%

5. Conclusions

In this paper, a layout design method for the large-scale box structures under moving loads based on multiworking-condition topology optimization is proposed to solve the problem of difficult identification and complex moving loads. According to the magnitude of loads and moments, the complex 3D structure is transformed into 2D functional sections including the main bending functional section, the main torsional functional section, and the auxiliary functional section, which makes the topology optimization simplify from 3D to 2D. The complex moving loads are equivalent to several working conditions, and the

comprehensive evaluation function is constructed by using the compromise programming method, which solves the problem of load sickness under the topology optimization of extreme single-working-condition and avoids that the result is only the local optimal solution rather than the global optimal solution. Taking a crossbeam of superheavy turning and milling machining center as an example, the optimization results show that the stiffness and strength of the crossbeam are increased by 17.39% and 19.9%, respectively, while the weight is reduced by 12.57%. It shows that the method proposed in this paper has better practicability and effectiveness for large-scale box structures.

Data Availability

The data can be obtained from the corresponding author.

Conflicts of Interest

The authors declare that they have no financial and personal relationships with other people or organizations that can inappropriately influence their work, and there is no professional or other personal interest of any nature or kind in any product, service, and/or company that could be construed as influencing the position presented in this manuscript.

Acknowledgments

This work was supported by the Chinese National Key Research and Development Program (2016YFC0802900) and the Key Natural Science Projects of Hebei Provincial Department of Education (ZD2020156).

References

[1] S. Liu, Y. Li, Y. Liao, and Z. Guo, "Structural optimization of the cross-beam of a gantry machine tool based on grey relational analysis," *Structural and Multidisciplinary Optimization*, vol. 50, no. 2, pp. 297–311, 2014.

[2] Q. X. Wang, X. F. Zhang, and C. B. Sun, "Lightweight design and research of box girder for double girder bridge crane," *Applied Mechanics and Materials*, vol. 229–231, pp. 478–481, 2012.

[3] C. Sun, T. Ying, J. C. Zeng, J. S. Pan, and Y. F. Tao, "The structure optimization of main beam for bridge crane based on an improved PSO," *Journal of Computers*, vol. 6, no. 8, pp. 1585–1590, 2011.

[4] H. Huang, H. An, H. Ma, and S. Chen, "An engineering method for complex structural optimization involving both size and topology design variables," *International Journal for Numerical Methods in Engineering*, vol. 117, no. 3, pp. 291–315, 2019.

[5] T. Liu, G. Sun, J. Fang, J. Zhang, and Q. Li, "Topographical design of stiffener layout for plates against blast loading using a modified ant colony optimization algorithm," *Structural and Multidisciplinary Optimization*, vol. 59, no. 2, pp. 335–350, 2019.

[6] D. Trias Mansilla, L. Marín Hernández, and M. Majó, "A comparative study of genetic algorithms for the multi-objective optimization of composite stringers under compression loads," *Composites Part B: Engineering*, vol. 47, pp. 130–136, 2013.

[7] H. Gao, J. Sun, W. Chen, Y. Zhang, and Q. Wu, "Structural bionic design for a machine tool column based on leaf veins," *Proceedings of the Institution of Mechanical Engineers, Part C: Journal of Mechanical Engineering Science*, vol. 232, no. 16, pp. 2764–2773, 2018.

[8] L. Zhao, J. Ma, W. Chen, and H. Guo, "Lightweight design and verification of gantry machining center crossbeam based on structural bionics," *Journal of Bionic Engineering*, vol. 8, no. 2, pp. 201–206, 2011.

[9] H. Zhang, X. Ding, X. Dong, and M. Xiong, "Optimal topology design of internal stiffeners for machine pedestal structures using biological branching phenomena," *Structural and Multidisciplinary Optimization*, vol. 57, no. 6, pp. 2323–2338, 2018.

[10] X. Dong, X. H. Ding, and M. Xiong, "Optimal layout of internal stiffeners for three-dimensional box structures based on natural branching phenomena," *Engineering Optimization*, vol. 51, no. 4, pp. 590–607, 2019.

[11] B. T. Li, J. Hong, S. N. Yan, and Z. F. Liu, "Multidiscipline topology optimization of stiffened plate/shell structures inspired by growth mechanisms of leaf veins in nature," *Mathematical Problems in Engineering*, vol. 201311 pages, Article ID 653895, 2013.

[12] S. Yan, B. T. Li, and J. Hong, "Bionic design and verification of high-precision machine tool structures," *International Journal of Advanced Manufacturing Technology*, vol. 81, no. 1–4, pp. 73–85, 2015.

[13] O. Sigmund and K. Maute, "Topology optimization approaches," *Structural and Multidisciplinary Optimization*, vol. 48, no. 6, pp. 1031–1055, 2013.

[14] L. Xia, L. Zhang, Q. Xia, and T. Shi, "Stress-based topology optimization using bi-directional evolutionary structural optimization method," *Computer Methods in Applied Mechanics and Engineering*, vol. 333, pp. 356–370, 2018.

[15] T. Kunakote and S. Bureerat, "Multi-objective topology optimization using evolutionary algorithms," *Engineering Optimization*, vol. 43, no. 5, pp. 541–557, 2011.

[16] D. Qin and Q. Zhu, "Structural topology optimization of box girder based on method of moving asymptotes (MMA)," in *Proceedings of the 2010 International Conference on Intelligent Computation Technology and Automation*, pp. 402–405, Changsha, China, May 2010.

[17] K. D. Tsavdaridis, J. J. Kingman, and V. V. Toropov, "Application of structural topology optimisation to perforated steel beams," *Computers & Structures*, vol. 158, pp. 108–123, 2015.

[18] Y.-S. Eom, K.-S. Yoo, J.-Y. Park, and S.-Y. Han, "Reliability-based topology optimization using a standard response surface method for three-dimensional structures," *Structural and Multidisciplinary Optimization*, vol. 43, no. 2, pp. 287–295, 2011.

[19] J. Liu, Y. Ma, A. J. Qureshi, and R. Ahmad, "Light-weight shape and topology optimization with hybrid deposition path planning for FDM parts," *International Journal of Advanced Manufacturing Technology*, vol. 97, no. 1–4, pp. 1123–1135, 2018.

[20] Z. L. Zhou, J. Song, and M. Cong, "Structure topology optimization of the spindle box of a machining center," *Advanced Materials Research*, vol. 421, pp. 225–229, 2011.

[21] Y. Yang, C. D. Moen, and J. K. Guest, "Three-dimensional force flow paths and reinforcement design in concrete via stress-dependent truss-continuum topology optimization,"

Journal of Engineering Mechanics, vol. 141, no. 1, Article ID 04014106, 2015.

[22] T. E. Johnson and A. T. Gaynor, "Three-dimensional projection-based topology optimization for prescribed-angle self-supporting additively manufactured structures," *Additive Manufacturing*, vol. 24, pp. 667–686, 2018.

[23] R. H. Zuberi, Z. X. Zuo, K. Long, and W. Li, "Topological optimization of constant beam section under moving load condition," in *Proceedings of the International Conference on Mechanic Automation and Control Engineering*, Wuhan, China, June 2010.

[24] F. Wu, Z. Wang, J. Han, and G. Pei, "Research on multi-objective topology optimization of diesel engine cylinder block based on analytic hierarchy process," *Mathematical Problems in Engineering*, vol. 2019, Article ID 6194634, 16 pages, 2019.

[25] A. Li, C. Liu, and S. Feng, "Topology and thickness optimization of an indenter under stress and stiffness constraints," *Journal of Mechanical Science and Technology*, vol. 32, no. 1, pp. 211–222, 2018.

[26] Q. Zhao, X. Chen, Z.-D. Ma, and Y. Lin, "Robust topology optimization based on stochastic collocation methods under loading uncertainties," *Mathematical Problems in Engineering*, vol. 2015, Article ID 580980, 14 pages, 2015.

[27] K. Liu and A. Tovar, "An efficient 3D topology optimization code written in Matlab," *Structural and Multidisciplinary Optimization*, vol. 50, no. 6, pp. 1175–1196, 2014.

[28] M. P. Bendsøe, *Topology Optimization: Theory, Methods, and Applications*, pp. 1–370, Springer, Berlin, Germany, 2004.

[29] G. Zhao, J. Liu, H. X. Wang, X. F. Yang, and G. L. Wen, "Strategy of sensitivity hierarchical filtering for overcoming load sickness phenomenon of continuum topology optimization," *Journal of Hunan University (Natural Sciences)*, vol. 8, pp. 79–85, 2018.

[30] D. Xiao, H. Zhang, X. Liu, T. He, and Y. Shan, "Novel steel wheel design based on multi-objective topology optimization," *Journal of Mechanical Science and Technology*, vol. 28, no. 3, pp. 1007–1016, 2014.